

สรุปผลการดำเนินงานวิจัย

โครงการทุนเมธีวิจัยประจำปี 2538

The Surface Structure and Catalytic Properties of Zeolite and Molecular Sieve Catalysts

เสนอ

ผู้อำนวยการฝ่ายสนับสนุนการวิจัยเชิงวิชาการ สำนักงานกองทุนสนับสนุนการวิจัย

โดย รศ.ดร.จำรัส ลิ้มตระกูล ภาควิชาเคมี คณะวิทยาศาสตร์ ม.เกษตรศาสตร์

วันที่ 6-7 ตุลาคม พ.ศ. 2541



สรุปผลการดำเนินงานวิจัย

โครงการทุนเมธีวิจัยประจำปี 2538

The Surface Structure and Catalytic Properties of Zeolite and Molecular Sieve Catalysts

เสนอ

ผู้อำนวยการฝ่ายสนับสนุนการวิจัยเชิงวิชาการ สำนักงานกองทุนสนับสนุนการวิจัย

| | วัน ท ี่ |
|---------------------------------|------------------------|
| โดย | กาเกรมซึ่งน |
| รศ.ดร.จำรัส ลิ้มตระ | กลื่อกหนังถือ 41 ชู |
| กาดวิชาเคมี คณะวิทยาศาสตร์ ม เร | |

วันที่ 6-7 ตุลาคม พ.ศ. 2541

สำนักงานกองทุนสบับสนุนการวิจัย (สถว.) ชั้น 14 อาคาร และเอีย กรายอร์ เลเบี 979/17-21 ถบบพบคโยธิบ แบวงสามเสนใน เราะกฤปิก กรุงเบพร 10400 โรร.298-0455 โกรสาร 298-0476 Home page : http://www.trf.or.th E-mail : trf-info@erf.or.th



สารบัญ

| | หน้า |
|--|------|
| กิตติกรรมประกาศ | |
| บทคัดย่อ | |
| สารบัญ | |
| ผลการวิจัย | 1 |
| Structures, energetics, vibrational frequencies of zeolitic catalysts, | 2 |
| a comparison between density functional and post Hartree-Fock | |
| approaches | |
| ■ บทน้ำ (Introduction) | |
| วิธีการทดลอง (Methods) | |
| ผลการทดลองและบทวิจารณ์ (Results and Discussion) | |
| ■ เอกสารข้างชิง (References) | |
| | |
| Cationic, structural, and compositional effects on the surface | 17 |
| structure of zeolitic aluminosilicate catalysts | |
| ■ บทน้ำ (Introduction) | |
| ■ วิธีกา รทด ลอง (Methods) | |
| ผลการทดลองและบทวิจารณ์ (Results and Discussion) | |
| • เอกสารข้างชิง (References) | |
| | |
| Structures and potential energy surface of faujasitic zeolite / water | 30 |
| ■ บทน้ำ (Introduction) | |
| ■ วิธีการทดลอง (Methods) | |
| ผลการทดลองและบทวิจารณ์ (Results and Discussion) | |
| 🛎 เอกสารจ้างชิง (References) | |

TRF Final-report; 25-Sep-98

| Coadsorption | of ammonia and methanol on H-zeolites and | |
|-------------------------------------|---|----|
| alkaline-excha | inged zeolites | 45 |
| • | บทน้ำ (Introduction) | |
| • | วิธีการทดลอง (Methods) | |
| • | ผลการทดลองและบทวิจารณ์ (Results and Discussion) | |
| • | เอกสารข้างอิง (References) | |
| | | |
| Structure and | Reaction Pathways in Zeolitic Systems | 60 |
| • | บทน้ำ (Introduction) | |
| | วิธีการทดลอง (Methods) | |
| • | ผลการทดลองและบทวิจารณ์ (Results and Discussion) | |
| • | เอกสารข้างชิง (References) | |
| | | |
| เคมีของชีโอไลต์ | (Chemistry of Zeolites) | 68 |
| ผลงาน | | 74 |
| ผลงานที่ตีพิมพ์และกิ | จกรรมอื่นๆ ที่เกี่ยวข้อง | |
| ภาคผนวก | | |
| รายงานการเงิน | | |

กิติกรรมประกาศ

งานวิจัยนี้ได้รับการสนับสนุนจากสำนักงานกองทุนสนับสนุนการวิจัย (สกว.) สถาบันวิจัยและพัฒนา มก. และภาควิชาเคมี คณะวิทยาศาสตร์ มหาวิทยาลัยเกษตรศาสตร์ ขอขอบคุณคณาจารย์และผู้ร่วมงาน : ผศ.ดร.สุภา หารหนองบัว อ.ดวงกมล ตัณฑนาค อ.ปิติ ตรีสุกล อ.อุษา อันทอง อ.มะยูโซ๊ะ กูใน และ คุณจรุงศักดิ์ ย้อยนวล และท้ายที่สุดขอขอบพระคุณที่คณะกรรมการ สภาวิจัยแห่งชาติได้ประกาศเกียรติคุณเป็นนักวิจัยดีเด่นแห่งชาติสาขา เคมี และเภสัช ประจำปี 2541

Acknowledgements

This research was supported by the Thailand Research Fund (TRF), Grant RSA/18/1995, The Kasetsart University Research and Development Institute (KURDI), and the chemistry department. We wish to thank the Kasetsart Computer Center for an allotment of CPU time to make some of the calculations presented here. The author wishes to express his sincere thanks to his talented co-workers: Supa Hannongbua, Piti Treesukol, Duangkamol Tantanak, Jurungsak Yoinuan and Usa Ongthong. J.L. also acknowledges the National Research Council of Thailand (NRCT) committees for naming him the outstanding researcher awards in chemistry and pharmaceutical sciences in 1998.

บทคัดย่อ

ชีโอไลต์เป็นสารประกอบอะลูมิโนซิลิเกต (crystalline aluminosilicates) มีโครงสร้าง เป็นรูพรุนมีโพรงและช่องว่างขนาดตั้งแต่ 2-10 Å ซึ่งเป็นลักษณะพิเศษเฉพาะตัวที่เด่นชัด สมบัติของชีโอไลต์ที่นำเอาไปใช้ประโยชน์ เช่น การแลกเปลี่ยนไอออน (ion exchange) การคูด ขับ (adsorption) การคูดขับแก๊ส สารอาหาร น้ำ ตลอดจนโมเลกุลอินทรีย์ และสมบัติที่สำคัญ มากอย่างหนึ่งคือเป็นตัวเร่งปฏิกิริยา ได้ทำการวิจัยโครงสร้าง พลังงาน ความถี่ของการสั่นของ ตัวเร่งปฏิกิริยาชีโอไลต์ และ ศึกษาถึงอิทธิพลของโลหะ องค์ประกอบ การเปลี่ยนแปลงโครง สร้าง ต่อโครงสร้างพื้นผิวของตัวเร่งปฏิกิริยา การศึกษาและค้นหา Local structure properties ของชีโอไลต์และซีโอไทป์ เพื่อที่ะเข้าใจถึงบทบาทที่สำคัญของซีโอไลต์แต่ละซนิด และนำมาเป็น โครงสร้างต้นแบบ (Zeolitic prototype) ในการพัฒนาตัวเร่งปฏิกิริยาชีโอไลต์ให้มีประสิทธิภาพ สูงขึ้น นอกจากนั้นศึกษากระบวนการการดูดขับของ adsorbate บน ตัวเร่งปฏิกิริยาชีโอไลต์ โดยการศึกษาโครงสร้าง พื้นผิวพลังงานศักย์ (potential energy surface) ของ Faujasite Zeolite กับน้ำ และศึกษากระบวนการดูดซับร่วมและกลไกการเกิดปฏิกิริยาของเมธานอลและ แอมโมเนียบน H-zeolite และ Alkaline-exchange zeolite

Abstract

Rational catalyst design, notably zeolites and molecular sieves, represents one of the most rewarding challenges in catalysis research. Zeolites possess three dimensional microporous crystalline solid. Their catalytically active acid-sites within the complex porous framework structure provide unique properties that make them very attractive industrial materials. They play a significant role in chemicals and fuels production worth over \$1000 billion per year. Zeolites and molecular sieves can be tailored or chosen to maximize the product of target molecules by employing state-of-the-art techniques. Our aim is to develop strategies for tailoring the structural and chemical properties of catalyst materials and to explore the potential of new catalytic materials. In the present research work the surface structure and catalytic properties of different zeolitic clusters have been investigated for the first time via density functional theory (DFT/B3LYP), Hartree-Fock(HF) and Perturbation theory(MP2). This includes

- Structures, energetics and vibrational frequencies of zeolitic catalysts: a comparison between density functional and post-Hartree-Fock approaches
- Cationic, structural, and compositional effects on the surface structure of zeolitic aluminosilicate catalysts
- Structures and potential energy surface of Faujasitic zeolite/water
- Coadsorption of ammonia and methanol on H-zeolites and alkalineexchanged zeolites
- Structure and reaction pathways for methylamine/zeolite system.

ผลการวิจัย

- Structures, energetics, vibrational frequencies of zeolitic catalysts:
 A comparison between density functional and post Hartree-Fock approaches.
- Cationic, structural, and compositional effects on the surface structure of zeolitic aluminosilicate catalysts
- 3. Structures and potential energy surface of faujasitic zeolite / water
- Coadsorption of ammonia and methanol on H-zeolites and alkalineexchanged zeolites
- 5. Structure and Reaction Pathways in Zeolitic Systems
- 6. เคมีของซีโอไลต์ (Chemistry of Zeolites)

Reprinted from

THEO CHEM

Journal of Molecular Structure (Theochem) 358 (1995) 179-193

Structures, energetics and vibrational frequencies of zeolitic catalysts: a comparison between density functional and post-Hartree-Fock approaches

Jumras Limtrakul*, Duangkamol Tantanak

Laboratory for Computational and Applied Chemistry, Chemistry Department, Faculty of Science, Kasetsart University, Bangkok 10900, Thailand





THEO CHEM

Journal of Molecular Structure (Theochem) 358 (1995) 179-193

Structures, energetics and vibrational frequencies of zeolitic catalysts: a comparison between density functional and post-Hartree-Fock approaches

Jumras Limtrakul*, Duangkamol Tantanak

Laboratory for Computational and Applied Chemistry, Chemistry Department, Faculty of Science, Kasetsart University,
Bangkok 10900, Thailand

Abstract

Structures, energetics and vibrational frequencies of zeolitic cluster models have been investigated with an ab initio method at the correlated level involving the second-order Møller-Plesset (MP2) and with the density functional theory (DFT) method including local and non-local spin density functions. Full optimization of structures has been carried out with 3-21G, 6-31G*, 6-31G*, DZVP basis sets. The comparison of geometries of zeolite clusters between the DFT (Becke-Lee-Yang-Parr and Vosko-Wilk-Nusair) and MP2 results agrees with 1 pm for Si-O and O-H, while the weaker Al-O bond length agrees with 2-4 pm depending on the exchange-correlation potential employed. The Si-O(H)-Al, Si-O-H, and Si-O-Si bond angles are in good agreement with MP2. The flexible Si-O-Si angle is well represented by BLYP but not by VWN, the latter yielding angles 12° and 18° smaller than the MP2 and coupled pair functional results, respectively. This suggests that BLYP should be used. The acidity of zeolites at the BLYP/6-311G* level is evaluated by proton affinity; it is virtually identical to that from MP2/DZP and is also close to the result for G1 theory within the desired 10 kJ mol⁻¹ accuracy. The DFT OH stretching frequencies of zeolite clusters are predicted to within 4% of the experimental value. The DFT methods are computationally efficient and appear to provide results that are generally of comparable quality to MP2.

Keywords: Density functional theory; MP2; Zeolite

1. Introduction

Zeolites are porous frameworks of crystalline aluminosilicates with a number of interesting physical and chemical properties. The hydroxyl groups in zeolites are acknowledged to be of prime importance for the catalytic properties and have led to numerous industrially important applications [1-11].

It is important to know the structures, energetics

and vibrational frequencies of the Brønsted acidic surface sites which are crucial for understanding the catalytic processes [9-12].

Recently, density functional theory (DFT) has been employed to investigate various chemical systems [13–18]. Not only does it require much less computational effort, but also the DFT results are very encouraging when compared with high level ab initio calculations and more reliable experimental data. This leads to the utilization of DFT approaches for large chemical systems.

To the best of our knowledge, no systematic

^{*} Corresponding author.

investigations of the structure and bonding of zeolitic cluster models have been explored by DFT employing both local (LSD) and non-local spin density (NLSD) approximations. We have selected H₃SiOHAlH₃, (OH)₃SiOHAl(OH)₃, H₃SiOHAl-(OH)₂-OSiH₃, and H₃SiOHAl(OSiH3)₂-OSiH₃ to test and gauge the usefulness of DFT by a direct comparison with the high level ab initio results, and also the available experimental results.

2. Methods and computational details

Full geometry optimization of all zeolitic cluster models was carried out with the DFT methods.

All density functional computations were carried out using the Dgauss program [19] implemented to run on the Cray-YMP EL98 at the NECTEC High Performance Computing Center.

In Dgauss, the electron density is expanded in terms of single-particle Gaussian-type functions, referred to as the "auxiliary basis set". The program includes approximate electron exchange and correlation effects. These contributions are evaluated on a finite grid and can be fitted to another auxiliary basis set. Most integrals are calculated analytically, but some integrals concerning exchange-correlation contributions are evaluated by a numerical integration technique using a finite grid.

Two different exchange-correlation functionals were selected for this investigation, namely the

local density approximation (LDA) and BLYP functionals. For LDA we employed the Vosko-Wilk-Nusair (VWN) correlation function [20]. It is generally believed that the VWN potential represents one of the best analytical functional forms currently available for LSD potentials. Gradient-type corrections have been included self-consistently using the non-local functions of Becke exchange [21] and the Lee, Yang and Parr [22] correlation (BLYP).

The cluster models (H₃SiOH, H₃SiOSiH₃, H₃SiOHAlH₃, (OH)₃SiOHAl(OH)₃, H₃SiOHAl-(OH)2-OSiH3, and H3SiOHAl(OSiH3)2-OSiH3) have been computed with 3-21G, 6-31G*, and 6-311G* basis sets. Additionally, to minimize the basis set superposition error (BSSE) and to improve the quality of valence orbitals, the recommended LSD-optimized orbital basis sets [23] were also employed. The following orbitals were used: (41) for hydrogen atoms, (621/41/1) for oxygen atoms, and (6321/521/1) for Si and Al atoms. The following auxiliary basis sets were used: [4] for hydrogen atoms, [7/3/3] for oxygen atoms, and [9/4/4] for Al and Si atoms. These LSD-optimized orbital basis sets can be considered as double-zeta split valence plus polarization (DZVP) basis sets.

For the ab initio calculations we employed the TURBOMOLE program, which is based on the direct self-consistent field (SCF) method of Almloef and co-workers [24-26]. Two two-electron repulsion integrals are recomputed when needed, rather than being kept. Three basis sets of 3-21G,

Table 1
Optimized parameters for the molecular models of H₃SiOH and H₃SiOSiH₃

| Methods | Basis sets | H ₃ SiOH | | H ₃ SiOSiH ₃ | | |
|---------|-----------------------|---------------------|----------|------------------------------------|-----------|---------------|
| | | Si-O (pm) | O-H (pm) | Si-O-H (pm) | Śi-O (pm) | Si-O-Si (deg) |
| BLYP | 6-31G* | 168.2 | 97.7 | 114.3 | 166.7 | 148.4 |
| | 6-311G* | 167.3 | 97.0 | 118.6 | 166.4 | 150.0 |
| VWN | 6-31G* | 165.8 | 97.6 | 115.1 | 165.0 | 137.8 |
| | 6-311G* | 164.9 | 96.8 | 119.6 | 165.1 | 132.1 |
| MP2 | 6-31G* | 167.2 | 96.9 | 116.4 | 166.0 | 143.7 |
| | 6-311G* | 165.5 | 95.6 | 121.7 | 164.3 | 155.7 |
| CPF | Extended ^a | 165.0 | 95.8 | 117.7 | 164.8 | 151.6 |

a [8s, 5p, 3d, 1f/4s, 2p].

Table 2
Optimized parameters for the molecular model H₃SiOHAlH₃ at the BLYP, VWN, MP2 and HF levels

| Methods | Si-O (pm) | | | | | | | | | |
|---------|-------------|--------|---------|-------|-------|-------|--|--|--|--|
| | 3-21G* | 6-31G* | 6-311G* | DZVP | DZVP2 | TZVI | | | | |
| BLYP | 176.9 | 173.4 | 173.1 | 173.4 | 173.3 | 173.0 | | | | |
| VWN | 174.3 | 171.2 | 170.2 | 171.4 | 171.1 | 170.4 | | | | |
| MP2 | 175.8 | 172.8 | 171.5 | • | _ | | | | | |
| HF | 173.6 | 170.6 | 169.9 | - | | | | | | |
| | Al-O (pm) | | | | | | | | | |
| BLYP | 197.5 | 207.1 | 207.0 | 210.9 | 210.2 | 209.7 | | | | |
| VWN | 191.8 | 199.8 | 189.4 | 201.8 | 201.3 | 199.1 | | | | |
| MP2 | 194.2 | 202.6 | 200.6 | - | ** | ~ | | | | |
| HF | 192.2 | 202.2 | 201.5 | | | | | | | |
| | O-H (pm) | | | | | | | | | |
| BLYP | 99.7 | 97.9 | 97.1 | 98.2 | 97.8 | 97.5 | | | | |
| VWN | 99.5 | 98.1 | 97.1 | 98.2 | 97.8 | 97.5 | | | | |
| MP2 | 98.6 | 97.3 | 96.0 | - | - | - | | | | |
| HF | 96.6 | 95.1 | 94.2 | | • | - | | | | |
| | Al···H (pm) | | | | | | | | | |
| BLYP | 256.1 | 258.2 | 261.7 | 255.5 | 256.2 | 256.0 | | | | |
| VWN | 252.7 | 245.2 | 253.5 | 248.9 | 250.2 | 255.2 | | | | |
| MP2 | 256.0 | 259.7 | 259.2 | - | - | - | | | | |
| HF | 249.5 | 258.1 | 255.8 | _ | | | | | | |
| | Si-O-Al (de | (g) | | | | | | | | |
| BLYP | 125.6 | 127.6 | 127.0 | 131.0 | 130.8 | 130.6 | | | | |
| VWN | 121.6 | 121.1 | 125.1 | 121.9 | 123.4 | 125.9 | | | | |
| MP2 | 123.5 | 123.3 | 123.8 | | _ | _ | | | | |
| HF | 124.9 | 126.7 | 126.2 | - | | | | | | |
| | Si-O-H (de | g) | | | | | | | | |
| BLYP | 119.2 | 116.9 | 119.2 | 115.7 | 116.2 | 116.3 | | | | |
| VWN | 121.5 | 116.9 | 121.2 | 117.7 | 118.1 | 119.5 | | | | |
| MP2 | 118.2 | 116.5 | 118.7 | - | | _ | | | | |
| HF | 119.7 | 117.6 | 118.9 | - | | *** | | | | |

6-31G*, and 6-311G* quality are used. In order to obtain the more reliable structures of zeolite, the correlated calculations were performed for the primary unit $H_3SiOHAlH_3$. Geometry optimization was terminated when the gradient norm with respect to internal coordinates was less than $10^{-3}E_ha_0^{-1}$. The energy change was then below $5 \times 10^{-6}E_h$. All SCF and second-order Møller-Plesset (MP2)

calculations were carried out on the HP 700 cluster at the Laboratory for Computational and Applied Chemistry at Kasetsart University.

3. Results and discussion

In order to assess the reliability of density

J. Limtrakul, D. Tantanak Journal of Molecular Structure (Theochem) 358 (1995) 179-193

Table 3
BLYP optimized parameters computed for different models

| Model | Si-O (pm) | | | | | | |
|--|--------------|-------|---------|---------|--|--|--|
| | 3-21G | DZVP | 6-31G* | 6-311G* | | | |
| H ₃ SiOHAlH ₃ | 176.9 | 173.4 | 173.4 | 173.1 | | | |
| H ₃ SiOHAl(OH) ₂ OSiH ₃ | 175.7 | 174.6 | 173.4 | 173.4 | | | |
| (OH) ₃ SiOHAl(OH) ₃ | 175.6 | 174.8 | 175.2 | 174.3 | | | |
| H ₃ SiOHAl(OSiH ₃) ₂ OSiH ₃ | 175.8 | 173.9 | 173.1 | 173.0 | | | |
| | Al-O (pm) | | | | | | |
| H ₃ SiOHAlH ₃ | 197.5 | 210.9 | 207.1 | 207.0 | | | |
| H ₃ SiOHAl(OH) ₂ OSiH ₃ | 188.8 | 197.9 | 195.3 | 195.7 | | | |
| (OH) ₃ SiOHAI(OH) ₃ | 184.8 | 191.9 | 190.9 | 191.7 | | | |
| H ₃ SiOHAl(OSiH ₃) ₂ OSiH ₃ | 190.0 | 197.4 | 196.4 | 197.6 | | | |
| | O-H (pm) | | | | | | |
| H ₃ SiOHAIH ₃ | 99.7 | 98.2 | 97.9 | 97.1 | | | |
| H ₃ SiOHAl(OH) ₂ OSiH ₃ | 99.4 | 98.1 | 97.8 | 97.0 | | | |
| (OH) ₃ SiOHAl(OH) ₃ | 99.4 | 98.0 | 97.8 | 97.0 | | | |
| H ₃ SiOHAl(OSiH ₃) ₂ OSiH ₃ | 99.9 | 98.2 | 98.0 | 97.4 | | | |
| | Al···H (pm) | | | | | | |
| H ₃ SiOHAlH ₃ | 256.1 | 255.5 | 258.2 | 261.7 | | | |
| H ₃ SiOHAl(OH) ₂ OSiH ₃ | 248.9 | 255.4 | 251.6 | 250.9 | | | |
| (OH) ₃ SiOHAI(OH) ₃ | 251.8 | 254.3 | 255.5 | 253.7 | | | |
| H ₃ SiOHAl(OSiH ₃) ₂ OSiH ₃ | 240.5 | 248.8 | 243.6 | 244.0 | | | |
| | Si-O-Al (deg | 3) | | | | | |
| H ₃ SiOHAlH ₃ | 125.6 | 131.0 | 127.6 | 127.0 | | | |
| H ₃ SiOHAl(OH) ₂ OSiH ₃ | 120.2 | 125.6 | 124.1 | 124.0 | | | |
| (OH) ₃ SiOHAl(OH) ₃ | 119.3 | 121.4 | 120.2 | 119.9 | | | |
| H ₃ SiOHAl(OSiH ₃) ₂ OSiH ₃ | 128.4 | 130.0 | 131.9 | 131.5 | | | |
| | Si-O-H (deg |) | | | | | |
| H ₃ SiOHAIH ₃ | 119.2 | 115.7 | . 116.9 | 119.2 | | | |
| H ₃ SiOHAl(OH) ₂ OSiH ₃ | 123.9 | 119.3 | 121.8 | 122.3 | | | |
| (OH) ₃ SiOHAl(OH) ₃ | 118.8 | 119.6 | 118.8 | 120.8 | | | |
| H ₃ SiOHAl(OSiH ₃) ₂ OSiH ₃ | 123.7 | 119.9 | 121.3 | 121.9 | | | |

functional methods (local and non-local approximations) and the validity of the molecular models employed, the structures, proton affinities and vibrational frequencies of the smallest model compound silanol, H₃SiOH, disiloxane, H₃SiOSIH₃, and different cluster models of zeolites (H₃SiOHAlH₃, (OH)₃SiOHAl(OH)₃, H₃SiOHAl (OH)₂OSiH₃, and H₃SiOHAl(OSiH₃)₂OSiH₃)

were computed at different levels of theory using 3-21G, 6-31G*, 6-311G* and DZVP basis sets, as documented in Tables 1-5, and also depicted in Fig. 1. Smaller clusters, H₃SiOHAlH₃, are also computed at MP2 levels employing the corresponding basis sets, and the results were compared with those of the more reliable coupled pair functional (CPF/[8s, 5p, 3d, 1f/4s,

J. Limtrakul, D. Tantanak/Journal of Molecular Structure (Theochem) 358 (1995) 179-193

Table 4
VWN optimized parameters computed for different models

| Model | odel Si-O (pm) | | | |
|--|----------------|------------|--------|---------|
| | 3-21G | DZVP | 6-31G* | 6-311G* |
| H ₃ SiOHAlH ₃ | 174.3 | 171.4 | 171.2 | 170.2 |
| H ₃ SiOHAl(OH) ₂ OSiH ₃ | 172.8 | 171.5 | 170.8 | 170.4 |
| H ₃ SiOHAI(OSiH ₃) ₂ OSiH ₃ | 173.0 | 171.0 | 170.7 | 170.3 |
| | Al-O (pm) | | | |
| H ₃ SiOHAIH ₃ | 191.8 | 201.8 | 199.8 | 198.4 |
| H ₃ SiOHAl(OH) ₂ OSiH ₃ | 184.0 | 190.0 | 188.9 | 189.0 |
| H ₃ SiOHAl(OSiH ₃) ₂ OSiH ₃ | 184.3 | 190.3 | 190.4 | 190.3 |
| | O-H (pm) | | | |
| H ₃ SiOHAlH ₃ | 99.5 | 98.2 | 98.1 | 97.1 |
| H ₃ SiOHAl(OH) ₂ OSiH ₃ | 99.3 | 98.0 | 97.8 | 97.2 |
| H ₃ SiOHAI(OSiH ₃) ₂ OSiH ₃ | 100.2 | 98.3 | 98.1 | 97.4 |
| | Al···H (pm) | | | |
| H ₃ SiOHAlH ₃ | 252.7 | 248.9 | 245.2 | 253.5 |
| H ₃ SiOHAl(OH) ₂ OSiH ₃ | 241.9 | 247.7 | 245.2 | 243.7 |
| H ₃ SiOHAl(OSiH ₃) ₂ OSiH ₃ | 231.2 | 243.7 | 241.7 | 241.0 |
| | Si-O-Al (deg | <u>;</u>) | | |
| H ₃ SiOHAlH ₃ | 121.6 | 121.8 | 121.1 | 125.1 |
| H ₃ SiOHAI(OH) ₂ OSiH ₃ | 118.2 | 121.9 | 122.2 | 121.8 |
| H ₃ SiOHAl(OSiH ₃) ₂ OSiH ₃ | 125.0 | 124.3 | 125.3 | 125.1 |
| | Si-O-H (deg |) | | |
| H ₃ SiOHAlH ₃ | 121.5 | 117.7 | 116.9 | 121.2 |
| H ₃ SiOHAl(OH) ₂ OSiH ₃ | 127.9 | 123.3 | 124.1 | 125.4 |
| H ₃ SiOHAl(OSiH ₃) ₂ OSiH ₃ | 130.1 | 124.5 | 125.1 | 125.4 |

2p]) method of Sauer and Alhrichs [27] and G1 [28,29], as well as available accurate experimental results.

3.1. Structures

Table 1 illustrates the results for H₃SiOH and H₃SiOSiH₃ structure parameters computed at different levels of theory. It is clearly seen that BLYP/6-311G* and MP2/6-31G* levels yield basically the same results, which are also close to the more accurate CPF structure given in Table 1.

Silanol

Bond lengths involving OH are consistently longer than CPF values (97.0 (BLYP), 96.8 (VWN), and 95.8 pm (CPF)). The DFT results are in good agreement with MP2/6-31G* (96.9 pm). For the Si-O bond length VWN/6-311G* yields a virtually identical value to CPF, while the corresponding value at the BLYP/6-311G* level is 2.3 pm too long. Si-O-H bond angles calculated with both DFT procedures compare well with MP2 and CPF results (119.6°, 118.6°, 116.4°, and 117.7° at the VWN, BLYP, MP2 and CPF levels, respectively).

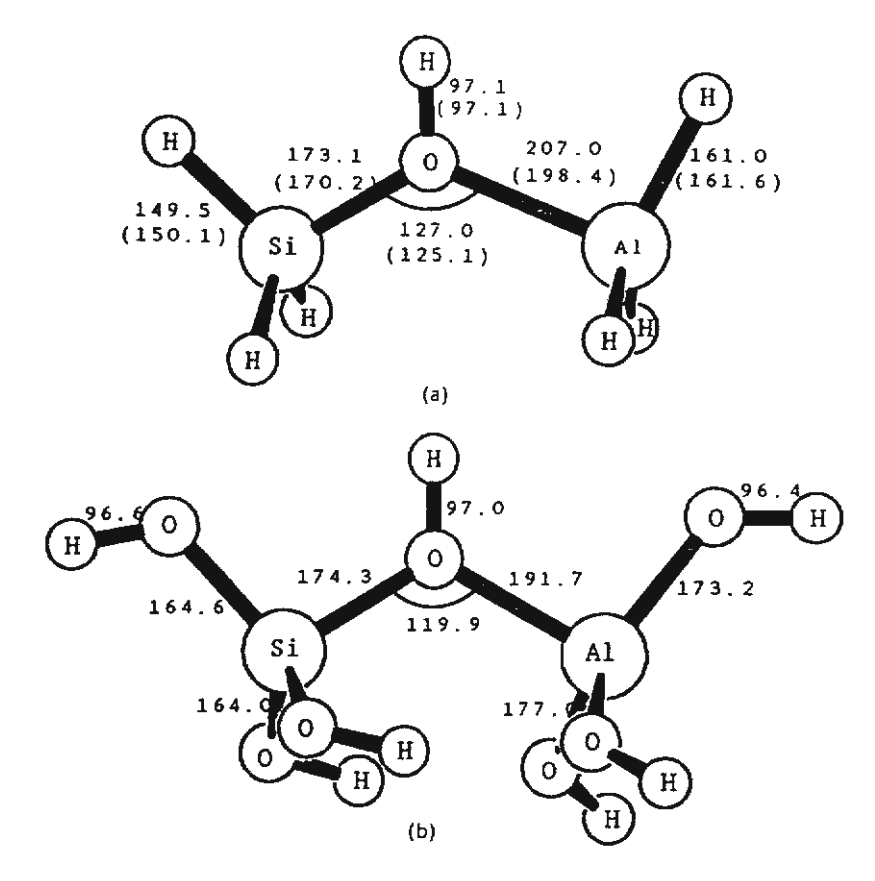
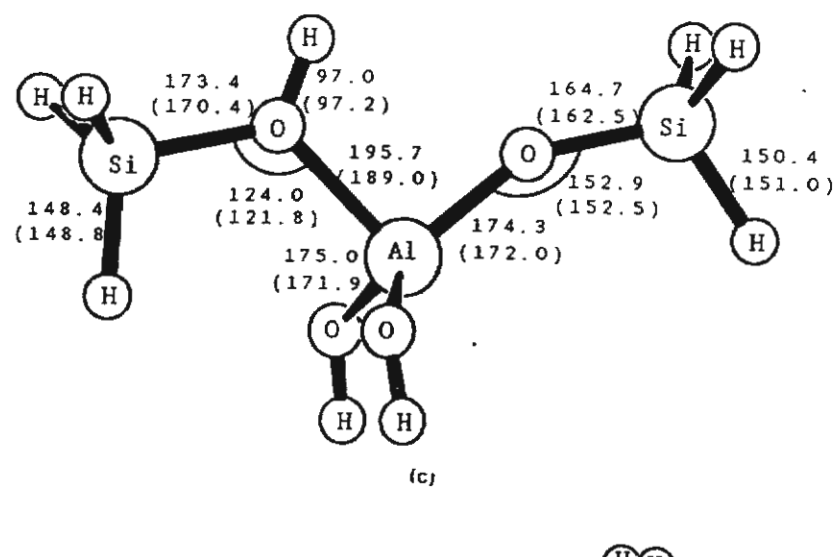


Fig. 1. Schematic representation of molecular models optimized at BLYP/6-311G* and VWN/6-311G* (values in parentheses) for (a) H₃SiOHAlH₃, (b) (OH)₃SiOHAl(OH)₃, (c) H₃SiOHAl(OH)₂OSiH₃, and (d) H₃SiOHAl(OSiH₃)₂OSiH₃.

Table 5
Computed OH bond lengths, proton affinities (kJ mol⁻¹), and vibrational frequencies (cm⁻¹) at the VWN and BLYP levels of theory for H₃SiOHAl(OH)₂OSiH₃ and H₃SiOHAl(OSiH₃)₂OSiH₃

| Cluster model | Basis set | r _{OH} (pm) | r _{OH} (pm) | | P.A. (kJ mol ⁻¹) | | |
|--|-----------|----------------------|----------------------|--------|------------------------------|--------|--------|
| | | VWN | BLYP | VWN | BLYP | vwn | BLYP |
| H ₃ SiOHAlH ₃ | 3-21G | 99.5 | 99.7 | 1333.5 | 1343.0 | 3550.0 | 3488.6 |
| 3 | 6-31G* | 98.1 | 97.9 | 1295.5 | 1323.3 | 3671.3 | 3662.7 |
| | 6-311G* | 97.1 | 97.1 | 1282.7 | 1307.9 | 3789.8 | 3757.0 |
| | DZVP | 98.2 | 98.2 | 1284.0 | 1314.1 | 3693.7 | 3660.4 |
| H ₃ SiOHAl(OH) ₂ OSiH ₃ | 3-21G | 99.3 | 99.4 | 1371.8 | 1382.4 | 3610.9 | 3516.0 |
| | 6-31G* | 97.8 | 97.8 | 1302.5 | 1324.0 | 3780.3 | 3720.8 |
| | 6-311G* | 97.2 | 97.0 | 1296.9 | 1316.2 | 3873.1 | 3812.9 |
| | DZVP | 98.0 | 1.89 | 1281.9 | 1310.4 | 3841.1 | 3749.4 |
| H2SiOHAl(OSiH3)2OSiH3 | 3-21G | 100.2 | 99.9 | 1305.7 | 1319.3 | 3455.0 | 3451.3 |
| 2 (3/2 3 | 6-31G* | 98.1 | 98.0 | 1253.6 | 1272.5 | 3675.2 | 3653.4 |
| | 6-311G* | 97.4 | 97.4 | 1242.3 | 1261.9 | 3702.6 | 3683.7 |
| | DZVP | 98.3 | 98.2 . | 1244.4 | 1264.9 | 3655.3 | 3647.6 |



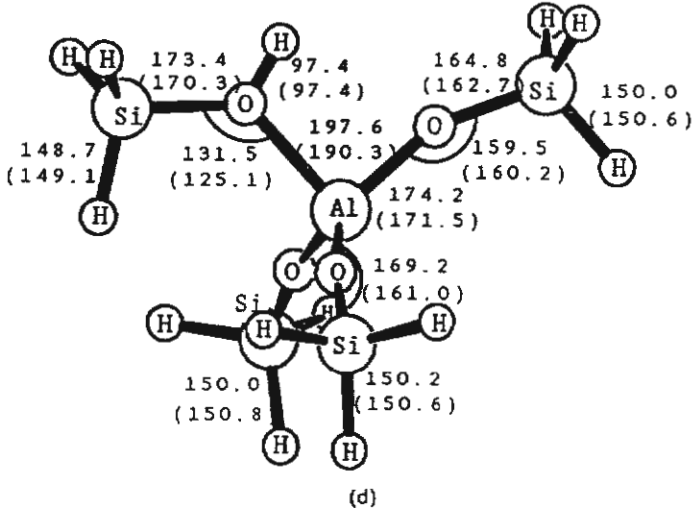


Fig. 1. Continued.

Disiloxane

For H₃SiOSiH₃, the computed Si-O bond lengths are 166.4 pm (BLYP/6-311G*) and 165.1 pm (VWN/6-311G*), which are in good agreement with the results of 166.0 pm at the MP2/6-31G* and 164.8 pm at the CPF level. However, the VWN Si-O-Si bond angles are too small by about 18° when compared to the CPF result. In contrast with this discouraging result, the BLYP/6-311G* approach yields of 150.0° which is close to the MP2/6-31G* (143.7°) and the most reliable

CPF angle of 151.6°, as well as experimental data (\approx 144°) [30].

Zeolites

A systematic deviation in bond lengths can be observed with different methods for H₃SiOHAlH₃ (see Figs. 2(a)-2(c) and Table 2). Bond lengths concerning hydroxyl O-H calculated at both the DFT-VWN/6-311G* and DFT-BLYP/6-311G* levels are comparable to those computed at the MP2/6-31G* level. The deviation for the O-H

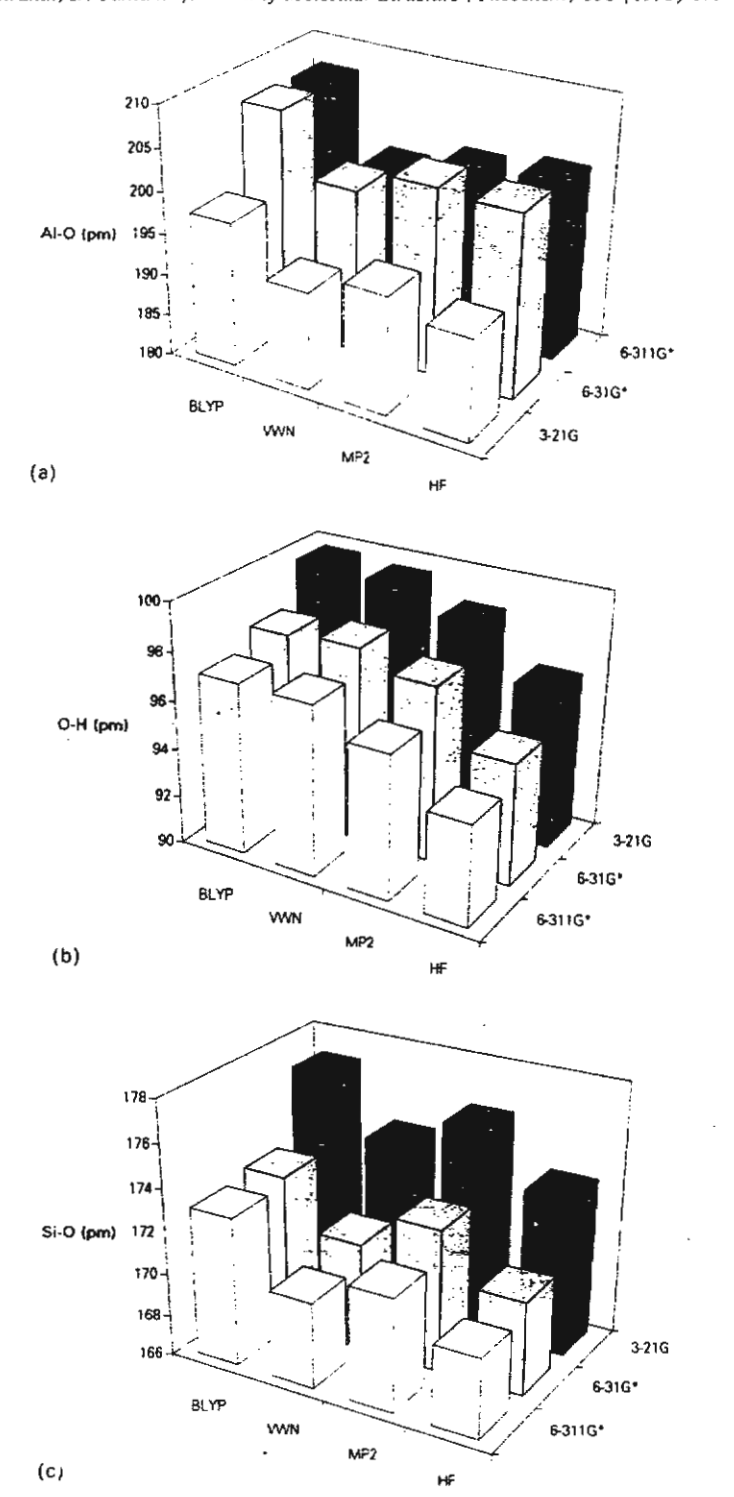


Fig. 2. Optimized parameters — (a) Al-O, (b) O-H. (c) Si-O, (d) Si-O(H)-Al and (e) Si-O-H — for the molecular model H_3 SiOHAl H_3 at the BLYP, VWN, MP2 and HF levels.

J. Limtrakul, D. Tantanak/Journal of Molecular Structure (Theochem) 358 (1995) 179-193

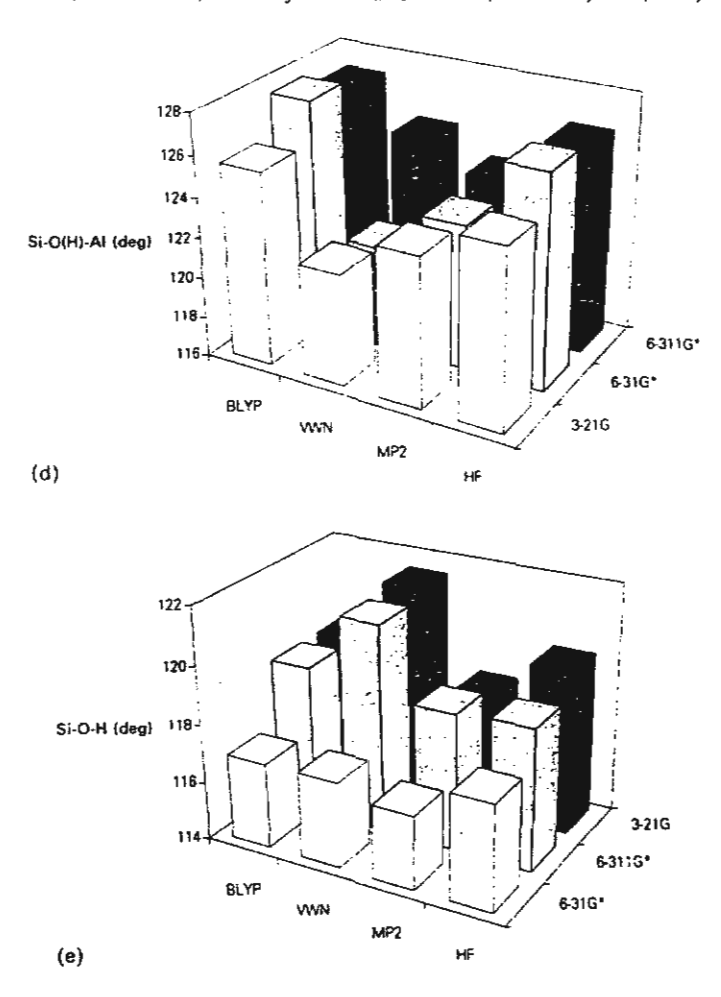


Fig. 2. Continued.

bond length is 1.1 pm at both the DFT-VWN/6-311G* and DFT-BLYP/6-311G* levels, as compared to the MP2/6-311G* level. Inclusion of NLSD has little effect on the O-H and Si-O bonds, but this is not the case for the weaker Al-O bonds: the Si-O, and Al-O bonds are lengthened by 2.9 and 8.7 pm, respectively. At the DFT-VWN/6-311G* level, the OH, Si-O and Al-O bond lengths are 97.1, 170.2 and 198.4 pm, respectively, which are in very good agreement with those determined at the MP2/6-31G* level; the corresponding MP2 values are 97.3, 172.8 and 202.6 pm.

Bond angles calculated at both the DFT/VWN and DFT/BLYP levels are in good agreement with those computed at the MP2 level (see Figs. 2(d)-

2(e)). At the DFT-BLYP/6-311G* level, maximum deviations of 3.2° and 0.5° are calculated for the bond angles of Si-O(H)-Al and Si-O-H, respectively. The corresponding deviation values using DFT-VWN/6-311G* are 1.3° and 2.5°.

There is little effect on the Si-O and Al-O bond lengths, and Si-O-Al and Si-O-H bond angles on going from the DFT-BLYP/6-31G* to the DFT-BLYP/6-31IG* level. The same corresponding effect is also observed for the DFT-VWN procedure. However, the bond lengths involving hydrogen atoms, especially the O-H bond, exhibit large deviations: 98.1 vs. 97.1 pm (at VWN/6-31G* and VWN/6-31IG*, respectively) and 97.9 vs. 97.1 pm (at BLYP/6-31G* and BLYP/6-31IG*, respectively). This implies that at least a 6-311G* basis

J. Limtrakul, D. Tantanak/Journal of Molecular Structure (Theochem) 358 (1995) 179-193

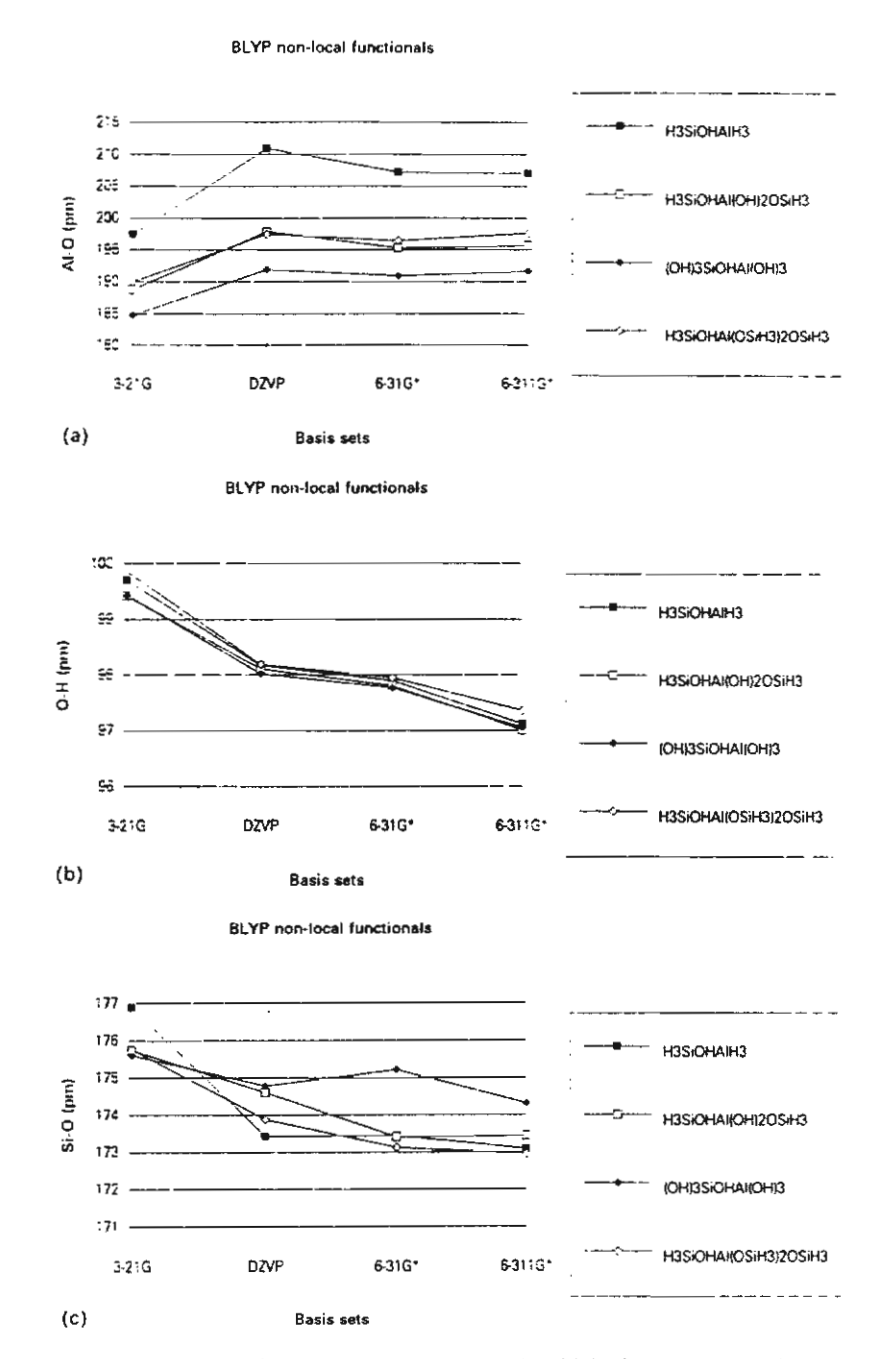


Fig. 3. Variation of calculated (a) Al-O, (b) O-H and (c) Si-O bond lengths with basis sets at the BLYP non-local density functional level.

J. Limtrakul, D. Tantanak/Journal of Molecular Structure (Theochem) 358 (1995) 179-193

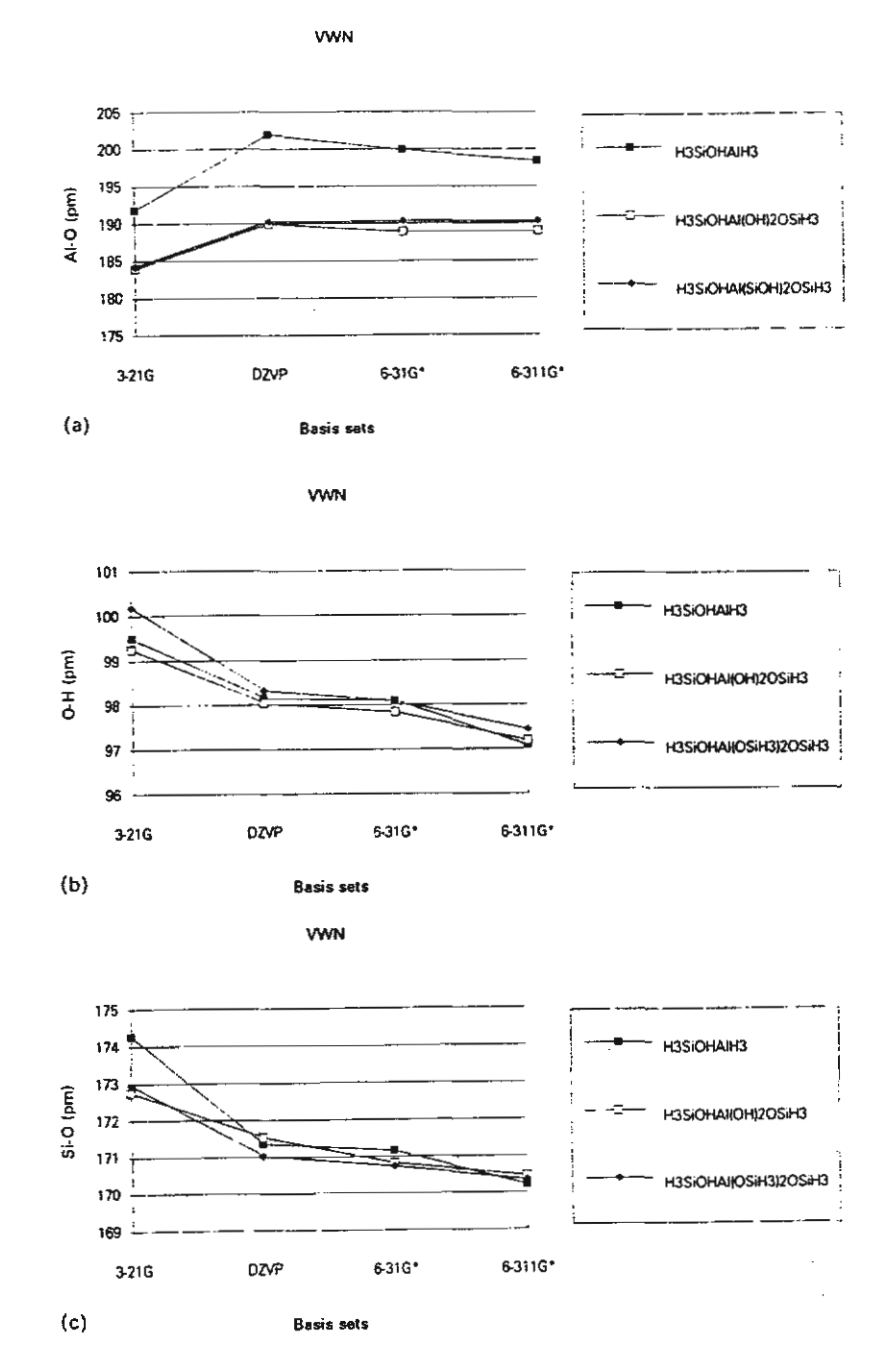


Fig. 4. Variation of calculated (a) Al-O, (b) O-H and (c) Si-O bond lengths with basis sets at VWN local density functional level.

set is required for the system involving hydrogen bonding.

Considering Tables 3 and 4, it is clearly seen that H₃SiOHAl(OSiH₃)₂OSiH₃ provides a better model than the widely employed H₃SiOHAlH₃. The smallest model yields an Al-O bond length that long compared with that of H₃SiOHAl(OSiH₃)₂OSiH₃. On increasing the level of basis set from 3-21G to 6-31G* to 6-311G*, the Al-O bond lengths of the cluster models increase whereas the Si-O and O-H bond lengths decrease, as shown in Figs. 3 and 4. The results obtained with the 6-311G* basis sets show that the Al-O bond lengths are contracted by 9.4 and 8.1 pm at the BLYP and VWN levels, respectively, while the Si-O bond lengths of these methods are almost identical upon expanding the model from H₃SiO(H)AlH₃ to H₃SiOHAl-(OSiH₃)₂OSiH₃ (see also Tables 3 and 4).

Further support for the reliability of using the $H_3SiOHAl(OSiH_3)_2OSiH_3$ unit in computations is given by the results of NMR studies: the Al··H distance of H-faujasite has been estimated to be $238 \pm 4 \,\mathrm{pm}$ [1], when our computed distances of $H_3SiOHAl(OSiH_3)_2OSiH_3$ are 244.0 and 241.0 pm (at the BLYP/6-311G* and VWN/6-311G* level, respectively), whereas the corresponding distances of $H_3SiO(H)AlH_3$ are 261.7 and 253.5 pm (at BLYP/6-311G* and VWN/6-311G*, respectively).

Tables 3 and 4 also give other important parameters, including the O-H distance which plays an important role in catalytic properties. The hydroxyl O-H bond length obtained from a neutron diffraction study of acidic faujasite [31,32] was $100 \pm 20 \,\mathrm{pm}$. It should be noted that for H₃SiOHAl(OH)₂OSiH₃ our BLYP/6-311G* OH bond length was calculated to be 97.0 pm, which is in very good agreement with the recent MP2/DZP result of 96.8 pm [33].

In order to observe changes in structure and bonding on going from the anionic framework site to Brønsted acid site, the anionic clusters were also computed at the 3-21G, 6-31G* and 6-311G* levels of theory. In the following discussion, we refer to the BLYP results obtained with the largest basis set, 6-311G*. Removal of a proton from the protonated cluster of H₃SiOHAl-

(OSiH₃)₂OSiH₃ strengthens the Si-O(H) and Al-O(H) bonds (173.0 pm vs. 160.6 pm for Si-O(H), and 197.6 pm vs. 174.8 pm for Al-O(H). The Si-O-Al angle (148.2°) in the deprotonated cluster is larger (by 16.7°) than the Si-O(H)-Al angle (131.5°) at the bridging hydroxyl site. The average Al-O bond length of the four Al-O bonds of the protonated form was calculated to be 179.9 pm, whereas for the anionic framework it was found to be 174.4 pm, which is in good agreement with the available experimental value of 174.5 pm determined by X-ray diffraction measurement of the zeolite [34].

3.2. Proton affinities

Proton affinities of Brønsted hydroxyl in zeolites can be used as a basis for the activity of catalysts in catalytic processes.

We can evaluate the performance of the DFT procedure in predicting gas phase proton affinities by comparison with highly reliable theoretical values of G1 and coupled pair functional levels. All calculated proton affinities at different basis sets for different cluster models are documented in Table 5.

Silanol

The calculated VWN/6-311G* and BLYP/6-311G* proton affinities are evaluated to be 1495.2 and 1520.4 kJ mol⁻¹. It can be seen that NLSD performs perfectly well at the BLYP/6-311G* level, which is in good agreement with the CPF (1521 kJ mol⁻¹) [27] and G1 (1490.3 kJ mol⁻¹) [28,29] results.

Zeolites

The BLYP proton affinities of zeolites are reduced on passing from 3-21G to 6-311G*, as shown in the following (VWN results in parentheses): 35.1 (50.8) kJ mol⁻¹ for H₃SiO(H)AlH₃, 66.2 (74.9) kJ mol⁻¹ for H₃SiOHAl(OH)₂OSiH₃ and 57.4 (63.4) kJ mol⁻¹ for H₃SiOHAl-(OSiH₃)₂OSiH₃. The improvement on going from 3-21G to 6-311G* is quite large, with a maximum difference of 75 kJ mol⁻¹.

The result of the proton affinity for the H₃SiOAlH₃ molecule with BLYP/6-311G* is also

encouraging. The deviation from the most accurate G1 [29,30] is about 12 kJ mol⁻¹. The MP2/6-31G* proton affinity yields a virtually identical value to the less expensive BLYP result (1307.9 kJ mol⁻¹ (MP2) vs. 1307.9 kJ mol⁻¹ (BLYP)). DFT results may be further improved by enlarging the basis to a size comparable to 6-311 + G (3df,2p) in order to obtain a deviation within the desired 10 kJ mol⁻¹ accuracy from experimental data.

For H₃SiOHAl(OH)₂OSiH₃, the BLYP/6-311G* yields a value 2kJ mol-1 lower than MP2/ DZP [33]. This agreement reflects the similar computed OH bond lengths at both levels of theory (96.8 pm (MP2) vs. 97.1 pm (BLYP)). It is also important to study the dependence of proton affinities on the employed cluster size. On expanding the model cluster from H₃SiOHAlH₃ to H₃SiOHAl(OSiH₃)₂-OSiH₃, the proton affinities are decreased by 40 and 46 kJ mol-1 with the LSD and NLSD procedures, respectively. For the largest model of our work, the proton affinities are calculated to be 1242 and 1262 kJ mol⁻¹ with LSD and NLSD, respectively. Using the systematic deviations between DFT and G1 theory, our predicted value is estimated to be 1215 kJ mol-1, which is in the range of experimentally determined values of 1180-1333 kJ mol⁻¹ [35,36]. The calculated AM1 proton affinity of Si₄₇AlO₁₁₄H₃₇, which is by far the largest zeolite cluster, is estimated to be 1295 kJ mol⁻¹ [37]. In order to properly study the acidity of the bridging hydroxyl group in zeolites, such a modestly-sized cluster model of H₃SiOHAl(OSiH3)₂-OSiH₃ at least is needed.

3.3. Vibrational frequencies

It has been noted previously by Pople et al. [38] that the frequencies obtained at the HF and MP2 levels using the 6-31G* basis set have been found to yield vibrational frequencies that are about 12% and 6% too high, respectively, on average compared with the experimentally observed frequencies.

It is one of our aims to evaluate the performance of DFT procedures in predicting vibrational frequencies, ν_{OH} . The ν_{OH} of zeolites increases with the size of the basis functions (see Table 5). The improvement on going from 3-21G to

6-311G* is quite large, with a maximum of 297 cm⁻¹.

Silanol

The VWN and BLYP OH frequencies, $\nu_{\rm OH}$, of 3807.2 and 3751.3 cm⁻¹ are in agreement with MP2/6-31G* calculations (3841.6 cm⁻¹). They are also in agreement with the Morse MP2 OH stretching frequency of Bates and Dwyer [39] (3818 cm⁻¹). The HF/6-31G* $\nu_{\rm OH}$ of 4148 cm⁻¹ is 306 cm⁻¹ higher than the MP2/6-31G* value. This is due partly to the neglect of electron correlation.

Zeolites

The VWN and BLYP OH frequencies, ν_{OH} , of H₃SiOHAlH₃ are 3789.8 and 3757.0 cm⁻¹, respectively. Andrews and Handy [40] have recently presented harmonic vibrational frequencies of this molecule at MP2/DZP. Their ν_{OH} is $3800 \, \text{cm}^{-1}$, in agreement with our results. The DFT result is about 300 cm⁻¹ lower than the SCF/6-31G* result reported by Fleischer et al. [41]. Their calculation at this level is 4090 cm⁻¹ which is known to yield an overly high voh. Calculations of the vibrational frequencies of all cluster models of zeolites employed here indicated that ν_{OH} are located in the region 3683-3757 cm⁻¹, which can be compared to the range of experimentally determined values of 3520-3630 cm⁻¹. It is well known that the observed von depends on the number of aluminium atoms and the distribution of the ≡SiOHAl≡ groups in the zeolite framework [42]. With the aim of quantifying the quality of the DFT data for zeolite clusters, we have compared our results with the most recent experimental data [43]. The maximum deviation occurs in the case of H₃SiO(H)Al(OH)₂OSiH₃. If we consider the relative error, we find for our models a deviation of 2-5% from the experimental data depending on the models employed. In the case of closest agreement, a deviation of less than 2% is derived for H₃SiO(H)Al(OSiH₃)₂OSiH₃ at the BLYP level, compared to experimental results.

4. Conclusions

We have carried out LSD and NLSD functional

methods with 3-21G, 6-31G*, 6-311G*, and DZVP basis sets to investigate the structures, energetics, and vibrational frequencies for silanol, disiloxane, and different zeolite clusters. Some smaller models have also been calculated at the MP2 level. The individual geometrical parameters calculated at the BLYP and VWN levels with a modestly-sized basis set (6-311G*) generally yield good results compared to MP2 with much less computational effort. Comparing BLYP and VWN results with MP2, the former has a significant lengthening effect on the weaker A-O bond which does not occur with the latter. The Si-O(H)-Al and Si-O-H bond angles of zeolites are not appreciably affected by the inclusion of NLSD. However, the NLSD was found to be important for a better description of the floppy Si-O-Si bond angle for disiloxane. The proton affinity of H₃SiOHAlH₃, a widely employed model of a Brønsted acid site in zeolites, is virtually identical to that of MP2/DZP and is also close to the result from G1 theory within the desired 10 kJ mol-1 accuracy. For this cluster model, the BLYP ν_{OH} value is calculated to within 130 cm⁻¹ of the experimental value. We expect that the same accuracy from the BLYP/6-311G* procedure will be applied to larger zeolite clusters in the future.

Acknowledgement

This work was supported by donors of the Thailand Research Fund (TRF) the Kasetsart University Research and Development Institute (KURDI), and through a grant of CPU time by the National High Performance Computing Center (NHPCC) of the NECTEC. Our sincere thanks are due to Professor R. Ahlrichs (Karlsruhe, Germany) for his continued support of this work. We thank Drs. Fitzgerald and Kasren for technical assistance in using UNICHEM codes. We also thank the staff of the NHPCC of NECTEC for their assistance.

References

[1] J. Klinowski, Chem. Rev., 91 (1991) 1459.

- [2] J.M. Thomas, Sci. Am., 266 (1992) 82.
- [3] G.J. Kramer, R.A. Van Santen, C.A. Emeis and A.K. Nowak, Nature, 363 (1993) 529.
- [4] E. Kassab, J. Fouquet, M. Allavena and E.M. Evleth, J. Phys. Chem., 97 (1993) 9034.
- [5] C.T.W. Chu and C.D. Chang, J. Phys. Chem., 89 (1985) 1569.
- [6] K.J. Chao and L.J. Len, in H.G. Karge and J. Weitkamp (Ed.), Zeolites as Catalysts, Sorbents and Detergent, Builders, Elsevier, Amsterdam, 1989.
- [7] J. Das, C.V.V. Satyanaryana, D.K. Chakrabarty, S.N. Piramanayagarn and S.N. Shringi, J. Chem. Soc., Faraday Trans., 88 (1992) 3255.
- [8] Y. Murakami, A. Iijima and J.W. Ward, New Developments in Zeolite Science and Technology, Kodancha, Tokyo, 1986.
- [9] J. Limtrakul and S. Pullman-Hannongbua, J. Mol. Struct. (Theochem), 280 (1993) 139.
- [10] J. Limtrakul, J. Mol. Struct., 288 (1993) 105.
- [11] J. Limtrakul and J. Yoinuan, Chem. Phys., 184 (1994) 51.
- [12] J. Limtrakul, J. Yoinuan and D. Tantanak, J. Mol. Struct., 312 (1994) 183.
- [13] J.W. Andzelm and J.K. Labanowski (Eds.), Density Functional Methods in Chemistry, Springer-Verlag, New York, 1991.
- [14] R.D. Amos, C.W. Murray and N.C. Handy, Chem. Phys. Lett., 202 (1993) 487.
- [15] N.C. Handy, P.E. Maslen, R.D. Amos, J.S. Andrew, C.W. Murray and G.I. Laming, Chem. Phys. Lett., 197 (1992) 506.
- [16] F. Sim, A. St-Amant, I. Papai and D.R. Salahub, J. Am. Chem. Soc., 114 (1992) 4391.
- [17] D.A. Dixon, J. Andzelm, G. Fitzgerald and E. Wimmer, J. Phys. Chem., 95 (1991) 9197.
- [18] J. Andzelm, E. Rodzio and D.R. Salahub, J. Comput. Chem., 6 (1985) 520.
- [19] (a) Dgauss is part of the Unichem system of program available from Cray Research Inc., Unichem 2.3, Cray Research Inc., Eagan, MN, (1994).
 (b) J. Andzelm and E. Wimmer, J. Chem. Phys., 96 (1992)
- [20] S.H. Vosko, L. Wilk and M. Nuisar, Can. J. Phys., 58 (1980) 1200.
- [21] A.D. Becke, Phys. Rev. A, 38 (1988) 3098.

1280.

- [22] C. Lee, W. Yang and R.G. Parr, Phys. Rev. B, 37 (1988)
- [23] N. Godbout, D.R. Salahub, J. Andzelm and E. Wimmer, Can. J. Chem., 70 (1992) 560.
- [24] R. Ahirichs, R. Baer, M. Haeser, H. Horn and C. Koemel, Chem. Phys. Lett., 162 (1989) 165.
- [25] J. Almloef, K. Faegri, Jr., and K. Korsell, J. Comput. Chem., 3 (1982) 385.
- [26] M. Haeser and R. Ahlrichs, J. Comput. Chem., 10 (1989) 104.
- [27] J. Sauer and R. Ahlrichs, J. Chem. Phys., 93 (1990) 2575.
- [28] J.A. Pople, M. Head-Gordon, D. Fox, K. Raghavachari and L.A. Curtiss, J. Chem. Phys., 90 (1989) 5622.

- [29] L.A. Curtiss, C. Jones, G.W. Trucks, K. Roghavachari and J.A. Pople, J. Chem. Phys., 93 (1990) 2537.
- [30] M. Ito, Y. Shimoyama and Y. Saito, Acta Crystallogr., Sect C, 41 (1985) 1698.
- [31] A.K. Cheetham, M.M. Eddy and J.M. Thomas, J. Chem. Soc., Chem. Commun., (1988) 1337.
- [32] M. Eddy, D. Phil. Thesis, University of Oxford, 1984.
- [33] J. Sauer, P. Ugliengo, E. Garrone and V.R. Sounders, Chem. Rev., 94 (1994) 2095.
- [34] J.J. Pluth and J.V. Smith, J. Am. Chem. Soc., 102 (1980) 4704.
- [35] J. Datka, M. Boczar and P. Rymarowicz, J. Catal., 114 (1988) 368.

- [36] J. Datka, M. Boczar and B. Gil, Langmuir, 9 (1993) 2496.
- [37] J. Limtrakul and D. Tantanak, in preparation.
- [38] J.A. Pople, W.J. Hehre, L. Radom and P.V.R. Schleyer, Ab initio Molecular Orbital Theory, Wiley, New York, 1991.
- [39] Bates and J. Dwyer, Chem. Phys. Lett., 225 (1994) 427.
- [40] J. Andrews and N.C. Handy, unpublished work, 1989.
- [41] U. Fleischer, W. Kutzelnigg, A. Bleiber and J. Sauer, J. Am. Chem. Soc., 115 (1993) 7833.
- [42] J. Limtrakul, J. Yoinuan and D. Tantanak, J. Mol. Struct., 332 (1995) 151.
- [43] M.A. Makaroma, K.M. Al-Ghefaili and J. Dwyer, J. Chem. Soc., Faraday Trans., 90 (1994) 383.

Reprinted from

Chemical Physics

Chemical Physics 208 (1996) 331-340

Cationic, structural, and compositional effects on the surface structure of zeolitic aluminosilicate catalysts

Jumras Limtrakul*, Duangkamol Tantanak

Laboratory for Computational and Applied Chemistry, Chemistry Department, Faculty of Science, Kasetsart University, Bangkok 10900, Thailand





Chemical Physics 208 (1996) 331-340

Chemical Physics

Cationic, structural, and compositional effects on the surface structure of zeolitic aluminosilicate catalysts

Jumras Limtrakul*, Duangkamol Tantanak

Laboratory for Computational and Applied Chemistry, Chemistry Department, Faculty of Science, Kasetsart University,
Bangkok 10900, Thailand

Received 28 January 1996

Abstract

The cationic, structural, and compositional influences on the structure and bonding of zeolitic aluminosilicates have been investigated with the density functional theory (DFT) method including local (VWN) and non-local spin density functionals (BLYP). Full optimization of structures has been carried out at the 6-31G */WWN and 6-31G */BLYP levels of theory for the different types of the =Si-OH-Al= unit in the secondary building unit of the zeolite cluster models $[(OH)_8H_vAl_rSi_{8-x}O_{12}]^{(x-y)-}$ (x, y = 0, 1, 2, 4) and the silica model (OH)₈Si₈O₁₂. Changes in the environment of the silicon and aluminium framework atoms with a given Si/Al ratio generate new different acid sites. The validity of Loewenstein's = Al-O-Al= avoidance rule is confirmed but Dempsey's = Al-O-Si-O-Al= avoidance rule does not hold with double four-membered ring aluminosilicate (D4R). The proton affinity (PA) of the silica model (OH)₈Si₆O₁₂ at BLYP/6-31G* are evaluated to be 1403 ± 15 kJ/mol which is in good agreement with the experimentally observed value of 1390 ± 25 kJ/mol. Proton affinities of Brønsted hydroxyl groups in H forms of zeolites associated with different Si/Al ratios indicate that the higher the ratio, the less the proton is constrained which results in a stronger acid strength. Cations are found to have profound effects on the structure and bonding of zeolite clusters. The H ion has a strong perturbation on the important parameters i.e. Si-O, Al-O, OH bond lengths while the Li(I) has a modest effect. The PA of the Brønsted OH groups in the zeolitic frameworks interacting with their cations are 1272.4 and 1279.3 kJ/mol for H₂(OH)₈Al₂Si₆O₁₂ and LiH(OH) Al 2Si O12, respectively, which correspond with decreasing bond lengths of the OH groups. These results indicate that the acid strength of the OH groups within the zeolitic framework is also determined by the presence of cations, in addition to compositional and structural effects.

1. Introduction

Zeolites are porous frameworks of crystalline aluminosilicates with a number of interesting physical and chemical properties. The hydroxyl groups in zeolites are of primary significance for the catalytic properties and have led to numerous industrially

important applications, such as adsorbents and catálysts [1-10].

The performance of zeolitic catalysts depends on the framework composition (the Si/Al ratio) and the framework topology (the environment of the Si and Al atoms)

The widely utilized primary building unit [11-15] H₃SiOHAlH₃ is too limited to investigate the effects mentioned above. The two-site binding model of

^{*} Corresponding author.

H₃Si-OH-Al(OH)₂-O-SiH₃ [16-21], which can be employed for studying the details of interaction with the adsorbed molecules i.e. H₂O, NH₃ and methanol still involves two Si tetrahedra and only one Al tetrahedron. Important information of the nature, the strength and the number of acid sites is limited if a small cluster is employed for modelling.

Extension of the cluster model from H₃SiOHAlH₃ over H₃SiOHAl(OH)₂OSiH₃ to more realistic models of double four-membered rings (D4R) should therefore permit us to investigate the cationic and compositional effects on the surface structure of zeolite aluminosilicate catalysts.

Recently the density functional theory (DFT) has been employed to investigate various chemical systems [22-27]. Not only does it require much less computational effort, but also the DFT results are very encouraging when compared with high level ab initio calculations and more reliable experimental data [27]. This leads to the utilization of DFT approaches for large chemical systems.

To the best of our knowledge, no systematic investigations of the cationic, structural, and compositional effects on the structure and bonding of zeolitic cluster models have been carried out by DFT employing both local (LSD) and non-local density (NLSD) approximations. In addition to the DFT calculations, smaller models have been studied at HF and MP2 levels.

2. Methods and computational details

Full geometry optimization of the zeolitic cluster models H₃SiOHAlH₃, H₃SiOHAl(OH)₂-OSiH₃, as well as the more realistic models of double four-membered rings (D4R: (OH)₈Si₈O₁₂, (OH)₈Si₇AlOXO₁₁, (OH)₈Si₆Al₂OHXO₁₁, (OH)₈Si₄Al₄H₄O₁₂, where X represents H⁺ and Li⁺, was carried out with the density functional theory methods.

All density functional computations were carried out by the DGAUSS program [28] implemented to run on the Cray-YMP EL98 at the NECTEC High Performance Computing Center.

Two different exchange correlation functionals were selected for this investigation, namely the LDA and BLYP functionals. For local density approximation (LDA) we employed the Vosko-Wilk-Nusair

(VWN) correlation function [29]. It is generally believed that the VWN potential represents one of the best analytical functional forms currently available for LSD potentials. Gradient-type corrections have been included self-consistently using the non-local functions of Becke exchange [30] and the Lee, Yang and Parr [31] correlation (BLYP). Studies [32,33] have shown that these functionals yield harmonic frequencies with mean absolute errors less than those of MP2 and produce respectable geometries.

All cluster models mentioned above have been computed with 6-31G* basis sets. Additionally, to minimize the basis set superposition error (BSSE) and to improve the quality of valence orbitals, the recommended LSD-optimized orbital basis sets [34] were also employed. The following orbitals were employed: (41) for the hydrogen atom, (621/41/1) for the oxygen atom, and (6321/521/1) for Si and Al atoms. The following auxiliary basis sets were used: [4] for the hydrogen atom, [7/3/3] for the oxygen atom, and [9/4/4] for Al and Si atoms. These LSD-optimized orbital basis sets can be considered as double-zeta split valence plus polarization (DZVP) basis sets.

For the ab initio calculations we employed the TURBOMOLE program, which is based on the direct SCF method of Almloef et al. [35-37]. The two-electron repulsion integrals are recomputed when needed, rather than being kept. In order to obtain zeolite structures at a (more reliable) higher level of theory some models, e.g. the primary building unit H_3 SiOHAl H_3 , are also evaluated at the correlated level of theory. Geometry optimization was terminated when the gradient norm with respect to the internal coordinates was less than $10^{-3} E_h a_0^{-1}$. The energy change was then below $5 \times 10^{-6} E_h$. All SCF and MP2 calculations were carried out on the HP 700 cluster at the Laboratory for Computational and Applied Chemistry at Kasetsart University.

3. Results and discussion

3.1. Comparison of density functional theory and post-Hartree-Fock results with experimental results

The different types of $\equiv Si-O(H)-Al \equiv$ units in the double four-membered ring of the zeolite frame-

Table I
Optimized parameters for H₃SiOH, H₃SiOSiH₃ and H₃SiOHAlH₃ at various methods

| Model | Method | Basis | Si-O | AI-O | O-H | Si-O-Si | Si-O-Al | Si-O-H |
|-------------------------------------|--------|------------|-------|-------|-------|---------|----------------|---------|
| I C'OU DI VI | set | (pm) | (pm) | (pm) | (deg) | (deg) | (deg) | |
| H,SiOH | BLYP | 6-31G * | 168.2 | | 97.7 | | ** | 114.3 |
| - | | 6-311G* | 167.3 | - | 97.0 | _ | - | 118.6 |
| | | DZVP | 168.6 | _ | 97.8 | _ | _ | 116.0 |
| | VWN | 6-31G* | 165.8 | _ | 97.6 | - | _ | 115.1 |
| | | 6-311G* | 164.9 | _ | 96.8 | - | _ | 119.6 |
| | | DZVP | 166.1 | - | 97.7 | _ | _ | 117.0 |
| | MP2 | 6-31G * | 167.2 | | 96.9 | - | _ | 116.4 |
| | | 6-311G* | 165.5 | - | 95.6 | _ | _ | 121.7 |
| | HF | 6-31G ° | 164.7 | | 94.6 | _ | - | 119.0 |
| | | 6-311G* | 163.6 | - | 93.7 | _ | _ | 124.2 |
| | CPF | extended * | 165.0 | _ | 95.8 | - | _ | 117.7 |
| H ₃ SiOSiH ₃ | BLYP | 6-31G* | 166.7 | _ | - | 148.4 | _ | _ |
| | | 6-311G* | 166.4 | - | - | 150.0 | - | _ |
| | | DZVP | 167.5 | | - | 140.3 | _ | _ |
| | VWN | 6-31G* | 165.0 | - | - | 137.8 | - | |
| | | 6-311G* | 165.1 | - | - | 132.1 | - | _ |
| | | DZVP | 164.7 | - | - | 149.1 | _ | - |
| | MP2 | 6-31G ° | 166.0 | _ | _ | 143.7 | . . | _ |
| | | 6-311G* | 164.3 | _ | - | 155.7 | · - | _ |
| | HF | 6-31G " | 162.7 | _ | - | 166.4 | _ | |
| | | 6-311G* | 162.0 | _ | - | 0.081 | _ | _ |
| | CPF | extended * | 164.8 | _ | _ | 151.6 | - | _ |
| H ₃ SiOHAIH ₃ | BLYP | 6-31G* | 173.4 | 207.1 | 97.9 | - | 127.6 | 116.9 |
| _ | | 6-311G* | 173.1 | 207.0 | 97.1 | - | 127.0 | 119.2 |
| | | DZVP | 173.4 | 210.9 | 98.2 | - | 131.0 | 115.7 |
| | VWN | 6-31G * | 171.2 | 199.8 | 98.1 | - | 121.1 | 116.9 |
| | | 6-311G * | 170.2 | 189.4 | 97.1 | - | 125.1 | 121.2 |
| | | DZVP | 171.4 | 201.8 | 98.2 | _ | 121.9 | 117.7 |
| | MP2 | 6-31G * | 172.8 | 202.6 | 97.3 | - | 123.3 | 116.5 |
| | | 6-311G* | 171.5 | 200.6 | 96.0 | - | 123.8 | · 118.7 |
| | HF | 6-31G* | 170.6 | 202.2 | 95.1 | _ | 126.7 | 117.6 |
| | | 6-311G* | 169.9 | 201.5 | 94.2 | - | 126.2 | 118.9 |

 $^{^{2} = [8}s,5p,3d,1f/4s,2p].$

Table 2
BLYP optimized parameters computed for H₃SiOAlH₃, H₃SiOHAlH₃, H₃SiOHAKOH)₂OSiH₃ and D4R cluster models and their complexes with ions

| BLYP/6-31G* | | | | | | | | | |
|--|-----------|-----------|----------|----------|---------------|--------------|--|--|--|
| System | Si-O (pm) | Al-O (pm) | O-H (pm) | AlH (pm) | Si-O-Al (deg) | Si-O-H (deg) | | | |
| H ₃ SiOAIH ₃ | 163.0 | 184.5 | _ | _ | 127.1 | _ | | | |
| H ₃ SiOHAIH ₃ | 173.4 | 207.1 | 97.9 | 258.2 | 127.6 | 116.9 | | | |
| H ₃ SiOLiAIH ₃ | 167.5 | 190.6 | 178.5 * | 170.3 | 128.6 | 142.3 | | | |
| H ₃ SiOHAl(OH) ₂ OSiH ₃ | 173.4 | 195.3 | 97.8 | 251.6 | 124.1 | 121.8 | | | |
| H3SiOLiAKOH)2OSiH3 | 167.3 | 186.0 | 182.6 | 258.3 | 124.8 | 146.2 | | | |
| H(OH), AlSi, O12 | 171.9 | 194.6 | 98.2 | 248.9 | 131.0 | 116.1 | | | |
| $H_2(OH)_8 Al_2 Si_6 O_{12}$ (a) | 173.3 | 193.7 | 98.2 | 248.9 | 131.0 | 116.1 | | | |
| H ₂ (OH) ₈ Al ₂ Si ₆ O ₁₂ (b) | 175.5 | 194.0 | 98.4 | 240.8 | 137.2 | 116.1 | | | |
| H ₂ (OH) ₈ Al ₂ Si ₆ O ₁₂ (c) | 169.8 | 199.8 | 98.4 | 247.6 | 133.4 | 119.3 | | | |
| LiH(OH), Al2Si6O12 | 172.8 | 194.1 | 98.1 | 248.4 | 131.2 | 116.6 | | | |
| H ₄ (OH) ₈ Al ₄ Si ₄ O ₁₂ | 176.4 | 191.4 | 98.1 | 247.0 | 132.4 | 113.6 | | | |

 $a = Li(1) \dots O.$

สำนักงานกองทุนสนับสนุนการวิจัย (สกา.) ชั้น 14 อาคาร เอส เก็ม ทามาวลร์ เสขที่ 979/17-21 กบบบาลก ใกรีบ และวงล เมเสนใน เขตหญิงไท กรุงเทพฯ 10400 โทร.298-0455 โทรสาร 298-0476 Home page : http://www.trf.or.th E-mail : trf-info(ætrf.or.th



J. Limtrakul, D. Tantanak / Chemical Physics 208 (1996) 331-340

Table 3
VWN optimized parameters computed for H₃SiOAlH₃, H₃SiOXAlH₃, H₃SiOXAKOH)₂OSiH₃, D4R cluster models and their complexes with ions

| VWN/6-31G* | | - | | | | |
|--|--------------|--------------|-------------|-------------|------------------|-----------------|
| System | Si-O (pm) | Al-O (pm) | O-X (pm) | AlH (pm) | Si-O-Al (deg) | Si-O-H (deg) |
| H ₃ SiOAlH ₃ | 161.2 | 180.9 | | _ | 125.4 | - |
| H,SiOHAIH, | 171.2 | 199.8 | 98.1 | 245.2 | 121.1 | 116.9 |
| H,SIOLIAIH, | 165.8 | 186.5 | 176.2 | 251.1 | 127.6 | 142.9 |
| H,SiOHAKOH),OSiH, | 170.8 | 188.9 | 97.8 | 245.2 | 122.2 | 124.1 |
| H,SiOLiAKOH),OSiH, | 165.2 | 182.1 | 179.1 | 254.8 | 119.4 | 150.8 |
| H(OH), AlSi, O12 | 168.6 | 189.2 | 98.4 | 243.0 | 129.9 | 118.8 |
| $H_2(OH)_1 Al_2 Si_6 O_{12}$ (a) | 169.7 | 188.6 | 98.4 | 243.6 | 130.8 | 117.0 |
| H ₂ (OH) ₈ Al ₂ Si ₆ O ₁₂ (b) | 170.5 | 186.9 | 98.4 | 241.8 | 130.4 | 117.4 |
| H2(OH), Al2Si6O12 (c) | 166.3 | 191.7 | 97.6 | 226.5 | 134.4 | 127.9 |
| LiH(OH), Al2Si6O12 | 169.4 | 188.6 | 98.3 | 242.5 | 130.4 | 118.1 |
| H4(OH)8 Al4Si4O12 | 172.5 | 186.2 | 98.3 | 240.7 | 132.8 | 115.3 |

⁼ Li(1)...O.

Table 4
Computed OH bond lengths and proton affinities (kJ/mol) at BLYP for the zeolite cluster models

| BLYP | | | | | |
|--|-----------|----------------------|-----------------------|---------|-------------|
| System | Basis set | r _{OH} (pm) | <i>9</i> _H | q0 · qH | PA (kJ/mol) |
| H,SiOH | 6-311G* | 97.0 | 0.405 | 0.294 | 1520.4 |
| H,SiOHAISiH, | 6-311G* | 97.1 | 0.454 | 0.372 | 1307.9 |
| H,SiOHAKOH),OSiH, | 6-311G * | 97.0 | 0.466 | 0.395 | 1316.2 |
| (OH) ₂ Si ₂ O ₁₂ | 6-31G * | 97.7 ' | _ | _ | 1403.1 |
| H(OH), Al, Si, O, | 6-31G * | 98.2 | 0.477 | 0.333 | 1249.1 |
| H ₂ (OH) ₈ Al ₂ Si ₆ O ₁₂ (a) | 6-31G* | 98.2 | 0.475 | 0.333 | 1272.4 |
| H2(OH), Al2Si6O12 (b) | 6-31G* | 98.4 | 0.475 | 0.335 | - |
| H ₂ (OH) ₈ Al ₂ Si ₆ O ₁₂ (c) | 6-31G* | 98.4 | 0.476 | 0.327 | - |
| H ₄ (OH) ₈ Al ₄ Si ₄ O ₁₂ | 6-31G* | 98.1 | 0.458 | 0.318 | 1285.2 |
| LiH(OH), Al2Si6O12 | 6-31G* | 98.1 | 0.474 | 0.332 | 1279.3 |

t = terminal hydroxyl groups =SiOH.

Computed OH bond lengths and proton affinities (kJ/mol) at VWN for the zeolite cluster models

| VWN | | | | | | |
|--|-----------|----------------------|----------------|---------|-------------|--|
| System | Basis set | r _{OH} (pm) | q _H | q0 · qH | PA (kJ/mol) | |
| H ₃ SiOH | 6-311G* | 96.8 | 0.434 | 0.317 | 1495.2 | |
| H,SiOHAISiH, | 6-311G* | 97.1 | 0.487 | 0.396 | 1282.7 | |
| H,SiOHAKOH),OSiH, | 6-311G* | 97.2 | 0.498 | 0.413 | 1296.9 | |
| (OH), Si, O12 | 6-31G ° | 97.5 ^t | _ | _ | 1413.2 | |
| H(OH), Al, Si, O, | 6-31G * | 98.4 | 0.504 | 0.351 | 1233.6 | |
| H ₂ (OH) ₈ Al ₂ Si ₆ O ₁₂ (a) | 6-31G ° | 98.4 | 0.503 | 0.329 | 1255.8 | |
| H ₂ (OH) ₈ Al ₂ Si ₆ O ₁₂ (b) | 6-31G ° | 98.4 | 0.502 | 0.329 | _ | |
| H ₂ (OH) ₈ Al ₂ Si ₆ O ₁₂ (c) | 6-31G ° | 97.6 | 0.498 | 0.318 | _ | |
| H ₄ (OH) ₄ Al ₄ Si ₄ O ₁₂ | 6-31G* | 98.3 | 0.499 | 0.330 | 1265.8 | |
| LiH(OH), Al2Si6O12 | 6-31G * | 98.4 | 0.501 | 0.327 | 1241.4 | |

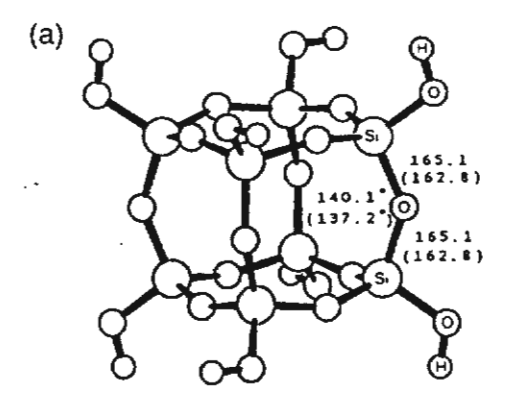
^{1 =} terminal hydroxyl groups #SiOH.

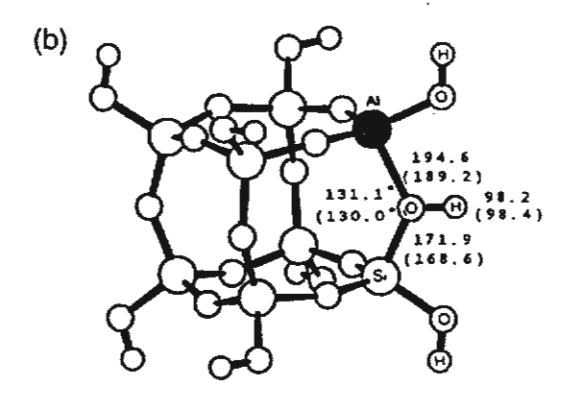
works with different Si/Al ratio computed using the DFT/BLYP and DFT/VWN methods are documented for the first time in Tables 1-5, and illustrated in Figs. 1-4. In order to compare the reliability of the DFT structure the highly symmetrical model compound H₈Si₈O₁₂ was fully optimized at the SCF/DZP level of theory and the results were compared with the more reliable experimental data. In addition to various isomers of the D4R model clusters the smaller models H₃SiOH, H₃SiOSiOH₃, H₃SiOHAlH₃, (OH)₃SiOHAl(OH)₃, H₃SiOAl (OH)₂-OHSiH₃ are also included at the SCF, DFT and MP2 methods.

The comparison of the geometry of the smaller zeolitic models between the DFT (Becke-Lee-Yang-Parr and Vosko-Wilk-Nasair) and MP2 results agrees with 1 pm for Si-O and O-H, while the weaker Al-O bond lengths agree with 2-4 pm depending on the exchange-correlation potential employed. The Si-O(H)-Al, Si-O-H, and Si-O-Si parameters are in good agreement with MP2. The flexible Si-O-Si angle of H₃SiOSiH₃ is well represented by BLYP but not by VWN, the latter giving angles 12° and 18° smaller than MP2 and coupled pair functional results, respectively. This suggests that BLYP should be employed for a silica model.

For $(OH)_8Si_8O_{12}$, Fig. 1a, the calculated values of r(Si-O) and $\angle Si-O-Si$ are 165.1 pm and 140.1° for BLYP/6-31G*, 162.8 pm and 137.2° for VWN/6-31G*, and 162.8 pm and 160.6° for SCF/DZP levels of theory. All DFT structures are in reasonable agreement with the experimental data $(r(Si-O) = 161.9 \text{ pm} \text{ and } \angle Si-O-Si = 148° [38])$.

Considering the D4R model H(OH)₈Si₇AlO₁₂, Fig. 1b, it is clearly seen that the unperturbed bridging hydroxyl unit, (OH)₃SiOHAl(OH)₃ is a better model than the widely employed H₃SiOHAlH₃ (Table 1). The smallest model yields an Al-O(H) bond length that is 12.4 pm too long, as compared with the D4R. There is a major difference between the D4R and the unperturbed models in the OH bond length. The D4R is more acidic than the unperturbed models, which is partly due to the larger SiOHAl angle of the former (131.1° versus 120.2°). Unfortunately, at present we cannot perform calculations at the 6-311G* level of theory for our largest model of H(OH)₈Si₇AlO₁₂ since this would take too much computer time. Thus, we have to rely on the 6-31G*





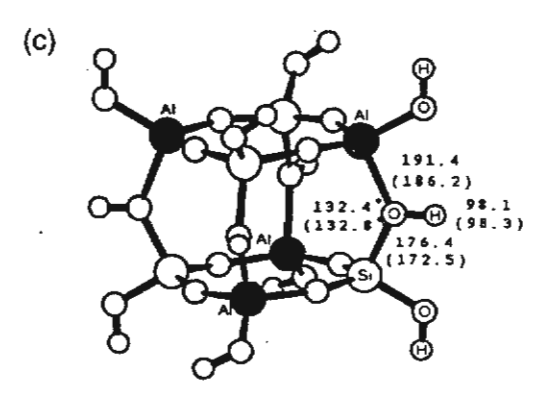
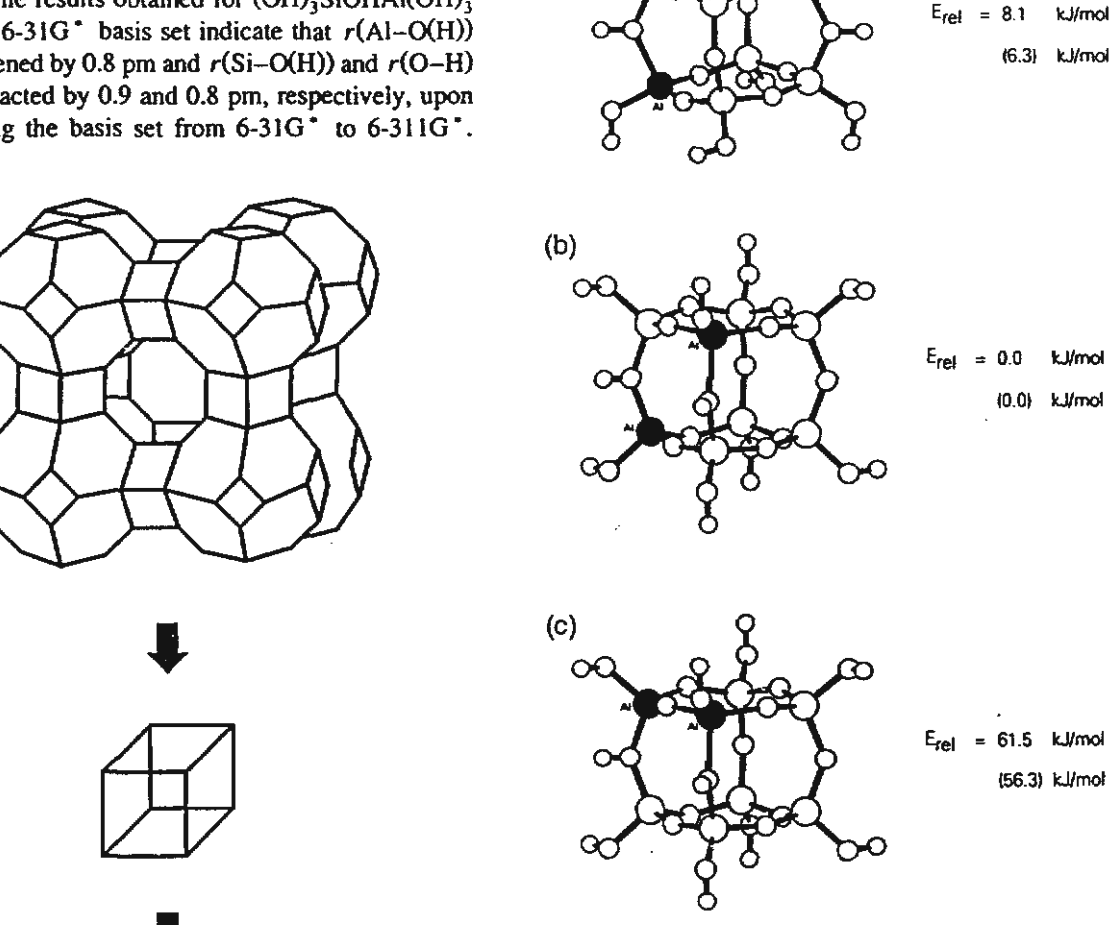


Fig. 1. Composition and variation of D4R with varying Si/Al ratio calculated at BLYP/6-31G° and VWN/6-31G° (values in parentheses). (a) $(OH)_8Si_8O_{12}$, (b) $H(OH)_6Si_7AlO_{12}$ and (c) $H_4(OH)_8Si_4Al_4O_{12}$.

(a)

results to estimate the changes of the selected parameters i.e. Si-O, Al-O and OH bonds on expansion of the (OH)₃SiOHAl(OH)₃ to the H(OH)₈Si₇AlO₁₂ model. The results obtained for (OH)₃SiOHAl(OH)₃ with the 6-31G* basis set indicate that r(Al-O(H)) is lengthened by 0.8 pm and r(Si-O(H)) and r(O-H) are contracted by 0.9 and 0.8 pm, respectively, upon expanding the basis set from 6-31G* to 6-311G*.



in parentheses).

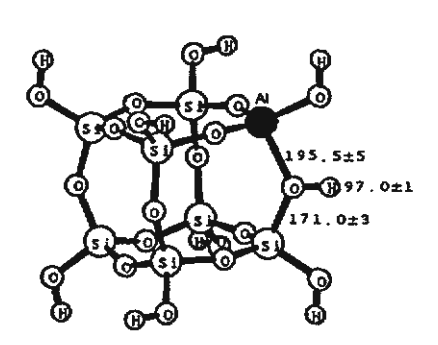
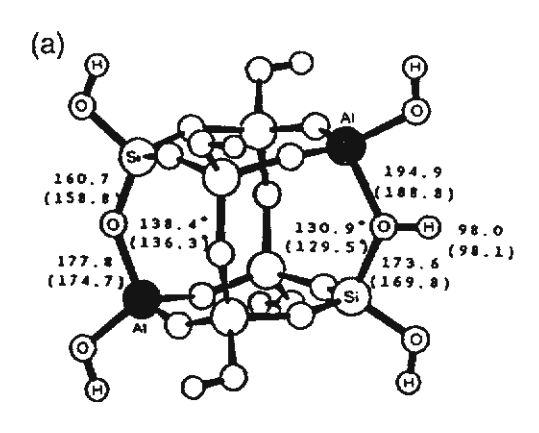


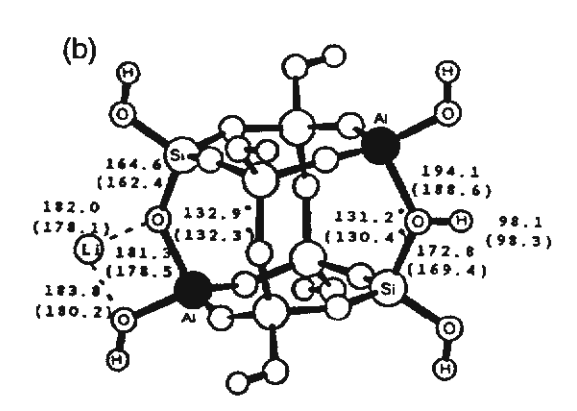
Fig. 2. Predicted local structure of Linde-type A zeolitic catalysts.

Using this systematic change in bond lengths (Table 1), the local structure of $H(OH)_8Si_7AlO_{12}$ can be reliably predicted (Fig. 2). The predicted results can be compared with the closely related experimental results observed by Feher et al. [39] (r(Si-O) = 165.2) versus 161.8 pm and r(Al-O) = 179.5 versus 174.5 pm).

Fig. 3. Relative isomer stability of D4R within given Si/Al ratio (6/2) calculated at BLYP/6-31G* and VWN/6-31G* (values

Further support for the reliability of the ≡Si-OH-Al≡ subunits by our calculations is given from NMR studies. Klinowski et al. have estimated the internuclear distance between aluminium and proton





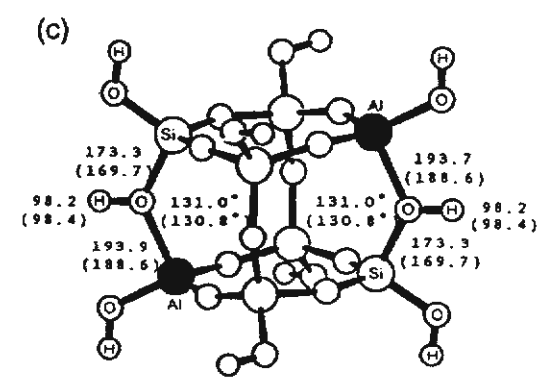


Fig. 4. Cationic effects on the catalytic acid sites of D4R calculated at BLYP/6-31G° and VWN/6-31G° (values in parentheses). (a) $H(OH)_8Si_6Al_2O_{12}^-$, (b) $LiH(OH)_8Si_6Al_2O_{12}^-$ and (c) $H_2(OH)_8Si_6Al_2O_{12}^-$.

nuclei in a Brønsted acid site, r(Al-H), of H-faujasite [40] and H-ZSM5 [41] to be 238.0 \pm 4 and 245.0 \pm 4 pm, respectively, whereas our computed r(Al-H) distance is 243.0 pm.

Tables 3 and 4 also show another important parameter, the r(O-H) distance which is of prime importance for catalytic properties. From neutron diffraction studies of the acidic faujasite, Cheetham et al. [42,43] have determined the OH distance to be 100 ± 20 pm, whereas our predicted value is 97.0 ± 1 pm. The result of lattice energy minimizations is also found to be as large as 100.0 pm. Such an unrealistic deviation is partly due to the Morse potential used in the simulation as already noted by Schröder et al. [44].

In order to observe changes in the structure and bonding on going from the anionic framework site [(OH)₈Si₇AlO₁₂] to the Brønsted acid site (H(OH), Si, AlO12), the anionic framework was also computed. Removal of a proton from the protonated D4R strengthens the Si-O and Al-O bonds (171.9 versus 160.0 pm for Si-O and 194.6 versus 178.5 pm for Al-O). The Si-O-Al angle (138.4°) in the deprotonated D4R is larger (by 7.3°) than that at the bridging hydroxyl site (131.1°). The average Al-O bond length of the four Al-O bonds of the deprotonated D4R was calculated as 177.3 pm whereas for the protonated D4R it was found to be 179.5 pm, which can be compared with the available experimental value of 174.5 pm found by X-ray diffraction measurements of the zeolite [45].

3.2. Proton affinities

Proton affinities of Brønsted hydroxyl groups in zeolites can be used as a basis for investigating the role of both composition and structure in describing the activity of catalysts in catalytic processes.

We can evaluate the performance of the DFT procedure in predicting gas phase proton affinities by comparing with highly reliable theoretical values of G1 and coupled pair functionals and experimental results. All calculated proton affinities for different cluster models are documented in Tables 4 and 5.

Silanol. The calculated VWN/6-311G* and BLYP/6-311G* proton affinities are evaluated to be 1495.2 and 1520.4 kJ/mol. It can be seen that NLSD performs perfectly well at the BLYP/6-

311G* level, which is in good agreement with the CPF (1521 kJ/mol) [46] and G1 (1490.3 kJ/mol) [47,48] results.

Octanuclear silsesquioxanes (cf. Fig. 1a). The calculated BLYP/6-31G° and VWN/6-31G° proton affinities of $(OH)_8Si_8O_{12}$ are evaluated to be 1403.0 and 1413.2 kJ/mol which is in good agreement with the recent experimental result (1390 \pm 25 kJ/mol) [49]. As can be seen that the calculated proton affinity of the most widely employed model H_3SiQH does not well represent silica which yields over 100 kJ/mol above the observed data. Thus the double four-membered silicate ring is highly recommended for studying the protonation process of a surface silica.

Zeolite. The result of the proton affinity for the H₃SiOAlH₃ molecule with BLYP/6-311G° is encouraging. The MP2/6-31G° proton affinity yields a virtually identical value to the less expensive BLYP result (1307.9 (MP2)) (see Table 4).

For H₃SiOHAl(OH)₂OSiH₃ BLYP/6-311G * yields a 2 kJ/mol lower value than MP2/DZP [50]. This agreement reflects the similar computed OH bond lengths at both levels of theory (96.8 pm (MP2) versus 97.1 pm (BLYP)). It is also important to study the dependence of proton affinities on the employed cluster models. On expanding the model cluster from H₃SiOHAlH₃ to H₃SiOHAl(OH)₂-OSiH₃, the proton affinities are decreased by 14 and 8 kJ/mol with VWN and BLYP procedures, respectively.

For the largest model of our work, the proton affinities are calculated to be 1233.6 and 1249.1 kJ/mol with LSD and NLSD, respectively. Using the systematic deviations between BLYP/6-311G* and BLYP/6-31G*, our predicted value is estimated to be 1234 kJ/mol, which is in the range of experimentally determined values of 1192 ± 29 kJ/mol [49].

Proton affinities of three types of Brønsted hydroxyl groups in H forms of zeolites associated with different Si/Al ratios are also determined, Tables 4 and 5, (i) $H(OH)_8Si_7AIO_{12}$: (PA) = 1249.1 kJ/mol, (ii) $H_2(OH)_8-Si_6Al_2O_{12}$: (PA) = 1272.4 kJ/mol, (iii) $H_4(OH)_8Si_4Al_4O_{12}$: (PA) = 1285.2 kJ/mol. The higher the Si/Al ratio, the less the proton is constrained which results in a stronger acid strength. These results indicate that the proton affinities are

proved to be dependent on the composition (Si/Al ratio) and the structure (distribution of the ≡Si-OH-Al≡ groups) in the zeolite framework.

3.3. The structural and compositional effects on the properties of zeolites

H(OH)₈Si₇AlO₁₂, 1b, with one catalytically active bridging hydroxyl group represents the "high" Si/Al zeolite corresponding to a ratio of 7. The Si-O(H), Al-O(H), and OH bond lengths at BLYP/6-31G* (VWN/6-31G*) are evaluated to be 171.9(168.6), 194.6(189.2), and 98.16(98.42) pm. respectively, where the values in parentheses are obtained at the VWN/6-31G* level. In this model the Al-O(H) bond is 0.7 pm shorter, the Si-O(H) bond 1.5 pm shorter, the OH distance is 0.36 pm longer, and the Si-O(H)-Al angle is more than 7° larger than in H₃Si-OH-Al(OH)₂-OSiH₃. This smaller cluster is widely employed as a two-site binding model when better methods and larger basis can be used. Compared with H₄(OH)₈Si₄Al₄O₁₂, 1c, with four Brønsted acid sites representing the "low" Si/Al zeolite (Si/Al = 4/4), the Si-O(H) distance in the "high" Si/Al zeolite is shorter by 4.5 pm, whereas the Al-O(H) bond length is longer by about 3.2 pm (Table 2). The net charge on the H proton, $q_{\rm H}$, in compound 1b is about 0.019 higher than in compound 1c, in accordance with the larger OH distance of the former as compared to the latter. These data indicate that H(OH)₈Si₇AlO₁₂ is more acidic than H₄(OH)₈ Si₄Al₄O₁₂. We note that absolute values from Mulliken population analysis are not very reliable, and are also basis set dependent [51]. However, comparison with closely related structures will give us certainly a very meaningful value.

H₂(OH)₈Si₆Al₂O₁₂, 3, with three isomers (3a, 3b, and 3c) is found to be a useful cluster model for structural investigations. Isomer 3a can be viewed as the structure with the largest Al... Al distance in the double four-membered zeolite ring. The calculated energy of this isomer is 8.1 kJ/mol less stable than that of the isomer 3b, in which two Al atoms are located in the same four-membered zeolite ring. Similar results for high-silica faujasite is also observed by Schroeder et al. [52] and Limtrakul et al. [53], which is in contradiction to Dempsey's rule

(i.e. an increased stability of the Al-O-Si-O-Al linkage in a zeolite framework structure). Using the relative stability of these isomers, the well known Loewenstein'rule, which states that two tetrahedrally coordinated aluminium atoms will not locate adjacent to each other (≡Al-O-Al≡), 3c, has been once again confirmed by us. Results of all the three isomers considered here show that the effects of local environment (other than chemical contents) are explicitly included.

On the basis of the charges on the hydroxyl proton, the OH bond lengths, the ionicity of the OH bonds and the proton affinities (see Tables 4 and 5), the Brønsted acidity is proved to be dependent on the number of aluminium atoms and the different environment of the =Si-OH-Al= groups in the zeolite framework.

3.4. Cationic effect on structure and bonding of zeolites

The selected geometrical parameters, proton affinities, charges on protons, bridging OH bonds of the $H_2(HO)_RAI_2Si_6O_{12}$ and $LiH(HO)_R-AI_2Si_6O_{12}$, zeolite clusters are given in Tables 2-5, and illustrated in Fig. 4. Comparison of H+ and Li+ cations indicates that the Al-O bond is lengthened by 15.9 and 3.5 pm for H+ and Li+ ions complexes, respectively. The Si-O bond is also weakened: it is about 12.6 pm for $H_2(HO)_8Al_2Si_6O_{12}$ and 3.9 pm for LiH(HO)₈ Al₂Si₆O₁₂. The Al-O-Si bridging angles are more bent in H₂(HO)₈Al₂Si₆O₁₂ than in LiH(HO)₈ Al₂Si₆O₁₂ (131.0° versus 132.9°). The OH bond is evaluated to be 98.1 pm whereas the O...Li bond is 182.0 pm. The marked difference between these cations is that the H+ is singly bonded while the Li+ is doubly bonded to the zeolitic framework structure.

The proton affinities of Brønsted OH groups in the zeolitic framework are 1272.4 and 1279.3 kJ/mol for H₂(HO)₈Al₂Si₆O₁₂ and LiH(HO)₈Al₂Si₆O₁₂, respectively, which corresponds with the decreased OH bond lengths (see Tables 4 and 5). These results indicate that the acid strength of the OH groups within the zeolitic framework is also determined by the presence of cations, in addition to the compositional and structural effects mentioned in Section 3.3; thus, the acid strength depends on the amount of

electron density transferred from the anionic framework to the cation which balances its negative charges.

4. Conclusions

The cationic, structural and compositional effects on the structure and bonding of different types of =Si-OH-Al= units in the secondary building unit of zeolite cluster models (OH)8H,Al,Si8-r- $O_{12}^{(x-y)-}$ (x, y = 0, 1, 2, 4) and the silica model (OH) SigO12 have been investigated with the DFT method. Full optimization of all mentioned structural isomer clusters have been carried out at VWN/6-31G* and BLYP/6-31G*. All isomers of the double four-membered ring aluminosilicate (D4R) demonstrate that Dempsey's rule may be violated in this type of zeolite. The well-known Loewenstein's =Al-O-Al= avoidance rule has been once again confirmed by us. The results of D4R with varying Si/Al ratio indicate that the higher the ratio, the lesser the proton is restricted which results in a higher acidic strength.

The cations, H⁺ and Li⁺, are found to have a profound effect on the important structural parameters (Si-O, Al-O, O-H bonds and SiOHAl angle) of D4R. The marked difference between the cations is that the H⁺ is singly bonded while the Li⁺ is doubly bonded to the framework. This excellent results indicate that the catalytic activity of zeolites is also enhanced by the presence of cations, in addition to a compositional effect.

Acknowledgements

This work was supported by the Thailand Research Fund (TRF) in supporting the research career development project and the KURDI for kindly providing a HP-715 workstation, and through a grant of CPU time by the national high performance computing center (nhpcc) of the NECTEC. Our sincere thanks are due to Professor R. Ahlrichs (Karlsruhe, Germany) for his continued support of this work. We thank Dr. Fitzgerald and Dr. Kasren (Cray Research Inc., Minnesoto) for technical assistance in using UNICHEM codes.

References

- C.T.W. Chu and C.D. Chang, J. Phys. Chem. 89 (1985) 1569.
- [2] S.L. Suib, Chem. Rev. 93 (1993) 803.
- [3] P. Ugliengo, V.R. Saunders and E. Garrone, Chem. Phys. Letters 169 (1990) 501.
- [4] J.V. Smith, Chem. Rev. 88 (1988) 149.
- [5] W.J. Mortier, J. Sauer, J.A. Lercher and H. Noller, J. Phys. Chem. 88 (1984) 905.
- [6] S. Beran, J. Phys. Chem. 94 (1990) 335.
- [7] W.D. de Almeida and P.J. O'Malley, J. Chem. Soc. Chem Commun. (1990) 445.
- [8] Y. Murakami, A. Iijima and J.W. Ward, New developments in zeolite science and technology (Kodansha, Tokyo, 1986).
- [9] J. Sauer, Chem. Rev. 89 (1989) 199.
- [10] B.M. Lok, C.A. Messian, R.L. Patton, R.T. Gajek, T.R. Cannon and E. M. Flanigen, J. Am. Chem. Soc. 106 (1984) 6092.
- [11] J. Limtrakul and S. Hannongbua, J. Mol. Struct. THEOCHEM 280 (1993) 139.
- [12] J. Sauer, J. Phys. Chem. 91 (1987) 2315.
- [13] L.A. Curtiss, H. Brand, J.B. Nicholas and L.E. Iton, Chem. Phys. Letters 184 (1991) 215.
- [14] M. Allavena, K. Seiti, E. Kassab, G. Ferenczy and J.G. A'ngyan, Chem. Phys. Letters 168 (1990) 461.
- [15] M.S. Stave and J.B. Nicholas, J. Phys. Chem. 97 (1993) 9630
- [16] R. Ahlrichs, M. Baer, M. Haeser, H. Horn and C. Koelmel, Chem. Phys. Letters 162 (1989) 165.
- [17] J. Limtrakul, J. Mol. Struct. 288 (1993) 105.
- [18] J. Limtrakul and J. Yoinuan, Chem. Phys. 184 (1994) 51.
- [19] J. Limtrakul, J. Yoinuan and D. Tantanak, J. Mol. Struct. 312
- [20] J.D. Gale, C.R.A. Catlow and J.R. Carruthers, Chem. Phys. Letters 216 (1993) 155.
- [21] J. Limtrakul, Chem. Phys. 193 (1995) 79.
- [22] J.W. Andzelm and J.K. Labanowski, Eds., Density functional methods in chemistry (Springer, New York, 1991).
- [23] R.D. Amos, C.W. Murray and N.C. Handy, Chem. Phys. Letters 202 (1993) 487.
- [24] N.C. Handy, P.E. Maslen, R.D. Amos, J.S. Andrew, C.W. Murray and G.I. Laming, Chem. Phys. Letters 197 (1992) 506.
- [25] F. Sim, A. St.Amant, I. Papai and D.R. Salahub, J. Am. Chem. Soc. 114 (1992) 4391.
- [26] D.A. Dixon, J. Andzelm, G. Fitzgerald and E. Wimmer, J. Phys. Chem. 95 (1991) 9197.

- [27] J. Limtrakul and D. Tantanak, J. Mol. Struct. 358 (1995) 179.
- [28] DGAUSS is available as part of Unichem software from Cray Research, Eagan, M.N.; J. Andzelm and E. Wimmer, J. Chem. Phys. 96 (1992) 1280.
- [29] S.H. Vosko, L. Wilk and M. Nuisar, Can. J. Phys. 58 (1980) 1200.
- [30] A.D. Becke, Phys. Rev. A 38 (1988) 3098.
- [31] C. Lee, W. Yang and R.G. Parr, Phys. Rev. B 37 (1988) 785.
- [32] J. Andzelm and E.Wimmer, J. Chem. Phys. 96 (1992) 1280.
- [33] B.G. Johnson, P.M.W. Gill and J.A. Pople, J. Chem. Phys. 98 (1993) 5612.
- [34] N. Godbout, D.R. Salahub, J. Andzelm and E. Wimmer, Can. J. Chem. 70 (1992) 560.
- [35] R. Ahlrichs, R. Baer, M. Haeser, H. Horn and C. Koemel, Chem. Phys. Letters 162 (1989) 165.
- [36] J. Almloef, K. Faegri Jr. and K. Korsell, J. Comput. Chem. 3 (1982) 385.
- [37] M. Haeser and R. Ahlrichs, J. Comput. Chem. 10 (1989) 104.
- [38] C.W. Earley, Inorg. Chem. 31 (1992) 1250.
- [39] F.J. Feher, T.A. Budzichowski and S.L. Weller, J. Am. Chem. Soc. 111 (1989) 7288.
- [40] R.L. Stevenson, J. Catal. 21 (1971) 113; D. Frende, J. Klinowski and H. Hamdan, Chem. Phys. Letters. 149 (1988) 355.
- [41] J. Klinowski, Chem. Rev. 91 (1991) 1459.
- [42] A.K. Cheetham, M.M. Eddy and J.M. Thomas, J. Chem. Soc. Chem. Commun. (1984) 1337.
- [43] M. Eddy, PhD Thesis, University of Oxford (1984).
- [44] K.P. Schroder, J. Sauer, M. Leslie, C.R.A. Catlow and J.M. Thomas, Chem. Phys. Letters 188 (1992) 320.
- [45] J.J. Pluth and J.V. Smith, J. Am. Chem. Soc. 102 (1980) 4704.
- [46] J. Sauer and R. Ahlrichs, J. Chem. Phys. 93 (1990) 2575.
- [47] J.A. Pople, M. Head-Gordon, D. Fox, K. Raghavachari and L.A. Curtiss, J. Chem. Phys. 90 (1989) 5622.
- [48] L.A. Curtiss, C. Jones, G.W. Trucks, K. Roghavachari and J.A. Pople, J. Chem. Phys. 93 (1990) 2537.
- [49] M.A. Makarova, K.M. Al-Gefaili and J. Dwyer. J. Chem. Soc. Faraday Trans. 90 (1994) 383.
- [50] J. Sauer, P. Ugliengo, E. Garrone and V.R. Sounders, Chem. Rev. 94 (1994) 2095.
- [51] J. Limtrakul, M. Baer and R. Ahlrichs, Chem. Phys. Letters 160 (1989) 479.
- [52] K.P. Schroeder and J. Sauer, J. Phys. Chem. 117 (1993)
- [53] J. Limtrakul, J. Yoinuan and D. Tantanak, J. Mol. Struct. 332 (1995) 151.

Reprinted from

Chemical Physics

Chemical Physics 215 (1997) 77-87

Structures and potential energy surface of Faujasitic zeolite/water

Junuas Compaked " , Piti Treesukol ", Christoph Ebner b, Roland Sansone b, Michael Probst

* Eaboratory for Companies 1 and Applied Chemistry, Chem as a Department, Equally of Second Nation and University, Bang to L. (1990)

That local

In these Americanic Chemistry, University of transpruck, Intrain 52a, A and transport & Austria





Chemical Physics

Chemical Physics 215 (1997) 77-87

Structures and potential energy surface of Faujasitic zeolite/water

Jumras Limtrakul a, Piti Treesukol a, Christoph Ebner b, Roland Sansone b, Michael Probst b

Received 19 August 1996

Abstract

The structures and the potential energy surface of the system faujasitic zeolite/water have been investigated by Hartree-Fock, second-order Moller-Plesset (MP2) and by the density functional theory (DFT) calculations, using five basis sets 6-31G(d), 6-31G(d,p), 6-311G(d), 6-311G(d,p) and 6-311 + G(d,p). The DFT calculations employ the Becke-3-Lee-Yang-Parr (B3LYP) and Becke-Lee-Yang-Parr (BLYP) density functional, and, for comparisons, the local density approximation with the Vosko-Wilk-Nusair (VWN) functional. The B3LYP approach is found to yield better agreement with the corresponding experimental results than the VWN and BLYP functionals. The B3LYP and MP2 levels of theory yield basically the same results. Results of B3LYP with a 6-311 + G(3df,2p) basis set are also very close to those of the very accurate coupled pair functional (CPF) method. Also proton affinities (PA) computed by B3LYP reproduce the corresponding CPF and G1 results very well. The predicted PA of faujasitic catalyst is estimated to be 294 ± 3 kcal/mol, which is in the range of the experimentally determined value of 291-300 kcal/mol. The interaction of faujasite catalyst with water has revealed that the structures can be stabilized by the formation of two hydrogen bonds with water molecules adsorbed at the bridging hydroxyl groups which can act either as a proton acceptor or as a proton donor. Comparison of the faujasite complexes with silanol and hydrogen halides has demonstrated that the faujasitic zeolite is a strong acid. The potential energy surfaces of faujasite zeolite/water has been investigated and analytical interaction potentials have been derived.

1. Introduction

Zeolites are microporous materials widely investigated for their numerous industrially important applications, e.g. as sorbents, catalysts, and molecular sieves [1-8]. The zeolitic framework structures of crystalline aluminosilicates present regular cavities

and open channels of molecular dimensions which allow molecular probes to interact with the Brønsted acidic sites. Their catalytic property of zeolite is involved with the site originating from bridging hydroxyl groups in zeolite catalysts.

For understanding the catalytic processes [9-18] it is of prime importance to know the structure and properties of Brønsted acidic sites, as well as the potential energy surface of the adsorbate/zeolite system.

Laboratory for Computational and Applied Chemistry, Chemistry Department, Faculty of Science, Kasetsart University, Bangkok 10900, Thailand

b Institute of Inorganic Chemistry, University of Innsbruck, Innrain 52a, A-6020 Innsbruck, Austria

^{*} Corresponding author.

Density functional theory (DFT) has been increasingly exploited to study various chemical systems [19-24]. Requiring less computational effort, DFT results compare well with high level ab initio calculations and reliable experimental data. The quality of DFT results is determined largely by the density functional employed. The Becke-3-Lee-Yang-Parr (B3LYP) functional, recently introduced by Stephens et al. [25], a modification of the BLYP functional [26], is often regarded as one of the best available choices. Bauschlicher and Partridge [27], and other groups [28] have demonstrated that this density functional can be employed to yield accurate results about molecular structures, atomic energies and harmonic vibrational frequencies for a large set of small molecules. To the best of our knowledge, no systematic investigations of the faujasitic zeolite properties have yet been performed with this functional.

In the present work, the catalytic properties of zeolites have been investigated for the first time via DFT employing B3LYP and the basis sets ranging from 6-31G(d), 6-31G(d,p), 6-311G(d), 6-311G (d,p), to 6-311 + G(3df,2p) with the aims of: (a) comparing the changes in structures and bonding on going from the smallest possible model to the more realistic cluster models; (b) determining the influence of the structure on the catalytic properties of zeolites; (c) predicting a local solid acid catalyst site of zeolite and comparing the structural parameters with available experimental data; (d) obtaining the potential energy surface of system zeolites/water and (e) investigating the effects of the size of the basis set.

2. Method and models

We employed different clusters, AlSi₁₀O₁₄H₁₇, Al(OSiH₃)₄H, H₃SiOHAlH₃ and H₃SiOH, illustrated in Fig. 1b-e, as the representative models of zeolites. We consider that to simulate the local framework of these clusters correctly, at least four silicon atoms and one aluminium atom have to be included in the model clusters. In the model employed, the dangling bonds of 'surface' oxygen atoms are saturated by hydrogen atoms. The Al(OSiH₃)₄H cluster, denoted as 'cluster C' (Fig. 1c), represents the active acidic site of zeolite. In this model the dangling bonds of the Si atoms are terminated by H

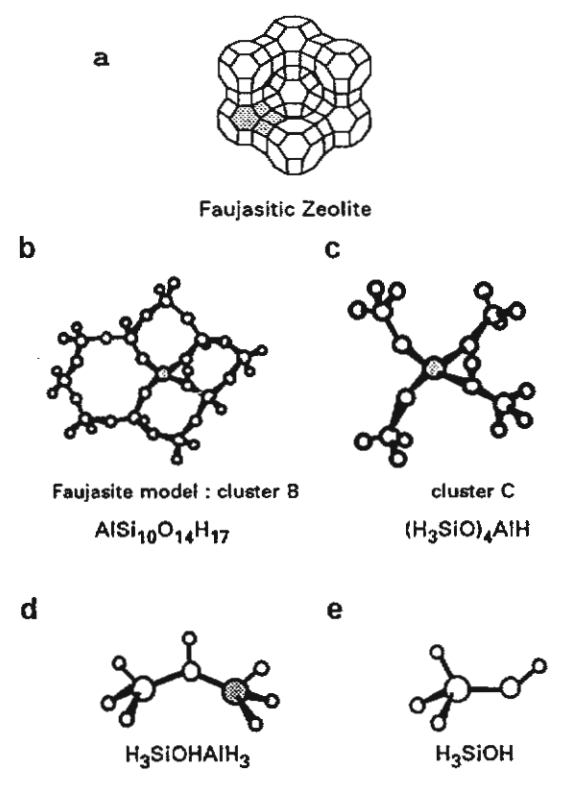


Fig. 1. Cluster models of faujasite zeolite.

atoms with a fixed Si-H bond length of 1.487 Å, and the Si-H bonds are aligned with the corresponding Si-O bonds of the structure of faujasite [29]. The local active site structure has been achieved by allowing the AlO₄H unit to relax, while the remainder SiH₃ groups are being fixed. In order to observe the effect of full relaxation, this cluster is compared to its fully optimized Al(OSiH₃)₄H structure.

The AlSi₁₀O₁₄H₁₇ cluster, denoted as 'cluster B' (Fig. 1b) consists of three four-membered rings (4MR) and one six-membered ring (6MR), representing the 'high' Si/Al zeolite(Si/Al = 10). This cluster can also be exploited to investigate the structural and compositional influences on the catalytic properties of faujasite.

Full geometry optimization of the mentioned cluster models was carried out with the DFT methods employing the B3LYP density functional. Again the basis sets 6-31G(d), 6-31G(d,p), 6-311G(d), 6-311G(d,p), and 6-311 + G(3df,2p) were used. Additionally, calculation with the Becke-Lee-Yang-Parr

(BLYP) [26] and Vosko-Wilk-Nusair (VWN) [30] functionals were performed for some models. All density functional computations were carried out using the program Gaussian-94 [31].

For the HF calculations we employed the TUR-BOMOL code [32,33] which is based on the direct SCF method of Almloef et al. [34]. In order to obtain the more reliable structures of zeolites, the correlated calculations were also included for the smallest model. Geometry optimization was terminated when the gradients norm with repect to internal coordinates was less than $10^{-3} E_h/a_0$. The energy change was then below 5×10^{-6} au.

The computations were carried out using an SGI power challenge XL computer at the Innsbruck University computing center, and DEC AlphaStation 250/4 266 and HP 9000/700 workstations at the Laboratory for Computational and Applied Chemistry at Kasetsart University.

3. Results and discussion

3.1. Structures

Table 1 illustrates the results for H₃SiOH and H₃COH structural parameters computed at different levels of theory. It is clearly seen that B3LYP density functional results are superior to the BLYP and VWN. The B3LYP and MP2 levels yield basically the same results, the B3LYP/6-311 + G(3df,2p) is also very close to the most accurate CPF [35] structure given in Table 1.

3.1.1. Silanol

B3LYP bond lengths involving bridging OH are virtually identical to CPF [35] value (cf. Table 1). For the Si-O bond length again B3LYP yield an excellent value to CPF, while the corresponding value at the BLYP level is about 0.02 Å too long. Si-O-H bond angles calculated with all DFT approaches compare well with MP2 and CPF data. Again a good agreement takes place for its anion, H₃SiO⁻, where B3LYP values of Si-O = 1.580 Å, Si-H = 1.531 Å and O-Si-H = 117.1° are compared to the CPF values of 1.563, 1.529 and 117.3°, respectively. The same trends are also observed for methanol (cf. Table 1).

3.1.2. Zeolite

The extension of 6-311G(d) basis set with the polarization functions on the hydrogen atoms influences the B3LYP structure only slightly. The O-H, Si-O, and Al-O bonds differ by less than 0.001 Å, the SiO(H)Al and Si-O-H bond angles differ by about less than 0.5° (Table 2). These results indicate that the B3LYP structural parameters are converged for the cluster C, Al(OSiH₃)₄H at B3LYP/6-311G(d) level of theory and the extension of the basis set will not lead to different structure results.

Comparing the cluster C, Al(OSiH₃)₄H, with the widely employed model cluster, H₃SiOHAlH₃ (Table 2), it is clearly seen that the smallest model yields an Al-O bond length that is too long. On increasing the levels of basis set from 6-31G(d) to 6-311G(d,p), the Al-O and Si-O bond lengths of the cluster models increase, as tabulated in Table 2.

Table 1
Optimized parameters for the molecular models of H_3SiOH and H_3COH at different levels of theory with the 6-311 + G(3df,2p) basis set (bond distances in Å, bond angles in degrees)

| Method | H₃SiOH | | | H ₃ COH | | | |
|--------|--------|-------------|---------------------|--------------------|----------------|--------|---|
| | rsio | <i>г</i> он | ∠ _{Si-O-H} | r _{co} | _{гон} | ∠с-о-н | , |
| HF | 1.630 | 0.937 | 121.4 | 1.398 | 0.938 | 110.3 | |
| VWN | 1.644 | 0.967 | 118.9 | 1.400 | 0.969 | 109.2 | |
| BLYP | 1.673 | 0.968 | 118.2 | 1.439 | 0.974 | 108.5 | |
| B3LYP | 1.654 | 0.958 | 119.3 | 1.421 | 0.960 | 109.1 | |
| MP2 | 1.655 | 0.957 | 118.6 | 1.418 | 0.959 | 108.5 | |
| CPF * | 1.650 | 0.958 | 117.7 | 1.419 | 0.959 | 108.1 | |
| Expt. | | *** | ** | 1.421 | 0.963 | 108.1 | |

^a 6s, 5p, 2d, 1f/5s, 3p, 2d, 1f/3s, 2p basis set.

The results obtained with 6-311G(d,p) basis sets show that the Al-O bond lengths is contracted by 0.11 Å, while the S-O bond length is lengthened by 0.013 Å upon expanding the model cluster from H₃SiOHAlH₃ to Al(OSiH₃)₄H.

Further support for the reliability of using the cluster C, $Al(OSiH_3)_4H$ in computation is given by the results of NMR studies: the Al...H distance of H-faujasite has been estimated to be 2.380 ± 0.04 Å_[36], whereas our computed distances in the fully optimized cluster C are 2.400 and 2.416 Å with 6-31G(d) and 6-31G(d,p) basis sets, respectively. The calculated distances of $H_3SiOHAlH_3$ are 2.539 Å (6-31G(d)) and 2.537 Å (6-31G(d,p)).

Table 2 also provides other vital parameters, including the O-H distance which plays an important role in catalytic properties. The hydroxyl O-H bond length derived from neutron diffraction measurement of acidic faujasite [37,38] is 1.000 ± 0.02 Å. Our O-H bond lengths (Table 2) are in good agreement with the previously predicted O-H bond distance [39].

In order to investigate changes in structure and bonding on going from the anionic framework site to Brønsted acid site, removal of a proton from the cluster C, Al(OSiH₃)₄H strengthens the Si-O(H) and Al-O(H) bonds (1.729 versus 1.602 Å for Si-O(H), and 1.961 versus 1.758 Å for Al-O(H)). The Si-O-Al angle in the deprotonated cluster is larger by 50.9° than the bridging $\equiv \text{SiO(H)-Al} \equiv \text{angle}$ (128.0°). The average Al-O bond length of the four Al-O bonds of the neutral form was calculated to be 1.778 Å, whereas the anionic framework it was found to be 1.755 Å, which is in good agreement with the available experimental value of 1.745 Å determined by X-ray diffraction study of zeolite [40]. The use of the 6-31G(d) basis set in the DFT prediction of the faujasite structure also yields good results and will be the basis set of choice in B3LYP calculations on much larger systems.

In order to know more about the nature of Brønsted acid site in Faujasitic zeolite, the larger cluster with three 4-membered oxygen rings and 6-membered oxygen ring around the active site has also been included (see Fig. 1b). In this 'cluster B' model, we have permitted full optimization of the site, AlO₄H, constraining the rest of the cluster fixed at the structure of faujasite [29]. In doing so, the 'cluster B' can lead to a structure that can mimic the real faujasitic zeolite framework, since full optimization of (sub-) structures can some times lead to wrong results, as noted by Sauer [39]. The results

Table 2
B3LYP optimized geometrical parameters computed for H₃SiOHAlH₃, (H₃SiO)₄AlH (cluster C), and AlO₁₄Si₁₀H₁₇ (cluster B) (distances in Å, angles in degrees).

| System | Basis set | ron | r _{SiO(H)} | FAIO(H) | r _{AlH} | $\langle r_{\rm AIO(H)} \rangle$ | ∠ _{SI-O-H} | ∠ _{SiO(H)A1} |
|--|----------------|-------|---------------------|---------|------------------|----------------------------------|---------------------|-----------------------|
| H,SiOHAIH, | 6-31G(d) | 0.969 | 1.716 | 2.037 | 2.539 | _ | 117.7 | 132.2 |
| | 6-31G(d,p) | 0.966 | 1.715 | 2.037 | 2.537 | - | 118.0 | 131.9 |
| | 6-311G(d) | 0.962 | 1.714 | 2.037 | 2.533 | _ | 119.1 | 130.9 |
| | 6-311G(d,p) | 0.963 | 1.715 | 2.041 | 2.535 | - | 118.5 | 131.7 |
| | 6-311 + G(d,p) | 0.963 | 1.718 | 2.048 | 2.543 | _ | 118.7 | 131.3 |
| Al(OSiH3)4H 4 | 6-31G(d) | 0.971 | 1.732 | 1.964 | 2.505 | 1.772 | 118.8 | 128.4 |
| • • | 6-31G(d,p) | 0.968 | 1.731 | 1.964 | 2,499 | 1.772 | 119.2 | 128.1 |
| | 6-311G(d) | 0.964 | 1.729 | 1.961 | 2.499 | 1.770 | 119.4 | 127.6 |
| | 6-311G(d,p) | 0.964 | 1.729 | 1.961 | 2.499 | 1.769 | 119.2 | 128.0 |
| Al(OSiH3)4H b | 6-31G(d) | 0.974 | 1.733 | 1.948 | 2.400 | 1.778 | 117.2 | 123.5 |
| • | 6-31G(d,p) | 0.970 | 1.732 | 1.947 | 2.416 | 1.777 | 117.5 | 123.0 |
| | 6-311G(d) | 0.962 | 1.734 | 1.936 | 2.556 | 1.774 | 118.4 | 121.7 |
| | 6-311G(d,p) | 0.963 | 1.735 | 1.938 | 2.561 | 1.775 | 117.9 | 121.8 |
| AlSi ₁₀ O ₁₄ H ₁₇ * | 6-31G(d) | 0.972 | 1.729 | 1.956 | 2.508 | 1.773 | 117.6 | 128.8 |
| | 6-311G(d,p) | 0.965 | 1.726 | 1.953 | 2.499 | 1.770 | 117.9 | 128.7 |

^{*} Partial optimization.

b Full optimization.

collected in Table 2 show the expected pattern. For the fully optimized cluster C, there is close agreement between 6-31G(d) and 6-31G(d,p) results: bond lengths differ by about 0.004 Å for the O-H bond, Si-O and Al-O bonds are virtually equal and Si-O-H bond angles vary by 0.3°. Comparing the fully optimized cluster C with its partially optimized structure, the Al-O bonds of the latter are longer while the Si-O bonds are slightly shorter than the former. The 6-31G(d,p) calculations of the partially optimized structure yields an O-H that is 0.002 Å too short. The comparative results for the optimized 'cluster C' (Si/Al = 4) and optimized 'cluster B' having high silica zeolite (Si/Al = 10) demonstrate the variation of acidity on chemical composition of Si/Al ratio i.e the acid strength of zeolite increases with decreasing Al content, which is in accordance with recent experimental data [41].

3.2. Proton affinities

Proton affinities (PAs) of Brønsted hydroxyl group in zeolites are considered to be an important feature of catalytic activity. The performance of the B3LYP method in predicting gas phase proton affinities is compared with highly the reliable coupled pair functional method [35] and G1 theory [42,43]. Both theoretical levels are reportedly capable of predicting PAs accurate to within 2 to 3 kcal/mol. All calculated PAs at different basis sets for different cluster models are documented in Table 3.

3.2.1. Silanol

The B3LYP/6-311G(d,p) and B3LYP/6-311 + G(d,p) proton affinites are found to be 368.6 and 363.7 kcal/mol. It is clearly seen that inclusion into the basis of a single diffuse function on heavy atoms,

Table 3

OH bond lengths (Å), proton affinities (PA in kcal/mol) and Mulliken charges of the acidic hydrogens computed with the B3LYP for the different models

| Model | Basis set | [₹] OH | PA | q_{H} | |
|-------------------------------------|----------------|-----------------|-------|---------|---|
| H ₂ O | 6-31G(d) | 0.969 | 431.8 | 0.3871 | |
| • | 6-31G(d,p) | 0.965 | 435.1 | 0.3049 | |
| | 6-311G(d) | 0.962 | 425.4 | 0.3987 | |
| | 6-311G(d.p) | 0.962 | 429.2 | 0.2367 | |
| | 6-311 + G(d,p) | 0.962 | 396.0 | 0.2529 | |
| Н ₃ СОН | 6-311G(d) | 0.963 | 397.2 | 0.3789 | |
| • | 6-311G(d,p) | 0.961 | 401.2 | 0.2355 | • |
| H ₃ SiOH | 6-311G(d,p) | 0.959 | 368.8 | 0.2808 | |
| - | 6-311 + G(d,p) | 0.959 | 363.7 | 0.2814 | |
| H ₃ AIOHSiH ₃ | 6-311G(d,p) | 0.963 | 314.3 | 0.3427 | |
| • | 6-311 + G(d,p) | 0.963 | 312.6 | 0.3303 | |
| Cluster C ^a | 6-31G(d) | 0.971 | 306.7 | 0.4768 | |
| | 6-31G(d,p) | 0.968 | 310.5 | 0.3777 | |
| | 6-311G(d) | 0.964 | 304.4 | 0.4882 | |
| | 6-311G(d,p) | 0.964 | 307.5 | 0.3568 | |
| Cluster C ^b | 6-31G(d) | 0.974 | 303.6 | 0.4740 | |
| Cluster B * | 6-31G(d) | 0.972 | 300.9 | 0.4773 | |
| | 6-311G(d,p) | 0.965 | 301.9 | 0.3497 | |
| H ₃ O ⁺ | 6-31G(d) | 0.982 | 173.8 | 0.5576 | |
| - | 6-31G(d,p) | 0.976 | 178.2 | 0.4653 | |
| | 6-311G(d) | 0.973 | 176.1 | 0.5796 | |
| | 6-311G(d,p) | 0.975 | 176.1 | 0.4193 | |
| | 6-311 + G(d,p) | 0.976 | 170.0 | 0.4182 | |

Partially optimized structure.

b Fully optimized structure.

 $6-311G(d,p) \rightarrow 6-311 + G(d,p)$, yields a significant improvement in the PA. The DFT performs perfectly well at the B3LYP/6-311 + G(d,p) level, which is in good agreement with the CPF and G1 results (363.5 and 363.4 kcal/mol).

3.2.2. Zeolites

A nearly linear relationship between the PAs and the net charge on the proton, q_H , has been derived for a set of structurally related molecules (HO-H, H₃CO-H, H₃SiO-H, H₃SiOHAlH₃, different types of zeolite cluster models, and H₃O⁺) and is illustrated in Fig. 2. As expected, the hydronium cation yields the lowest PA, while the nonacidic water molecule provide the largest PA value. Comparing the PAs of H, SiOH with H, SiO(H)AlH, the PA of the latter is 50.9 kcal/mol lower than the PA of the former which corresponds to the lengthening of the OH in the H₃SiO(H)AlH₃. This results from the interaction of the Lewis acid, AlH3, with the basic oxygen site in the Lewis acid-base complex, $H_3SiOH...AlH_3$. The B3LYP/6-311G+(d,p) result of the PA for [H3SiOAlH3] is also encouraging. The deviation from the most accurate G1 [38,39] is about 2.86 kcal/mol. The MP2/DZ2P proton affinity yields a virtually identical value to the less expensive B3LYP result (312.5 kcal/mol (MP2) versus 312.6 kcal/mol (B3LYP)).

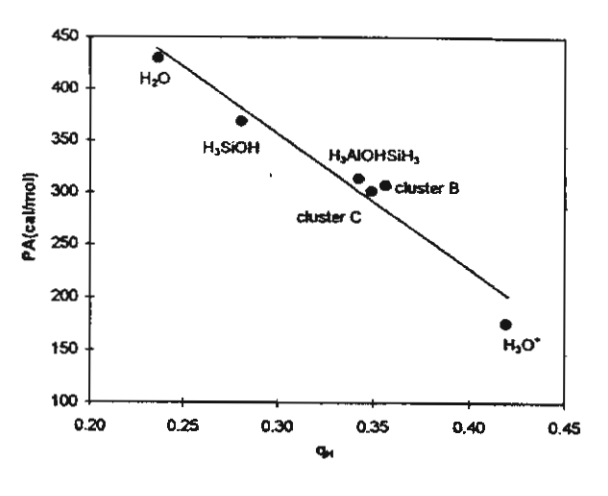
For cluster C, $Al(OSiH_3)_4H$, the B3LYP/6-311G(d,p) calculation yields a PA value of 307.5 kcal/mol. It is also important to study the dependence of PA on the employed cluster size. On expanding the model cluster from $H_3SiO(H)AlH_3$ to $Al(OSiH_3)_4H$, PA is decreased by 6.8 kcal/mol. For the largest faujasitic zeolite model, Fig. 1b, the PA is evaluated to be 301.9 kcal/mol. Using the systematic deviation between B3LYP/6-311G+(d,p) and G1 theory, our predicted value is estimated to be 294 ± 3 kcal/mol, which is in the range of experimentally determined values of 291-300 kcal/mol [44,45].

3.3. The interaction of faujasitic zeolite with water

3.3.1. Structures and energetics

Two representative cluster models of water adsorption on zeolites are investigated. In one of these, the hydrogen-bonded structures are stabilized on the

B3LYP/6-311G(d,p)



B3LYP/6-311+G(d,p)

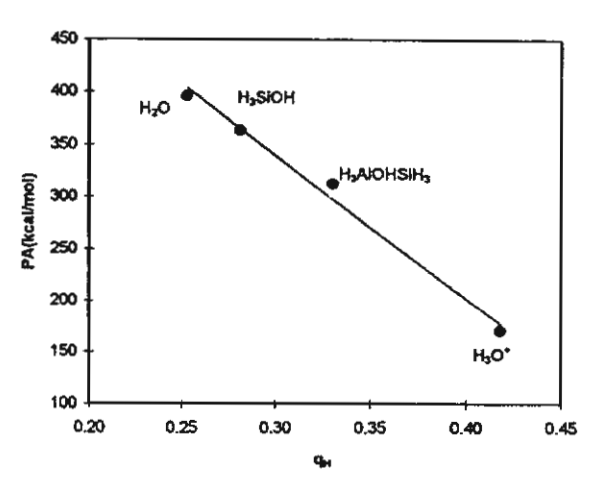


Fig. 2. The proton affinities of a set of structurally related molecules (HO-H, H_3 COH, H_3 SiO-H, H_3 SiOHAl H_3 , different types of zeolite cluster models, and H_3 O⁺) as a function of the net charge on the proton, q_H .

bridging OH. The other is a type of protonated model, in which hydronium cation forms two hydrogen bonds towards the unprotonated zeolitic framwork. Attempts were made to search for the minimum structure of zeolite cluster model/H₃O⁺. All investigated cluster models yield only one minimum as hydrogen-bonded physisorbed water complexes regardless of whether the initial framework structure having H₂O or hydronium ion. It is noted that in the case of ion-pair complexes, an initial structure with a

J. Limirakul ei al. / Chemical Physics 215 (1997) 77-87

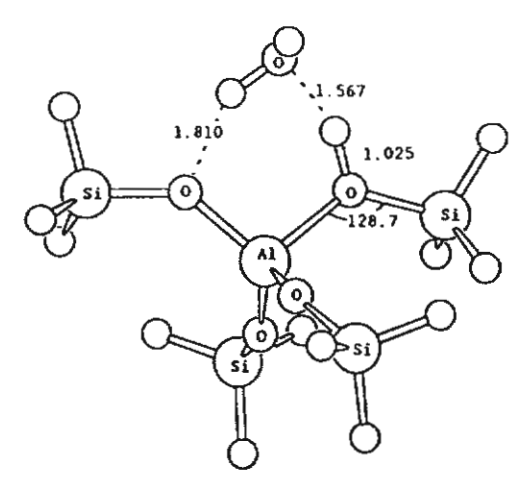


Fig. 3. Schematic representation of molecular model for the cluster C, Al(OSiH₃)₄H/H₂O.

hydronium ion is optimized. The OH bond of H₃O⁺ and the hydrogen bond angle (O...H-O) in the complex is constrained at the optimized H₃O⁺ and 180, respectively. The final complex can be derived by removing the fixed internal coordinates from the former constrained optimization structure. Similar conclusions to our predicted results have just recently been reported by Sauer et al. [11]. Recent FT-IR [17] and ab initio [14] studies of H₂O adsorption on zeolite support the direct clear evidence for the hydrogen-bonded adsorption of water. In the present study we concentrate only on the most probable hydrogen-bonded models.

The optimized geometry of cluster C with water (Fig. 3) and the extended model cluster B with water (Fig. 4) are investigated at the B3LYP/6-31G(d) level. The geometric parameters are summarized in Table 4. The results for the surface complexes clus-

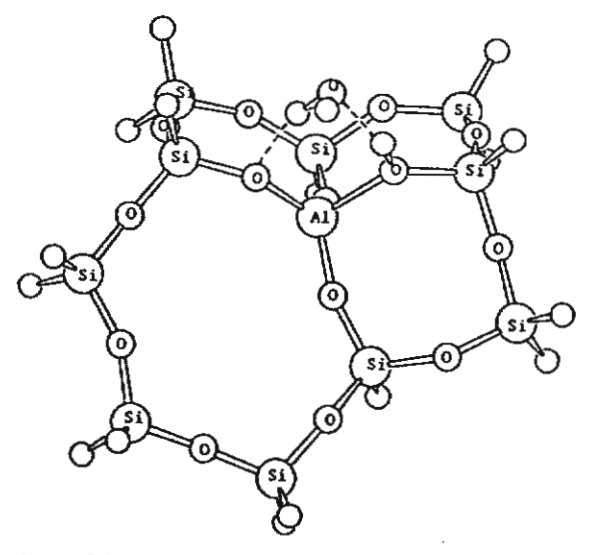


Fig. 4. Schematic representation of molecular model for the faujasitic zeolite/water.

ter C/water and cluster B/water indicate that the adsorbed water can act both as a proton acceptor and as a proton donor. The two hydrogen bonds are part of a cyclic structure, which have also been reported at HF/DZP level of theory by Sauer et al. [13].

The changes in the structural parameters of the faujasitic zeolite upon complexation with water are impressive. The results are in accordance with Gutmann's rules [46], i.e. a lengthening of the bridging O-H bond, a shortening of Al-O adjacent to this bond and a lengthening of Al-O (not adjacent to it).

The intermolecular O...O distance in the optimized and rigid structure of faujasite/water adducts (within the O-H...O hydrogen bond) are evaluated to be 2.605 and 2.555 Å, respectively. The con-

Table 4
B3LYP optimized structure parameters for Al(OSiH₃)₄H/H₂O (cluster C, cf. Fig. 3) and faujasitic zeolite catalyst/water (cluster B, cf. Fig. 4)

| Model/parameter | Rigid cluster C | Optimized cluster C | Rigid cluster B | Optimized cluster B |
|----------------------|-----------------|---------------------|-----------------|---------------------|
| r _{AlO} | 1.961 | 1.912 | 1.953 | 1.909 |
| rsio | 1.729 | 1.714 | 1.726 | 1.710 |
| r _{OH} | 0.964 | 1.026 | 0.965 | 1.024 |
| ⁷ Q(H)0 | 2.598 | 2.546 | 2.605 | 2.555 |
| r _{но} | 1.685 | 1.567 | 1.693 | 1.581 |
| r _{он} | 1.933 | 1.811 | 1.981 | 1.863 |
| ∠ _{Al-O-Si} | 128.0 | 128.8 | 128.7 | 129.2 |

tracted O...O distance of the latter model reflects an increase of the binding energy (-20.3 versus -22.5 kcal/mol). The adsorption energy for the largest model investigated, cluster B (Fig. 1b) is -20.3 kcal/mol, which is close to the result for the smaller cluster C (-20.5 kcal/mol, Fig. 1c). The binding energy of the latter cluster can be compared to the MP2 result of Sauer et al. [11] (-20.3 versus -18.98 kcal/mol). The heat of adsorption of water with H-ZSM-5 has been recently obtained by Gorte [[15],[16]], which is an excellent agreement with our largest model (-20.4 versus -20.3 kcal/mol).

In order to check the reliability of the calculated intermolecular O...O distance of faujasite/water, the water dimer was also carried out and compared to the experimental data. The calculated O...O distance of water dimer is found to be 2.909 Å, only 0.009 Å longer than the corresponding MP2 value and 0.03 Å less than the experimentally determined value of the O...O distance [47].

In order to compare the relative acidity with the other types of hydrogen-bonded systems we have performed calculations with the same theoretical model on the systems $HF...H_2O(-11.68)$, $HCl...H_2O(-8.94)$, $H_3SiOH...H_2O(-9.52)$ and $H_3SiOHAlH_3...H_2O$ (-19.24); the values in parentheses are the hydrogen bonding energies in kcal/mol. The B3LYP results suggest that in comparison with hydrogen halides, the faujasitic zeolite/ H_2O system is a strong acid.

3.3.2. Analytical potentials

The interaction of faujasite catalyst with water for different conformations has been calculated at DFT and HF levels of theory. The Hartree-Fock calculations were performed with the effective-core potential and corresponding basis sets of Stevens et al. [48-50] (denoted as SBKJC) in valence doule-zeta contraction. For the DFT calculations the B3LYP functional and the 6-31G(d) basis set were used. In order to construct potential functions for faujasitic zeolite/water, four main steps have been employed: (1) selection of the dimer conformations, (2) perfoming the B3LYP/6-31G(d) and HF/SBKJC calculations, (3) selecting the analytical form, and (4) fitting the computed DFT/B3LYP and HF/SBKJC energies to the selected functional forms.

The water geometry has been kept at the experimental values ($r_{OH} = 0.9572 \text{ Å}$, $\angle HOH = 104.52^{\circ}$ [51]), while the faujasite structure has been taken from the B3LYP/6-311G(d,p) optimization. Fig. 5 shows the faujasitic zeolite/water potential curves as a function of the O...H distance for three different levels of theory. The figure also reveals that HF/STO-3G yields a steeper minimum at a shorter distance than B3LYP/6-31G(d). This large difference shows that calculations on the STO-3G level are not useful here. The HF/SBKJC results are encouraging when compared to B3LYP/6-31G(d). The two potential curves are quite similar despite of the fact that the HF/SBKJC calculations are much

Table 5
Atomic charges for water and faujasite (cluster B)

| Water molecule | | | | | |
|-----------------------|---------------|---------------|---------------|---------------|---|
| O = -0.7401 | | | | | |
| H = 0.3700 | | | | | |
| Faujasite (Cluster B) | | | | | |
| H1 = -0.1356 | H10 = -0.1445 | H14 = -0.1465 | H15 = -0.1449 | H16 = -0.1365 | , |
| H21 = 0.5165 | H23 = -0.1490 | H24 = -0.1663 | H28 = -0.1197 | H33 = -0.1630 | |
| H34 = -0.1621 | H35 = -0.1613 | H36 = -0.1313 | H38 = -0.1551 | H39 = -0.1428 | |
| H41 = -0.1650 | H42 = -0.1639 | O3 = -1.1567 | O4 = -1.0252 | O5 = -1.0110 | |
| O9 = -1.1400 | O11 = -1.1141 | O12 = -1.0356 | O13 = -1.0424 | O17 = -1.0340 | |
| O22 = -1.0249 | 025 = -1.0048 | Q26 = -1.0156 | O27 = -1.0398 | O32 = -1.0168 | |
| O37 = -1.0271 | A16 = 1.9752 | Si2 = 1.5934 | Si7 = 1.3417 | Si8 = 1.3511 | |
| Si18 = 1.6386 | Si19 = 1.6427 | Si20 = 1.6616 | Si29 = 1.3454 | Si30 = 1.3438 | |
| Si31 = 1.3254 | Si40 = 1.3404 | | | | |

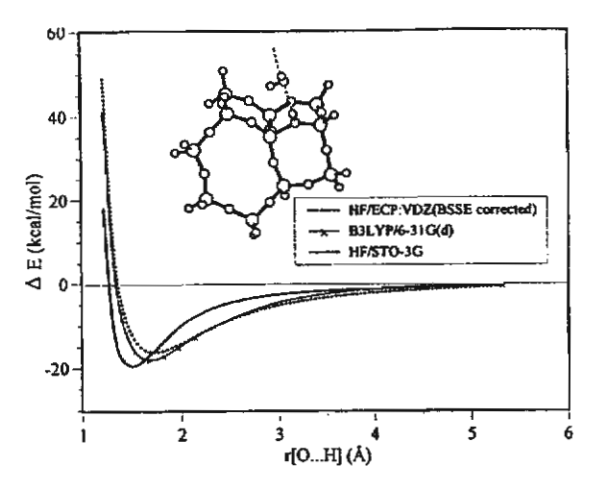


Fig. 5. Comparison of adsorption energies from B3LYP/6-31G(d), HF/ECP-VDZ, and HF/STO-3G for the faujasitic zeolite/water system.

faster (on an SGI Challenge about 50 times). After testing a variety of functional forms, a simple 2-6-10-12 potential energy expression for the interaction of faujasitic zeolite with water was employed:

$$E_{\text{fit}}^{z-w}(r_{ki}) = \sum_{k,i} \left[\frac{q_k q_i}{r_{ki}} + \frac{A_{ki}}{r_{ki}^2} + \frac{B_{ki}}{r_{ki}^6} + \frac{C_{ki}}{r_{ki}^{10}} + \frac{D_{ki}}{r_{ki}^{12}} \right].$$

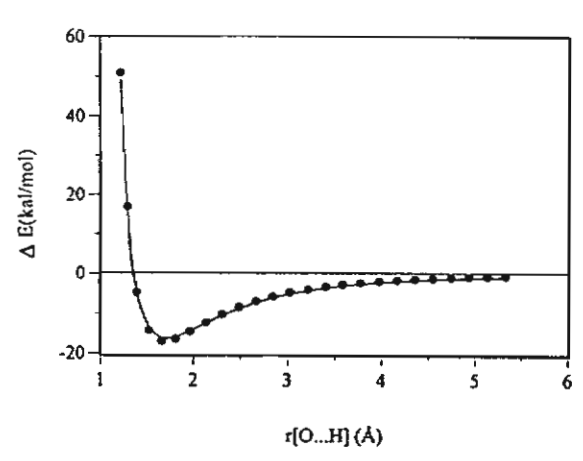


Fig. 6. Comparison between ab initio energy surface data (Δ) and analytical potential curves (lines) for the configuration presented in Fig. 4.

 r_{ki} is the distance between atom k on the zeolite molecule and atom i on the water molecule. q_k and q_i are atomic charges taken from a Mulliken population analysis (cf. Table 5). A_{ki} , B_{ki} , C_{ki} and D_{ki} are the parameters determined by least-squares fitting. The fitted parameters of the potential energy functions are tabulated in Table 6 (in kcal/mol). The quality of the fit is illustrated in Figs. 6 and 7. Fig. 6

Table 6
The fitted parameters of the potential energy functions (see text)

| Parameter | A | В | С | D |
|-----------|----------------------------|--------------------------------|----------------------------|----------------------------|
| H1-O | -1.0331905×10^{2} | 1.8382883 × 10 ² | -1.5083348×10^{2} | 8.9420565 × 101 |
| H1-H | 1.2645426×10^{2} | -2.8999846×10^{2} | 2.4324152×10^{2} | -5.5234880×10^{2} |
| H2-O | 2.8574043×10^{1} | 5.2740608×10^{2} | -3.3482893×10^{2} | -2.6299890×10^{2} |
| H2-H | -8.3599299×10^{1} | 1.4191032×10^{2} | 5.9935692×10^{1} | -1.0575208×10^{2} |
| 01-0 | -2.2914121×10^{1} | 1.3536682×10^{3} | -3.9274513×10^{3} | 6.0327825×10^{3} |
| O1-H | -9.2895111×10^{1} | 1.2641836×10^{2} | -3.6371045×10^{1} | 1.2479447×10^{1} |
| O2-O | 2.5865495×10^{2} | -1.3296107×10^{3} | 1.5674254×10^{5} | -3.4876443×10^{5} |
| O2-H | -1.1555464×10^{2} | 2.1024226×10^{2} | -1.9198437×10^{2} | 1.0763633×10^{2} |
| O3-O | 2.8803433×10^{2} | -6.7006798×10^{2} | 1.0924449×10^{5} | -2.4821535×10^{5} |
| O3-H | -1.4723644×10^{2} | 1.9241469×10^{2} | 6.6505733×10^{2} | -1.0651945×10^{3} |
| 04-0 | -7.4289775×10^{1} | 1.9661823×10^{3} | 4.0700384×10^{3} | -1.2381189×10^4 |
| O4-H | -1.3862499×10^{2} | 4.6499706×10^{1} | 7.3627116×10^{3} | 1.8873061×10^3 |
| O5-O | -3.2716430×10^{0} | 8.9273658 × 101 | 2.8112535×10^{5} | -1.1607496×10^6 |
| O5H | -1.1941986×10^{2} | 1.4535989×10^{2} | 2.1379764×10^{3} | -3.3723297×10^{3} |
| O6-O | -1.1715990×10^{2} | 1.5436984×10^{3} | 2.0774143×10^4 | -8.0412282×10^4 |
| O6-H | -9.7118742×10^{1} | 1.7816578×10^{2} | -1.3496463×10^{2} | 7.1361063×10^{1} |
| Si1-O | -5.7071178×10^{1} | -2.3134268×10^{3} | 8.2071595×10^4 | -4.9494428×10^4 |
| Sil-H | 2.8669836×10^{2} | -2.9201129×10^{2} | 3.0196516×10^{3} | -3.7259970×10^{3} |
| Si2-O | 1.6333832×10^{2} | -4.9009698×10^{0} | 3.4294755×10^{5} | -1.4582774×10^{5} |
| Si2-H | 2.3662032×10^{2} | $-1.2223283 \times 10^{\circ}$ | 2.2845654×10^4 | -5.9072913×10^4 |
| Al-O | -5.1438777×10^{2} | 1.1459039×10^{3} | 1.3088621×10^{5} | -5.1532513×10^{5} |
| Al-H | 1.1556943×10^{2} | 5.7061768×10^{2} | -9.1190710×10^{3} | 1.4812055×10^4 |

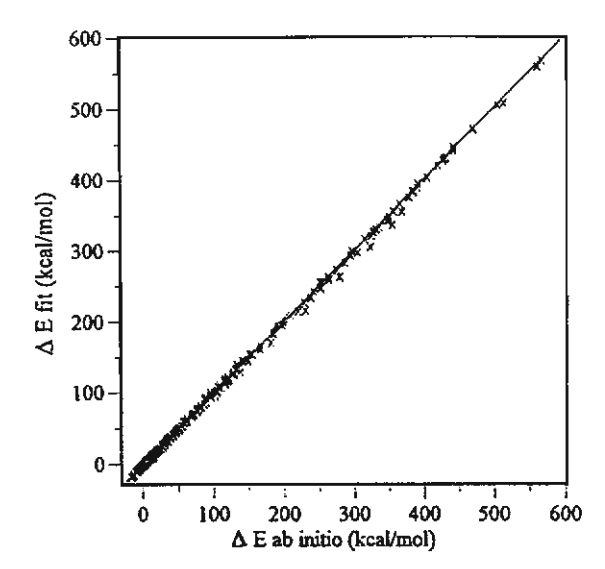


Fig. 7. Correlation between interaction energy ($\Delta E_{ab~laitio}$) from the ab initio calculations and those derived from analytical expressions as described in the text.

shows the fitted values for the same curve as Fig. 5 whereas Fig. 7 illustrates the correlation between all ab initio and fitted energies. The standard deviation obtained between fitted and ab-initio energies is 2.14 kcal/mol. Since among the 500 points used in the fitting there are many with high energies, this is a good value. Our newly developed potentials will be further employed in the simulation of zeolite/water system.

4. Conclusions

We have presented a density-functional study of faujasitic zeolites and their complexes with water using the B3LYP functionals and the basis sets 6-31G(d), 6-31G(d,p), 6-311G(d), 6-311G(d,p) and 6-311 + G(d,p). The agreement between DFT/B3LYP-6-311 + G(d,p) proton affinities and the corresponding CPF and G1 values are excellent. Comparing the older BLYP and VWN functionals with the recently introduced B3LYP functionals, the latter yields superior accuracy. This artificial significant lengthening effect on the weaker Al-O bond in the BLYP and VWN calculations does not occur with B3LYP. The Si-O(H)-Al and Si-O-H bond angles of zeolites do not appreciably depend on the

inclusion of non-local effects in the density functional. The 6-31G(d) basis set in the DFT prediction of the faujasite structure yields good results and is an economic choice for large systems. The predicted PA of the faujasitic catalyst is estimated to be 294 ± 3 kcal/mol, which is in the range of experimentally determined value of 291-300 kcal/mol. The faujasite catalyst/water structure (see Fig. 1b) is stabilized at the bridging O-H group by two H-bonds with binding energy of -20.3 kcal/mol. Comparison with hydrogen halides and related complexes of water demonstrates that the faujasite is a strong acid. An analytical potential for the interaction fo faujasitic zeolite with water was derived by fitting the ab initio interaction energies which we plan to employ simulations studies of petrochemical catalyst/water systems.

Acknowledgements

This work was supported by donors of the Thai- I land Research Fund (TRF) and the Kasetsart University Research and Development Institute (KURDI) and by Jubiläumsfonds der Österreichischen Nationalbank (project 5621). Our sincere thanks are due to Professor R. Ahlrichs (Karlsruhe, Germany) for his continued support of this work. We would like to express our gratitude to the referees for their critical and useful remarks and suggestions on this paper.

References

- [1] J. Klinowski, Chem. Rev. 91 (1991) 1459.
- [2] J.M. Thomas, Sci. Am. 266 (1992) 82.
- [3] G.J. Kramer, R.A. Van Santen, C.A. Emeis and A.K. Nowak, Nature 363 (1993) 529.
- [4] E. Kassab, J. Fouquet, M. Allavena and E.M. Evleth, J. Phys. Chem. 97 (1993) 9034.
- [5] C.T.W. Chu and C.D. Chang, J. Phys. Chem. 89 (1985) 1569.
- [6] K.J. Chao and L.J. Leu, Zeolite 9, (1989) 193.
- [7] J. Das, C.V.V. Satyanaryana, D.K. Chakrabarty, S.N. Pira-manayagarn and S.N. Shringi, J. Chem. Soc. Faraday Trans. 88 (1992) 3255.
- [8] Y. Murakami, A. Iijima and J.W. Ward, New Developments in Zeolite Science and Technology (Kodansha, Tokyo, 1986).
- [9] E. Nusterer, P.E. Blöchl and K. Schwarz, Chem. Phys. Lett. 253 (1996) 448.

- [10] S.A. Zygmunt, L.A. Curtiss, L.E. Iton and M.K. Erhardt, J. Phys. Chem. 100 (1996) 6663.
- [11] M. Krossner and J. Sauer, J. Phys. Chem. 100 (1996) 6199.
- [12] J. Sauer, P. Vglieugo, E. Garrone and V.R. Saunders, Chem. Rev. 94 (1994) 2095.
- [13] J. Sauer, H. Horn, M. Häser and R. Ahlrichs, Chem. Phys. Lett. 26 (1990) 173.
- [14] F. Haase and J. Sauer, J. Am. Chem. Soc. 117 (1995) 3780.
- [15] A. Ison and R.J. Gorte, J. Catal. 89 (1984) 150
- [16] R.J. Gorte, 1993, personal communication as referred by ref. 11
- [17] F. Wakabayashi, J.N. Kondo, K. Domen and C. Hirose, J. Phys. Chem. 100 (1996) 1442.
- [18] J. Limtrakul, J. Yoinuan, Chem. Phys. 184 (1994) 51; J. Limtrakul, Chem. Phys. 193 (1995) 79; J. Limtrakul and D. Tantanak, J. Mol. Struct. 358 (1995) 179; J. Limtrakul and D. Tantanak, Chem. Phys. 208 (1996) 331.
- [19] J.W. Andzelm and J.K. Labanowski, eds., Density Functional Methods in Chemistry (Springer, New York, 1991).
- [20] R.D. Amos, C.W. Murray, and N.C. Handy, Chem. Phys. Letter 202 (1993) 487.
- [21] N.C. Handy, P.E. Maslen, R.D. Amos, J.S. Andrew, C.W. Murray and G.I. Laming, Chem. Phys. Lett. 197 (1992) 506.
- [22] F. Sim, A. St-Amant, I. Papai and D.R. Salahub, J. Am. Chem. Soc. 114 (1992) 4391.
- [23] D.A. Dixon, J. Andzelm, G. Fitzgerald and E. Wimmer, J. Phys. Chem. 95 (1991) 9197.
- [24] J. Andzelm, E. Rodzio and D.R. Salahub, J. Comput. Chem. 6 (1985) 520.
- [25] P.J. Stephens, F.J. Devlin, L.F. Chablowski and M.J. Frisch, J. Phys. Chem. 98 (1994) 11623.
- [26] A.D. Becke, Phys. Rev. A 38 (1988) 3098; C. Lee, W. Yang and R.G. Parr, Phys. Rev. 13 (1988) 785.
- [27] C.W. Bauschlicher Jr. and H. Partridge, Chem. Phys. Lett. 240 (1995) 533-540.
- [28] J.W. Finley and P.J. Stephens, J. Mol. Struct (Theochem) 357 (1995) 255-235.
- [29] J. Limtrakul, unpublished results.
- [30] S.H. Vosko, L. Wilk and M. Nuisar, Can. J. Phys. 58 (1980) 1200.

- [31] M.J. Frisch, G.W. Trucks, H.B. Schlegel, P.M.W. Gill, B.G. Johnson, M.W. Wong, J.B. Foresman, M.A. Robb, M. Head-Gordon, E.S. Replogle, R. Gomperts, J.L. Andres, K. Raghavachari, I.S. Binkley, C. Gonzalez, R.L. Martin, D.J. Fox, D.J. DeFrees, J. Baker, J.J.P. Stewart and J.A. Pople, Gaussian 94 (Gaussian Inc., Pittsburgh, PA, 1994).
- [32] R. Ahlrichs, R. Baer, M. Haeser, H. Horn and C. Koemel, Chem. Phys. Lett. 162 (1989)165.
- [33] M. Haeser and R. Ahlrichs, J. Comput. Chem. 10 (1989) 104
- [34] J. Almloef, K. Faegri Jr. and K. Korsell, J. Comput. Chem. 3 (1982) 385.
- [35] J. Sauer and R. Ahlrichs, J. Chem. Phys. 93 (1990) 2575.
- [36] D. Freude, J. Klinowski and H. Hamdan, Chem. Phys. Lett. 149 (1988) 355.
- [37] A.K. Cheetham, M.M. Eddy and J.M. Thomas, J. Chem. Soc. Chem. Commun. (1988) 1337.
- [38] M. Eddy, PhD Thesis, University of Oxford, 1984.
- [39] J. Sauer, Chem. Rev. 89 (1989) 199.
- [40] J.J. Pluth and J.V. Smith, J. Am. Chem. Soc. 102 (1980) 4704.
- [41] D. Barthomeuf, Mater. Chem. Phys. 17 (1987) 49.
- [42] J.A. Pople, M. Head-Gordon, D. Fox, K. Raghavachari and L.A. Curtiss, J. Chem. Phys. 90 (1989) 5622.
- [43] L.A. Curtiss, C. Jones, G.W. Trucks, K. Raghavachari and J.A. Pople, J. Chem. Phys. 93 (1990) 2537.
- [44] J. Datka, M. Boczar and P. Rymarowicz, J. Catal. 114 (1988) 368
- [45] J. Datka, M. Boczar and B. Gil, Langmuir 9 (1993) 2496.
- [46] V. Gutmann, The donor-acceptor approach to molecular interactions (Plenum Press, New York, 1978).
- [47] J.A. Odutola and T.R. Dyke, J. Chem. Phys. 72 (1980) 5062.
- [48] W.J. Stevens, H. Basch and M. Krauss, J. Chem. Phys. 81 (1984) 6062.
- [49] W.J. Stevens, M. Krauss, H. Basch and P.G. Jasien, Can. J. Chem. 70 (1992) 612.
- [50] T.R. Cundari and W.J. Stevens, J. Chem. Phys. 98 (1993) 5555
- [51] W.S. Benedict, N. Gailar and E.K. Plyler, J. Chem. Phys. 24 (1956) 1139.

Reprinted from

Journal of MOLECULAR STRUCTURE

Journal of Molecular Structure 435 (1997) 181-192

Coadsorption of ammonia and methanol on H-zeolites and alkaline-exchanged zeolites

Jumras Limtrakul*, Usa Onthong

Laboratory for Computational and Applied Chemistry, Chemistry Department, Faculty of Science, Kasetsart University, Bangkok 10900, Thailand





Journal of
MOLECULAR
STRUCTURE

Journal of Molecular Structure 435 (1997) 181-192

Coadsorption of ammonia and methanol on H-zeolites and alkaline-exchanged zeolites

Jumras Limtrakul*, Usa Onthong

Laboratory for Computational and Applied Chemistry, Chemistry Department, Faculty of Science, Kasetsart University,
Bangkok 10900, Thailand

Received 17 February 1997; revised 10 April 1997; accepted 10 April 1997

Abstract

The interactions of methanol and ammonia on H-zeolites (H-Z) and alkaline-exchanged zeolites (Na-Z) have been investigated using Hartree-Fock (HF) and density functional theory (DFT) approaches. Full optimization of all clusters and their complexes has been optimized at B3LYP/6-31G* and HF/6-31G* theoretical levels. The reaction mechanism of coadsorption of methanol and ammonia on H-Z is that the ammonia is found to bound to the Brønsted acid site of H-Z, yielding ammonium cation, which in turn operates as an active site for methanol. The result of coadsorption processes indicates that the stronger base ammonia is preferentially bonded to the Brønsted acid sites of H-Z, while methanol is interacted with the Lewis acid of Na-Z. Our findings are in excellent agreement with very recently reported data (Kogelbauer, A., Grundling, G., Lercher, J.A., J. Phys. Chem. 100 (1996) 1852–1837). © 1997 Elsevier Science B.V.

Keywords: Quantum chemical calculations; Adsorption; Catalysis; Zeolites; Methanol-ammonia interaction

1. Introduction

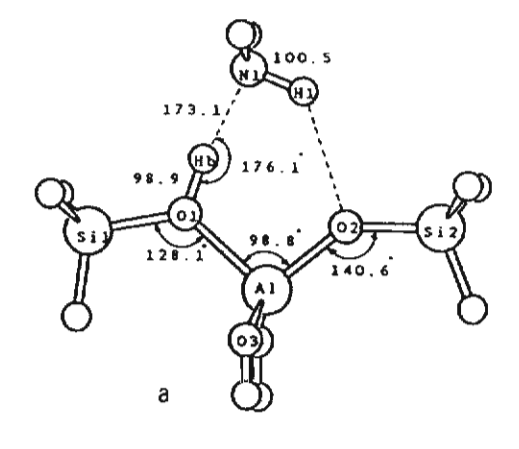
The acidity of zeolitic catalysts released from the surface hydroxyls (≡Si-OH-Al≡) is responsible for their catalytic function and has led to numerous important industrial applications, such as the application of catalysts and adsorbents in petrochemical processes and for the production of fine chemicals [1-15]. Of particular interest in this active research is the products generated from the adsorption of methanol (i.e. conversion of methanol to gasoline) [16-21] and the coadsorption of methanol and ammonia [22,23] (production of methylamines, which are essential chemical building subunits for important industrial materials such as resins, fibers,

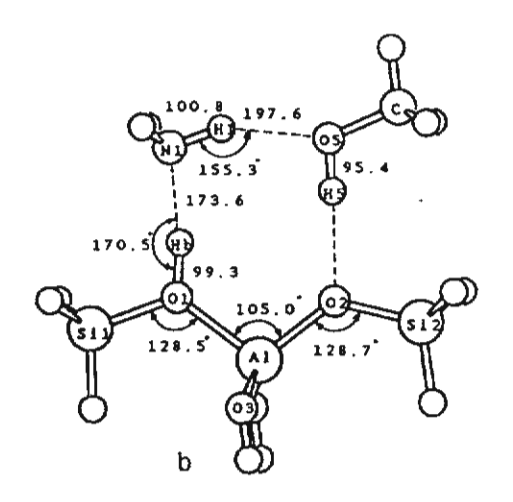
In this work, the interactions of methanol and ammonia with H-zeolites (H-Z) and alkaline-zeolites (Na-Z) are investigated for the first time by the density functional theory (DFT), and Hartree-Fock (HF) with the aim of; a) investigating the important consequences of different types of adsorbed probe molecules at low and high coverages, i.e. (CH₃OH)_n, (NH₃)_n, (CH₃OH)(NH₃) and (NH₃)(CH₃OH), where

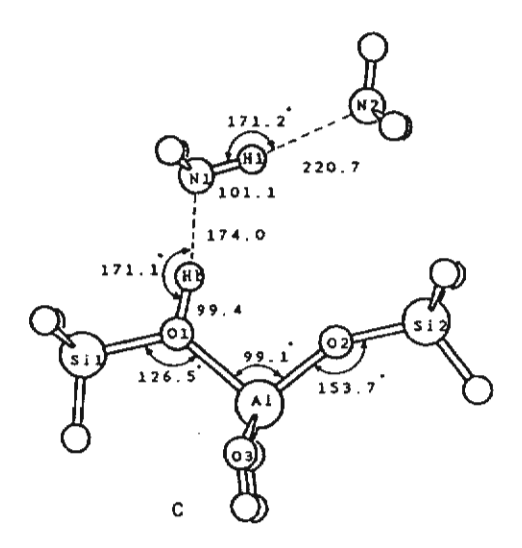
0022-2860/97/\$17.00 © 1997 Elsevier Science B.V. All rights reserved PII S0022-2860(97)00189-0

dyes and pharmaceuticals). One of the crucial steps of these chemically interesting systems involves the probed molecules adsorption on the catalyst surface. In spite of a large number of documents about zeolite research, details of the structures and reaction mechanisms of adsorption and, particularly of coadsorption, are still incomplete and only partially solved [17,23]. This understanding is the basis for the rational design of improved catalysts.

^{*} Corresponding author.







n denotes the amount of probed molecule coverages; b) determining the reaction mechanism of coadsorption; c) comparing the influence of H-Z and Na-Z on the coadsorption structure of methanol and ammmonia.

2. Method

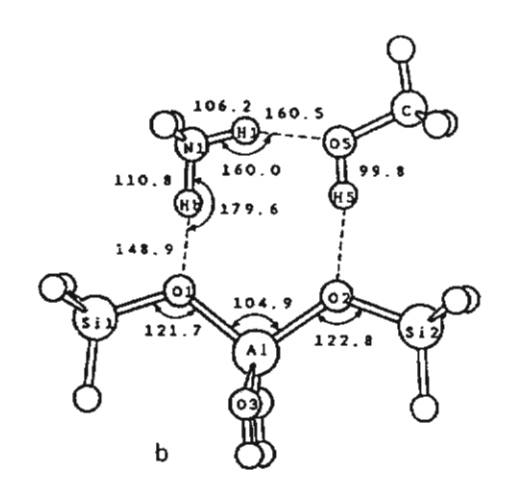
We employed the adsorption clusters illustrated in Figs. 1-3 as the models of the probed molecules' adsorption on zeolites {H₃SiOHAl(OH)₂OSiH₃}/ [NH₃][CH₃OH],and [H₃SiOHAl(OH)₂OSiH₃]/ [CH₃OH][NH₃], and their possible ion-pair species. The alkaline-exchanged systems, [H₃SiONaAl(OH)₂ OSiH₃]/[NH₃][CH₃OH] and [H₅SiONaAl(OH)₂ OSiH₃]/[CH₃OH][NH₃] are modelled for the coadsorption of methanol and ammonia on Na-exchanged zeolites (see Fig. 4 and Fig. 5). The isolated Nacomplexes, Na(I)/[NH₃][CH₃OH], and [CH₃OH][NH₃] are also included for comparison. We have also investigated the adsorption of methanol and ammonia at low and high coverages, with similar absorbent models of [H₃SiOHAl(OH)₂SiH₃]/ ICH₃OH₁. [H₃SiOHAl(OH)₂OSiH₃/[CH₃OH]₂, [H₃SiOHAl(OH)₂OSiH₃]/[NH₃], H₃SiOHAl(OH)₂ OSiH₃]/[NH₃]₂. In the models employed, the clusters have been terminated by hydrogen atoms.

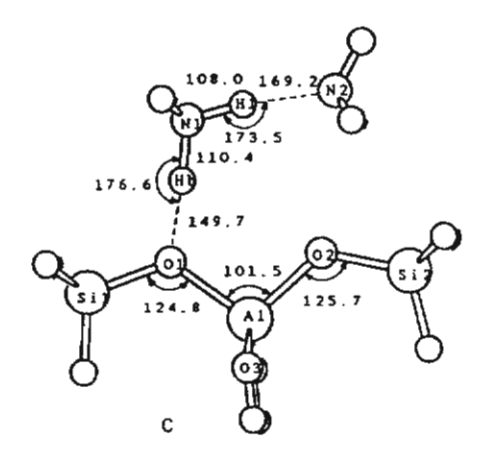
Full geometry optimization of the cluster models mentioned above was carried out with the DFT methods employing the B3LYP density functional. This functional has been recently demonstrated to yield accurate results for the molecular structures and vibrational frequencies for zeolites [24–26]. All density functional computations were performed using the program Gaussian-94 [27].

For the HF calculations, we employed the TURBO-MOLE code [28,29] which is based on the direct SCF method of Almloef et al. [30]. Geometry optimizations were terminated when the gradients norm with respect of internal coordinates was less than $10^{-3} E_b/a_0$. The energy change was then below 5×10^{-6} a.u.

The computations were carried out using DEC

Fig. 1. Schematic representation of molecular models for the systems Brønsted acid site [H₃SiOHAl(OH)₂OSiH₃]; (H-Z): a) [H₃SiOHAl(OH)₂OSiH₃]/[NH₃]; b) [H₃SiOHAl(OH)₂OSiH₃]/[NH₃].





Alphastation 250 and HP 9000/700 workstations at the Laboratory for Computational and Applied Chemistry at Kasetsart University.

3. Results and discussion

3.1. Coadsorption of ammonia and methanol on H-zeolite (H-Z)

3.1.1. Interaction of ammonia and methanol on H-Zeolite

The fully optimized geometrical structures constrained at Cs symmetry for [H₃SiOHAl(OH)₂OSiH₃]/[NH₃][CH₃OH] (see Fig. 1b) were investigated at HF levels of theory using 6-31G* basis set. The optimized parameters for the two theoretical approaches are summarized in Table 1.

Comparing the HF structure of H₃SiOHAl(OH)₂ OSiH₃ with the B3LYP structure, it is seen that the Si-O, Al-O and O-H bonds of the former are shorter than with the latter (see Table 2). Note that the HF results always yield an OH bond which is too short as compared to the experimental result [31].

Further support for the reliability of using this model is confirmed by the results of NMR measurement [32]: the Al...H of H-faujasite has been estimated to be $238 \pm 4 \,\mathrm{pm}$ whereas our computed distances at the B3LYP and HF levels of theory are 239.7 and 241.6 pm, respectively.

The changes in the structural parameters of tertiary upon complexation are in line with Gutmann's rules [33], i.e. a lengthening of the bridging OH bond, a shortening of Al-O and a lengthening of Al-O (not adjacent to the bridging OH bond).

In order to compare the structure and bonding with the related types of adsorbed molecules, we have also performed calculations on the systems H-Z/[NH₃], H-Z/[NH₃]₂. H-Z/[CH₃OH][NH₃], and H-Z/[CH₃OH] [CH₃OH] (see Table 4). The results suggest that the H-Z/[NH₃][CH₃OH] is energetically favoured in the coadsorption process of methanol and ammonia. The methanol has a pronounced effet on the H-Z/[NH₃] complex, indicating the capability of donating a

Fig. 2. Schematic representation of molecular models for the deprotonated framework {H₃SiOAl(OH)₂OSiH₃];(Z⁻): a) {H₃SiOAl(OH)₂SiH₃]⁻/{NH₄]⁺; b) {H₃SiOAl(OH)₂SiH₃]⁻/{NH₄]⁺(CH₃OH); c) {H₃SiOAl(OH)₂SiH₃]⁻/{NH₄]⁺(NH₃}.

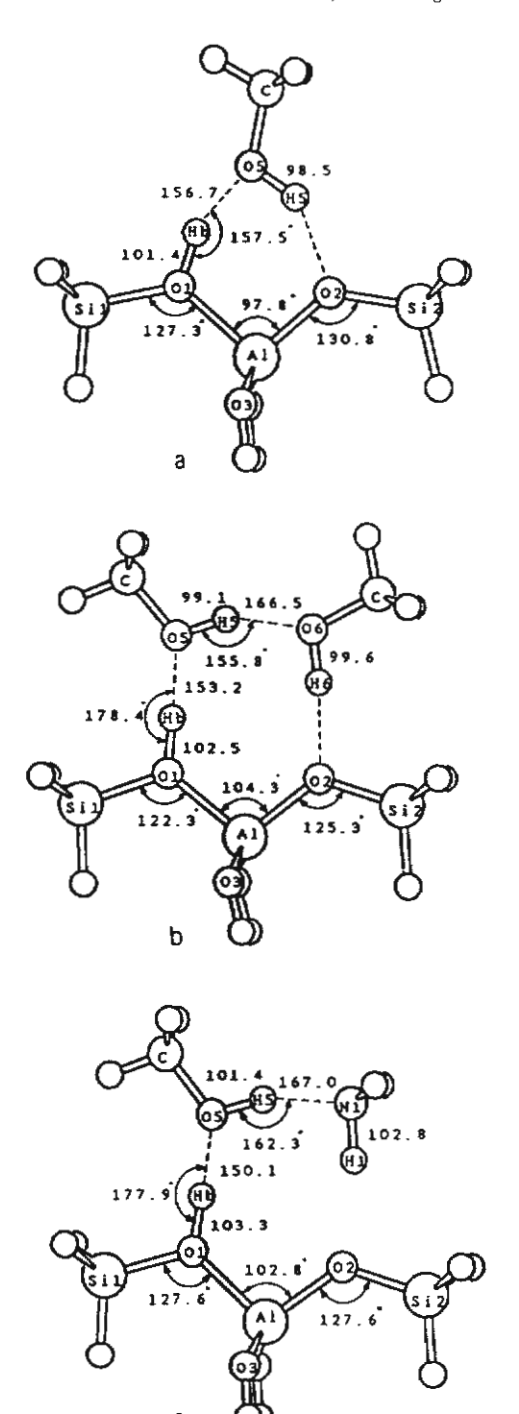


Fig. 3. Schematic representation of molecular models for the systems Brønsted acid site [H₂SiOHAl(OH)₂OSiH₃]; (H-Z): a) [H₃SiOHAl(OH)₂OSiH₃]/[CH₃OH]; b) [H₃SiOHAl(OH)₂OSiH₃]/[CH₃OH]; c) [H₃SiOHAl(OH)₂OSiH₃]/[CH₃OH][NH₃].

zeolitic proton onto the adsorbed ammonia. The Brønsted OH bonds of zeolitic catalysts are lengthened for the H-Z/[NH₃][CH₃OH] as compared to the corresponding binary complex of H-Z/[NH₃] (99.3 vs. 98.9 pm, see Fig. 1a,b).

3.1.2. Ion-pair formation

The optimized structure parameters of [H₃SiOAl (OH)₂SiH₃]⁷[NH₄][†], [H₃SiAl(OH)₂SiH₃]⁷[NH₄][†] [NH₃] and [H₃SiOAl(OH)₂SiH₃]⁷[NH₄][†] [CH₃OH] are reported. For the system [H₃SiOAl(OH)₂SiH₃]⁷ [NH₄][†], the ammonium cation forms two very strong hydrogen bonds towards the negatively charged zeolite (see Fig. 2a). The Al-O1, and Al-O2 distances are virtually equal and about 4.6 pm longer than that found in the anionic zeolite. For the high coverages, the ammonia is found to bond to the Bronsted acid site of H-Z, yielding ammonium cation, which operates as the centre site for further hydrogen bonding to methanol of ammonia (see Fig. 2b and 2c).

Attempts have been to observe the Z⁻[CH₃OH₂]⁺ [NH₃]; an initial structure with a methoxonium ion is optimized. The OH bond of [CH₃OH₂]⁺ and the hydrogen bond angle (O-H...N) in the complex is constrained at the optimized [CH₃OH₂]⁺ and 180°, respectively. However, during the optimization, the proton of [CH₃OH₂]⁺ is transferred to the ammonia molecule, and the final equilibrium complex H-Z/[CH₃OH][NH₄]⁺ is obtained. Note that this complex is achieved only at B3LYP, while only hydrogenbonded H-Z/[CH₃OH][NH₃] is obtained at the HF level of theory.

The energy for conversion of [H₃SiOHAl(OH)₂SiH₃]/[NH₃][CH₃OH] to [H₃SiOAl(OH)₂SiH₃]⁻/[NH₄]⁺[CH₃OH] is 0.74 kcal/mol. The details of the sorption processes were evaluated as follows. The coadsorption energy of ammonia and methanol on the cluster zeolite (H-Z) is the energy of reaction

$$H-Z+[NH_3]+[CH_3OH] \rightarrow H-Z/[NH_3][CH_3OH]$$
(1)

_....

Whilst for an anion (Z⁻) and ammonium cation (NH₄), the energies are those of the reactions

$$H - Z \rightarrow Z^- + H^+ \tag{2a}$$

$$NH_3 + H^+ \rightarrow [NH_4]^+ \tag{2b}$$

The energy for reaction (2a) is called the deprotonation energy and the protonation energy is represented by

| Bond/pm or | H-Z[NH ₃] | H-ZINHAL | H-Z/INH, J[CH,OH] | Z./INH.1 | | Z-/[NIL] TNH. | NH. | Z-/INH.] '[CH.,OH] | СН,ОН |
|------------|-----------------------|----------|-------------------|----------|-------|---------------|-------|--------------------|-------|
| angic/ocg | HF | HF | HF | HF | ВЗСУР | HF | ВЗСУР | HF | взгур |
| A1-01 | 190.4 | 190.0 | 189.4 | 180.3 | 182.2 | 180.1 | 182.8 | 180.9 | 182.7 |
| 1-02 | 173.5 | 172.4 | 174.8 | 180.3 | 182.2 | 177.4 | 178.5 | 178.5 | 180.6 |
| AI-03 | 172.2 | 172.5 | 172.4 | 173.1 | 174.2 | 173.6 | 175.1 | 173.6 | 174.8 |
| 9 | 172.2 | 172.5 | 172.4 | 173.1 | 174.2 | 173.6 | 175.1 | 173.6 | 174.8 |
| < 0-17 > | 177.1 | 176.8 | 177.2 | 176.7 | 178.2 | 176.2 | 6771 | 176.6 | 178.2 |
| Si1-01 | 168.7 | 168.5 | 169.4 | 162.9 | 165.4 | 162.3 | 165.3 | 163.3 | 1991 |
| 2-02 | 161.5 | 160.2 | 163.7 | 162.9 | 165.4 | 160.6 | 163.4 | 162.6 | 165.0 |
| I-Hb | 6'86 | 99.4 | 99.3 | 1.67.7 | 157.7 | 163.7 | 149.7 | 158.7 | 148.9 |
| I-H1 | 100.5 | 101.1 | 100.8 | 104.0 | 108.1 | 102.6 | 108.0 | 102.8 | 106.2 |
| NI-N2 | , | 321.0 | ı | t | f | 296.3 | 276.8 | ı | ı |
| 1-01 | 271.4 | 7.2.72 | 272.0 | 263.4 | 258.4 | 267.4 | 260.0 | 264.4 | 259.6 |
| -05 | ı | 1 | 292.3 | 1 | 1 | i | 1 | 269.4 | 262.8 |
| 5-H5 | 1 | 1 | 95.4 | 1 | 1 | 1 | 1 | 96.4 | 8.66 |
| Si1-01-A1 | 128.1 | 126.5 | 128.5 | 128.7 | 127.1 | 130.6 | 124.8 | 124.0 | 121.7 |
| Si2-02-Al | 140.6 | 153,7 | 128.7 | 128.6 | 127.0 | 131.9 | 125.7 | 124.7 | 122.8 |
| 01-A1-02 | 8'86 | 1.66 | 105.0 | 100.8 | 8.96 | 99.4 | 101.5 | 106.2 | 104.9 |
| NI-HI-N2 | 1 | 171.2 | | 1 | 1 | 161.7 | 173.5 | 1 | 1 |
| OI-HP-N | 171.6 | 171.1 | 170.5 | 150.8 | 152.5 | 170.3 | 176.6 | 1.77.1 | 179.6 |
| 20 111 | | | | | | | | | |

Table 2

| Bond/pm or | .2 | | Z-H | | н-х/сн,он] | H] | н-2/[СН,ОН] | OH] ₂ | H-Z/CH30H][NH3] | [FHN][HC |
|------------|-------|--------|--------|-------|------------|-------|-------------|------------------|-----------------|----------|
| angie/0eg | HF. | B31,YP | HF | B3LYP | HF | ВЗГУР | HF | ВЗСУР | Ή | ВЗГУР |
| AI-01 | 176.1 | 177.6 | 194.4 | 194.7 | 191.3 | 190.8 | 190.2 | 189.3 | 190.7 | 189.4 |
| A1-02 | 176.1 | 177.6 | 171.9 | 173.9 | 174.4 | 177.2 | 174.8 | 177.6 | 173.9 | 176.7 |
| AI03 | 176.4 | 177.7 | 171.6 | 173.1 | 171.9 | 173.4 | 172.2 | 173.7 | 172.3 | 174.0 |
| A1-04 | 176.4 | 177.7 | 171.6 | 173.1 | 171.9 | 173.4 | 172.2 | 173.7 | 172.3 | 174.0 |
| < AI-0 > | 176.2 | 177.6 | 177.4 | 178.7 | 177.4 | 178.7 | 177.4 | 178.6 | 177.3 | 178.5 |
| Si1-01 | 158.5 | 160.8 | 170.1 | 171.3 | 169.4 | 170.4 | 6.691 | 170.9 | 1.69.1 | 170.4 |
| 12-02 | 158.5 | 160.8 | 161.4 | 163.5 | 162.4 | 164.8 | 162.8 | 165.1 | 6.191 | 164.4 |
| OI-Hb | | ı | . 95,3 | 97.3 | 97.3 | 101.4 | 5.76 | 102.5 | 0.86 | 103.3 |
| 05-06 | 1 | , | t | 1 | 97.3 | 101.4 | 271.7 | 260.1 | i | , |
| 01-05 | 1 | ı | í | ı | 264.4 | 253,3 | 267.6 | 255.6 | 266.3 | 253.4 |
| 5-Hb | ı | ı | 1 | ı | 170.7 | 156.7 | 170.8 | 153.2 | 169.0 | 150.2 |
| O6-H6 | ı | t | 1 | 1 | 1 | • | 95.5 | 9.66 | į | ı |
| 05-H5 | ι | ı | ı | 1 | 95.4 | 98.5 | 6.7 | 99.1 | 5.96 | 101.4 |
| Sil-Ol-Al | 149.1 | 141.4 | 131.4 | 133.0 | 128.1 | 127.3 | 124.2 | 122.3 | 124.4 | 122.6 |
| Si2-02-Al | 149.1 | 141.4 | 152.3 | 146.9 | 135.5 | 130.8 | 128.8 | 125.3 | 134.8 | 127.6 |
| 01-A1-02 | 106.5 | 104.6 | 92.8 | 89.7 | 0.66 | 8'.26 | 104. | 104.3 | 103.0 | 102.8 |
| 05-H5-06 | ı | ı | i | ı | 1 | t | 154.9 | 155.8 | 160.7 | 162.3 |
| 01-Hb-05 | 1 | 1 | ŀ | 1 | 160.5 | 157.5 | 171.7 | 178.4 | 171.4 | 177.9 |
| NI-H6 | ŧ | ı | 1 | , | ı | i | 1 | 1 | 9:001 | 102.8 |
| 05-Mt | i | ı | 1 | t | i | ı | 1 | 1 | 280.8 | 265.4 |
| 05-H5-M1 | ı | , | ŀ | 1 | ì | , | i | t | 160.7 | 162.3 |

reaction (2b). For an ion-pair, Z⁻/[NH₄] [CH₃OH], the complexation energy is the energy of the reaction

$$[Z^{-}]+[NH_{4}]^{+}+[CH_{3}OH] \rightarrow Z^{-}/[NH_{4}]^{+}[CH_{3}OH]$$

Finally, the conversion energy of a covalent structure to an ion-pair structure is the sum of the energies of the three reactions above, i.e.

 $H-Z/[NH_3][CH_3OH] \rightarrow Z^-/[NH_4]^+[CH_3OH]$ (4) The reaction energies of each step are summarized in the schematic diagram in Scheme 1. From the reaction energies (see Table 4) of all the complexes, we can propose the reaction mechanism of coadsorption of methanol and ammonia on H-Z as depicted in Scheme 2.

3.2. Coadsorption of methanol and ammonia on Na-zeolites (Na-Z)

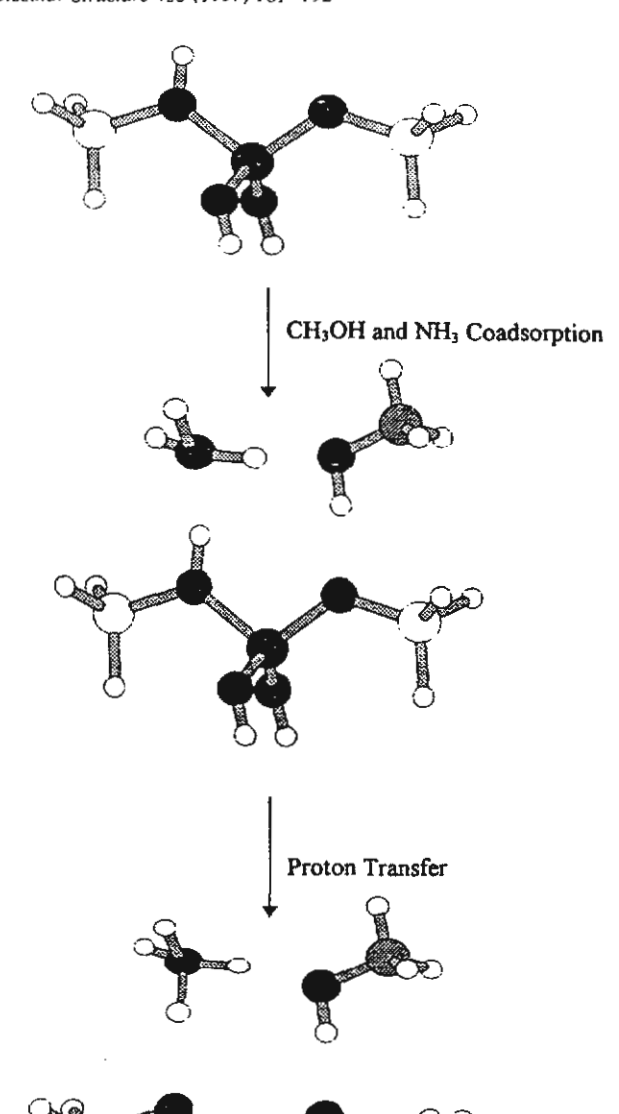
The effect of the cation on the structure of zeolitic catalysts and the coadsorption process is investigated at B3LYP/6-31G* and HF/6-31G* levels of theory. The fully optimized geometry structures for Na-Z, Na-Z/[NH₃], Na-Z/[CH₃OH], Na-Z/[NH₃][CH₃OH] and Na-Z/[CH₃OH][NH₃] are documented in Table 3.

3.2.1. The Na(1)/zeolite complex

The Na(I) does not bind with a particular bridging oxygen atom in the [AlO₄]⁻ but is symmetrically bidentated to the O1 and O2 of the [AlO₄]⁻ tetrahedron and the interaction has ionic character. The symmetric binding between Na(I) and [AlO₄]⁻ has been confirmed by an ESR experiment [34]. The optimized Na(I)...O distance is found to be 216.0 pm and the corresponding energy is 134.09 kcal mol⁻¹. Table 3 further indicates that the charge compensating Na(I) can affect the ≡Si-O-Al≡ by weakening the Si-O and Al-O bonds, as compared to the anionic framework (see Table 2).

H-Z+[NH₃]+[CH₃OH]
$$\xrightarrow{97.99}$$
 Z'+[NH₄]++[CH₃OH]
(i) 22.42 (iii) -119.67
H-Z/[NH₃][CH₃OH] $\xrightarrow{0.74}$ Z'/[NH₄]+[CH₃OH]

Scheme 1.



Scheme 2.

3.2.2. The Na-Z/[CH3OH] complex

The optimized Na(I)...O(Z) distance in the Na-Z/[CH₃OH] complex is 2.8 pm larger than in the Na(I)/zeolite complex. The Na...O(m) equilibrium distance of the Na-Z/[CH₃OH] complex is about 7.7 pm longer than the corresponding distance in the isolated Na(I) complex, Na(I)/[CH₃OH], in

Table 3
HF/6-31G* and B3LYP/631G* optimized structure parameters for H₃SiONaAl(OH)₂OSiH₃, H₃SiONaAl(OH)₂OSiH₃/[CH₃OH], H₃SiONaAl(OH)₂OSiH₃/[CH₃OH], H₃SiONaAl(OH)₂OSiH₃/[CH₃OH][NH₃] and H₃SiONaAl(OH)₂OSiH₃/[CH₃OH]

| | Z-gN | | Na-2/(NH) | = | Na-Z/CH OH | ОНІ | Na-Z/INH | Na-Z/[NH]][CH,OH] | Na-Z/CH | Na-Z/[CH,OH][NH,] |
|-----------|-------|-------|-----------|-------|------------|-------|----------|-------------------|---------|-------------------|
| angio ock | HF | B3LYP | H | B3LYP | 표 | B3LYP | HF | взгур | Ή | B3LYP |
| AI-01 | 180.3 | 182.0 | 179.8 | 181.5 | 179.8 | 181.5 | 179.6 | 181.2 | 179.6 | 181.3 |
| N-02 | 180.4 | 182.0 | 179.8 | 181.4 | 179.8 | 181.6 | 179.8 | 181.4 | 179.7 | 181.2 |
| 1-03 | 172.8 | 174.1 | .173.1 | 174.4 | 173.1 | 174.4 | 173.1 | 174.4 | 173.1 | 174.5 |
| 50 | 172.8 | 174.1 | 173.1 | 174.4 | 173.1 | 174.4 | 173.1 | 174.4 | 173.1 | 174.5 |
| < 0-14 > | 176.6 | 178.0 | 176.4 | 177.9 | 176.4 | 178,0 | 176.4 | 177.8 | 176.4 | 177.9 |
| IO-1 | 162.8 | 164.9 | 162.3 | 164.4 | 162.3 | 164.5 | 162.3 | 10-17-01 | 162,3 | 162,4 |
| 2-02 | 162.8 | 164.9 | 162.3 | 164.4 | 162.3 | 164.4 | 161.7 | 163.5 | 161.7 | 163.6 |
| 무 | ı | ì | 100.5 | 102.1 | ı | 1 | 8:001 | 10.28 | 100.4 | 102.0 |
| 01-05 | , | ı | ı | ţ | 424.0 | 420.8 | i | ı | 438.7 | 436.9 |
| 1×-1 | ŧ | t | 439.0 | 433.0 | ı | 1 | 450.9 | 449.2 | ì | ı |
| S-NI | 1 | ı | t | ı | ı | , | 310.6 | 298.6 | 289.0 | 276.9 |
| -Na | 217.6 | 216.0 | 220.9 | 219.5 | 220.6 | 219.1 | 221.7 | 220.7 | 221.7 | 220.6 |
| I-Na | ı | t | 242.3 | 238.8 | 1 | 1 | 239.6 | 235.7 | ı | i |
| 5-Na | ı | ı | ŀ | 1 | 227.8 | 225.7 | i | t | 223.6 | 220.6 |
| S-H5 | ı | ì | I | ı | 94.8 | 6'96 | 94.8 | 97.0 | 96.4 | 100.3 |
| Si1-01-Al | 129.8 | 127.5 | 131.0 | 128.6 | 131.1 | 128.5 | 131.4 | 129.0 | 131.1 | 128.8 |
| 2-02-AI | 130.1 | 127.6 | 131.0 | 128.6 | 131.1 | 128.6 | 132.0 | 130.5 | 132.1 | 130.4 |
| 01-AI-02 | 96.5 | 94.9 | 97.1 | 95.5 | 97.0 | 96.6 | 97.1 | 95.5 | 97.2 | 95.7 |
| 01-Na-05 | ı | t | 1 | ı | 142.0 | 142.2 | i | ı | 160.3 | 170.0 |
| I-Na-NI | 1 | 1 | 142.7 | 141.7 | 1 | t | 155.7 | 159.7 | ı | ı |
| 05-H5-NI | ŀ | ı | ı | ı | i | ı | ı | ı | 176.0 | 175.0 |
| N1-H1-05 | | | 1 | | , | ŀ | 168.7 | 168.8 | | |

accordance with the lower binding energy; $\Delta E(\text{Na(I)/CH}_3\text{OH}) = -31.08 \text{ kcal mol}^{-1}$, $\Delta E(\text{Na-Z/CH}_3\text{OH}) = -18.39 \text{ kcal mol}^{-1}$.

One point of interest is that the Na-Z/[CH₃OH] leads to an increased positive charge for the methanol hydrogen by about 0.0462. This suggests that the ability of the methanol molecule to form a hydrogen bond as a proton-donor molecule is enhanced with Na-Z attached to the methanol oxygen atom. We note that the absolute values from Mulliken population analysis are not very reliable, and also depend on the basis set employed. However, within closely related structures a useful value will be yielded.

3.2.3. The Na-Z/[CH₃OH][NH₃] complex

The changes in structural parameters of the coadsorption complexes Na-Z/[CH₃OH][NH₃] are in agreement with Gutmann's rule [33], i.e. a lengthening of the methanol OH bond, a shortening of Na...O(m), a lengthening of Na...O(Z), and a shortening of the Al-O (adjacent to sodium atom) and Si-O bonds, as illustrated in Fig. 4c. The optimized Na(I)...O(m) distance in the Na-Z/[CH₃OH][NH₃] is 5.1 pm smaller than in the Na-Z/[CH₃OH] complex, where O(m) and O(Z) denote methanol oxygen and oxygen of zeolite, respectively. The rotational energy barrier around the O-H...N bond of the Na-Z/[CH₃OH][NH₃] complex is lower than KT. Thus Na-Z does not seem to hinder the free rotation of the ammonia molecule.

Another additional point of interest is that the OH...N distance is contracted from the 289.2 pm found in the H-bonded dimers of CH₃OH...NH₃ to 276.9 pm for Na-Z/[CH₃OH][NH₃]. This reduced O-H...N distance reflects an increase of binding energy due to the Na-Z. This can also be simply rationalized on the basis of the hydrogen atom population. The Na-Z leads to a decrease in electron density at the methanol proton in the Na-Z/[CH₃OH][NH₃] of 0.1088 units, compared to 0.0588 units in the CH₃OH...NH₃.

From the reaction energies in Table 4, the reaction mechanism may be proposed as depicted in Scheme 3.

Fig. 4. Schematic representation of molecular models for the systems: a) $[H_3SiONaAl(OH)_2OSiH_3]$; [Na-Z); b) $[H_3SiONaAl(OH)_2OSiH_3]$ / $[CH_3OH]$; c) $[H_3SiONaAl(OH)_2OSiH_3]$ / $[CH_3OH]$ [$[NH_3]$.

Table 4
Computed binding energies

| Systems | Binding energy | y (– Δ <i>E</i> /kcał mol ⁻¹) |
|--|----------------|--|
| | HF/6-31G* | B3LYP/6-31G* |
| [H ₃ SiOHAl(OH ₂)OSiH ₃]/ [CH ₃ OH] | 13.50 | 18.48 |
| [H ₃ SiOHAl(OH ₂)OSiH ₃)/ [CH ₃ OH] ₂ | 21.51 | 29.60 |
| [H ₃ SiOHAl(OH ₂)OSiH ₃]/ [CH ₃ OH][NH ₃] | 22.13 | 31.64 |
| [H ₃ SiOHAl(OH ₂)OSiH ₃]/ [NH ₃] | 15.81 | - |
| [H ₃ SiOAl(OH ₂)OSiH ₃]/ [NH ₄] ⁺ | 112.25 | 120.96 |
| [H ₃ SiOHAl(OH ₂)OSiH ₃]/ [NH ₃] ₂ | 21.47 | - |
| (H ₃ SiOAt(OH ₂)OSiH ₃)/ [NH ₄)*(NH ₃) | 120.08 | 130.02 |
| [H ₃ SiOHAl(OH ₂)OSiH ₃]/ [NH ₃][CH ₃ OH] | 22.42 | - |
| [H ₃ SiOAl(OH ₂)OSiH ₃]/ [NH ₄] [†] [CH ₃ OH] | 119.67 | 131.59 |
| [H ₃ SiONaAl(OH ₂)OSiH ₃]/ [NH ₃] | 19.72 | 21.57 |
| [H ₃ SiON ₂ AI(OH ₂)OSiH ₃]/ [NH ₃][CH ₃ OH] | 27.07 | 31.03 |
| [H ₃ SiONaAl(OH ₂)OSiH ₃]/ [CH ₃ OH] | 17.33 | 18.39 |
| [H ₃ SiON ₂ Al(OH ₂)OSiH ₃]/ [CH ₃ OH][NH ₃] | 30.34 | 35.76 |

Scheme 2 and Scheme 3 indicate that when the methanol and ammonia are coadsorbed, the methanol preferentially adsorbs on Na-Z, while the ammonia binds favorably to H-Z. Our findings are in excellent agreement with very recent experimental data [23].

4. Conclusion

We have carried out HF and B3LYP methods with 6-31G* basis set to investigate the coadsorption of methanol and ammonia on H-zeolities (H-Z) and alkaline-exchanged zeolites (Na-Z). Comparing HF and B3LYP results with available experimental data, the B3LYP yields structural parameters which are in good agreement with experimental data. The Al...H distance of zeolite has been estimated experimentally as 238 ± 4 pm, whereas our B3LYP value is 239.7 pm.

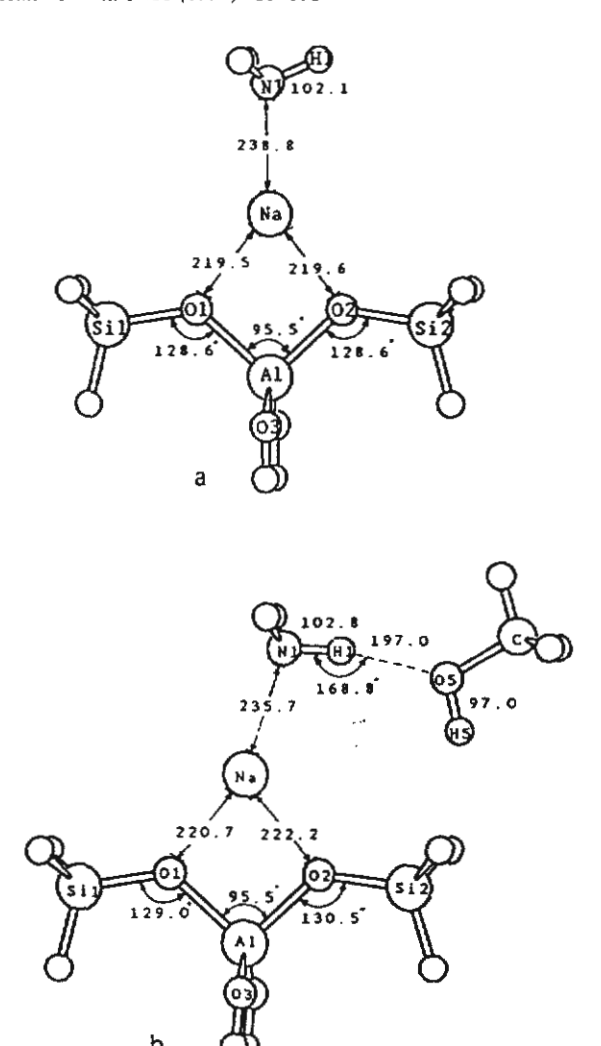
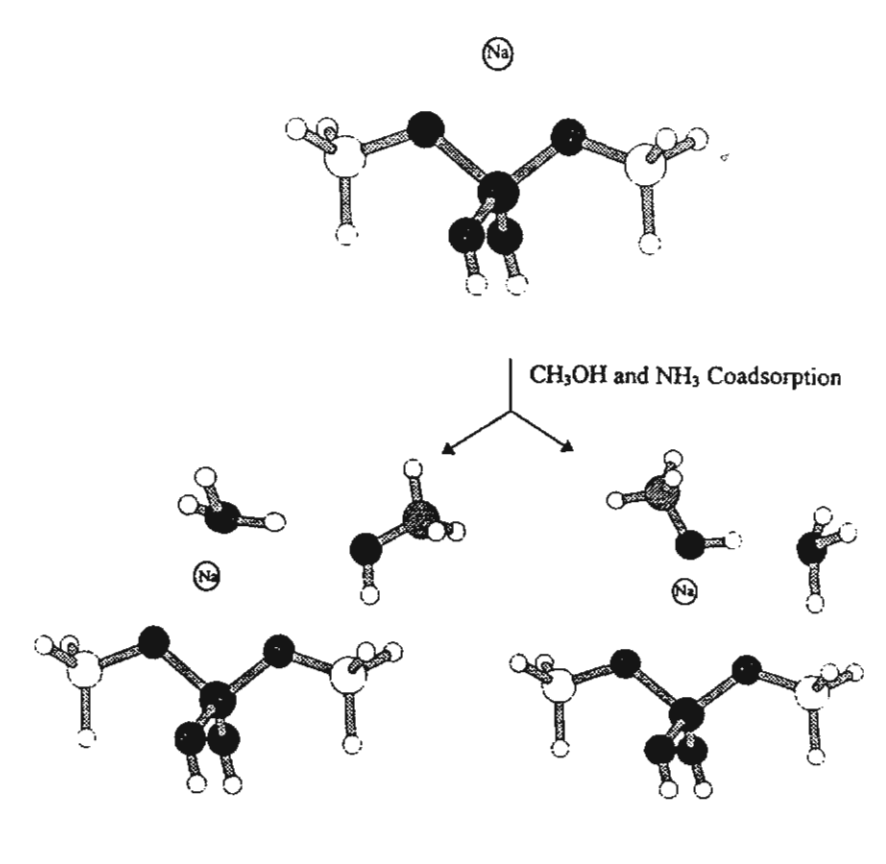


Fig. 5. Schematic representation of molecular models for the systems: a) [H₃SiONaAl(OH)₂OSiH₃]/[NH₃]; b) [H₃SiONaAl(OH)₂OSiH₃]/ [NH₃][CH₃OH].

A comprehensive study of the coadsorption of absorbate molecules with the surface hydroxyl reveals several interesting points. Structure Na-Z/[CH₃OH][NH₃] is lower in energy than Na-Z/[NH₃][CH₃OH], which suggests that the former is more favourable in the coadsorption process. The reaction mechanism of coadsorption of methanol and ammonia on H-Z is that the ammonia is found to stabilize to the Brønsted acid site of H-Z, generating an ammonium cation, which acts as an active site for methanol.



 $\Delta E = -31.03 \text{ kcal/mol}$

 $\Delta E = -35.76 \text{ kcal/mol}$

Scheme 3.

The results obtained in the present study are very useful from the experimental point of view, since the adsorption and coadsorption processes on the surface site are found to play a significant role in catalytic processes.

Acknowledgements

This work was supported by donors of the Thailand Research Fund (TRF) in supporting the research career development project (The TRF research scholar) and the Kasetsart University Research and Development Institute (KURDI). Our sincere thanks are due to Professor R. Ahlrichs (Karlsruhe, Germany) for his continued support of this work.

References

- [1] J. Klinowski, Chem. Rev. 91 (1991) 1459.
- [2] J.M. Thomas, Sci. Am. 266 (1991) 82.
- [3] G.J. Kramer, R.A. van Santen, C.A. Emeis, A.K. Nowak, Nature 363 (1993) 529.
- [4] E. Kassab, J. Fouquet, M. Allavena, A.M. Evleth, J. Phys. Chem. 97 (1993) 9034.
- [5] C.T.W. Chu, C.D. Chang, J. Phys. Chem. 89 (1985) 1569.
- [6] M.A. Makarova, S.P. Bates, J. Dwyer, J. Am. Chem. Soc. 117 (1995) 11309.
- [7] J. Das, C.V.V. Satyanaryana, D.K. Chakrabarty, S.N. Piramanayagarn, S.N. Shringi, J. Chem. Soc., Faraday Trans. 88 (1992) 3255.
- [8] S.R. Blazkowski, R.A. van Santen, J. Phys. Chem. 99 (1995) 11728.
- [9] H.J. Soscun, P.J. Omalley, A. Hinchcliffe, J. Mol. Struct. (Theochem) 341 (1995) 237.
- [10] J. Limtrakul, S. Pollman-Hannongbua, J. Mol. Struct. (Theochem) 280 (1993) 139.

- [11] J. Limtrakul, J. Mol. Struct. 288 (1993) 105.
- [12] J. Limtrakul, J. Yoinuan, D. Tantanak, J. Mol. Struct. 312 (1994) 183.
- [13] J.A. Zygmunt, L.A. Curtiss, L.E. Iton, M.K. Erhardt, J. Phys. Chem. 100 (1996) 6663.
- [14] M. Krossner, J. Sauer, J. Phys. Chem. 100 (1996) 6199.
- [15] F. Haase, J. Sauer, J. Am. Chem. Soc. 117 (1995) 3780.
- [16] J. Limtrakul, Chem. Phys. 193 (1995) 79.
- [17] J. Sauer, P. Ugliehgo, E. Garrone, V.R. Saunders, Chem. Rev. 94 (1994) 2095.
- [18] G. Mirth, J.A. Lercher, M.W. Anderson, J. Klinowski, J. Chem. Soc. Faraday Trans. 86 (1990) 3039.
- [19] R.A. van Santen, G.J. Kramer, Chem. Rev. 95 (1995) 637.
- [20] S.L. Meisel, J.P. McCullogh, C.H. Lechthaler, P.B. Weisz, Chem. Tech. 6 (1976) 86.
- [21] E. Nusterer, P.E. Blochl, K. Schwarz, Angew. Chem. Int. Ed. Eng. 35 (1996) 175.
- [22] W.E. Farneth, R.J. Gorte, Chem. Rev. 95 (1995) 615.
- [23] A. Kogelbauer, G. Grundling, J.A. Lercher, J. Phys. Chem. 100 (1996) 1837-1852.
- [24] J. Limtrakul, P. Treesakol, Chem. Phys. 215 (1997) 77.

- [25] J. Limtrakul, D. Tantanak, J. Mol. Struct. 358 (1995) 179.
- [26] J. Limtrakul, D. Tantanak, Chem. Phys. 208 (1996) 331.
- [27] Frisch, M.J., Trucks, G.W., Schlegel, H.B., Gill, P.M.W., Johnson, B.G., Wong, M.W., Foresman, J.B., Robb, M.A., Head-Gordon, M., Replogle, E.S., Gomperts, R., Andres, J.L., Raghavachari, K., Binkley, I.A., Gonzalez, C., Martin, R.L., Fox, D.J., DeFrees, D.J., Baker, J., Stewart, J.J.P., Pople, J.A., Gaussian 94 (Gaussian Inc., Pittsburgh, 1994).
- [28] R. Ahlrichs, R. Baer, M. Haeser. H. Horn, C. Koemel, Chem. Phys. Lett. 162 (1989) 165.
- [29] M. Haeser, R. Ahlrichs, J. Comput. Chem. 10 (1989) 104.
- [30] J. Almtoef Jr, K. Faegri, K. Korsell, J. Comput. Chem. 3 (1982) 385.
- [31] J.A. Pople, D.L. Beveridge, Approximate Molecular Orbital Theory, McGraw-Hill Inc., New York, 1970.
- [32] D. Freude, J. Klinowski, H. Hamdan, Chem. Phys. Letters 149 (1988) 355.
- [33] V. Gutmann, The Donor-Acceptor Approach to Molecular Interactions, Plenum Press, New York, 1978.
- [34] H. Hozono, H. Kawazoc, J. Nishii, J. Kanazawa, J. Non-Cryst. Solid 51 (1982) 217.

Structure and Reaction Pathways for Methylamine/Zeolite System

Jumras Limtrakul and Mayuso Kuno

Laboratory for Computational & Applied Chemistry, Chemistry Department, Faculty of Science, Kasetsart University, Bangkok 10900/THAILAND; fscijrl@ku.ac.th

ABSTRACT

Reaction pathways of methylamine synthesis from methanol and ammonia on zeolite (ZOH) have been carried out using Hartree-Fock (HF) and density functional theory (DFT) approaches. Structures of the adsorption reactants, transition states, intermediates, and adsorption products were optimized at DFT(B3LYP) and HF levels of theory using 6-31G(d). Four different reaction pathways, including Langmuir-Hinshelwood (methanol and ammonia are both bound to Brønsted acid sites) and Eley-Rideal (two adsorbing molecules react; methanol is unbound, the ammonia is bound to a Brønsted acid site) mechanisms of methylamine production, were investigated. The reaction pathway which involves dehydration of one methanol and generating surface methoxy species was found to possess a substantially higher activation energy barrier. The lower corresponding energy was estimated for methoxy-zeolite formation from coadsorption of CH₃OH and NH₃ at Brønsted acid sites. The reaction pathways involving an associative reaction were, however, found to be more preferable in methylamine formation.

INTRODUCTION

For many years, zeolites have been found in industrial applications as catalysts in petrochemical processes, because of their unique catalytic activity, excellent selectivity as well as superior stability in many important conversions and upgrading processes as compared to other materials [1]. The acidity of zeolitic catalysts released from the surface hydroxyls (\equiv Si-OH-Al \equiv) is responsible for catalytic function [2-3]. The structure of such catalytic sites and their mode of interaction with simple adsorbates have been investigated as a crucial step in elucidating the catalytic reaction mechanism occurring at these active sites.

Of particular interest in this active research is the products generated from the adsorption of methanol (i.e., conversion of methanol to gasoline) and the coadsorption of methanol and ammonia (the production of methylamines which are essential chemical building subunits for important industrial materials such as resins, fibers, dyes and pharmaceuticals) [4]. One of the crucial steps of these chemically interesting systems involves the adsorption of probed molecules on the catalyst surface.

Structure and Reaction Pathways for Methylamine/Zeolite System

Jumras Limtrakul and Mayuso Kuno

Laboratory for Computational & Applied Chemistry, Chemistry Department, Faculty of Science, Kasetsart University, Bangkok 10900/THAILAND; fscijrl@ku.ac.th

ABSTRACT

Reaction pathways of methylamine synthesis from methanol and ammonia on zeolite (ZOH) have been carried out using Hartree-Fock (HF) and density functional theory (DFT) approaches. Structures of the adsorption reactants, transition states, intermediates, and adsorption products were optimized at DFT(B3LYP) and HF levels of theory using 6-31G(d). Four different reaction pathways, including Langmuir-Hinshelwood (methanol and ammonia are both bound to Brønsted acid sites) and Eley-Rideal (two adsorbing molecules react; methanol is unbound, the ammonia is bound to a Brønsted acid site) mechanisms of methylamine production, were investigated. The reaction pathway which involves dehydration of one methanol and generating surface methoxy species was found to possess a substantially higher activation energy barrier. The lower corresponding energy was estimated for methoxy-zeolite formation from coadsorption of CH₃OH and NH₃ at Brønsted acid sites. The reaction pathways involving an associative reaction were, however, found to be more preferable in methylamine formation.

INTRODUCTION

For many years, zeolites have been found in industrial applications as catalysts in petrochemical processes, because of their unique catalytic activity, excellent selectivity as well as superior stability in many important conversions and upgrading processes as compared to other materials [1]. The acidity of zeolitic catalysts released from the surface hydroxyls (\equiv Si-OH-Al \equiv) is responsible for catalytic function [2-3]. The structure of such catalytic sites and their mode of interaction with simple adsorbates have been investigated as a crucial step in elucidating the catalytic reaction mechanism occurring at these active sites.

Of particular interest in this active research is the products generated from the adsorption of methanol (i.e., conversion of methanol to gasoline) and the coadsorption of methanol and ammonia (the production of methylamines which are essential chemical building subunits for important industrial materials such as resins, fibers, dyes and pharmaceuticals) [4]. One of the crucial steps of these chemically interesting systems involves the adsorption of probed molecules on the catalyst surface.

In spite of a large number of documents about zeolite research, the details of structures and reaction mechanisms of adsorption [2,5-8], and particularly of coadsorption [9] are still incomplete and only partially solved.

METHODS

We employed the adsorption clusters illustrated in Figure 1-5 as the models of all possible adsorption reactants: [XOHAl(OH)₂OX]/[CH₃OH], [XOHAl(OH)₂OX]/[CH₃OH][NH₃], [XOHAl(OH)₂OX]/[NH₃] [CH₃OH]; adsorption surface methoxy intermediates, [XOCH₃Al(OH)₂OX]/[NH₃], [XOCH₃Al(OH)₂OX]/[H₂O]; transition state complexes, and adsorption products, [XOHAl(OH)₂OX]/[CH₃NH₂], [XOHAl(OH)₂OX]/[CH₃NH₂], [XOHAl(OH)₂OX]/[CH₃NH₂], where X=H and SiH₃, hereafter referred to as 1T and 3T cluster models for HOHAl(H)₂OH and H3SiOHAl(H)₂OSiH₃, respectively.

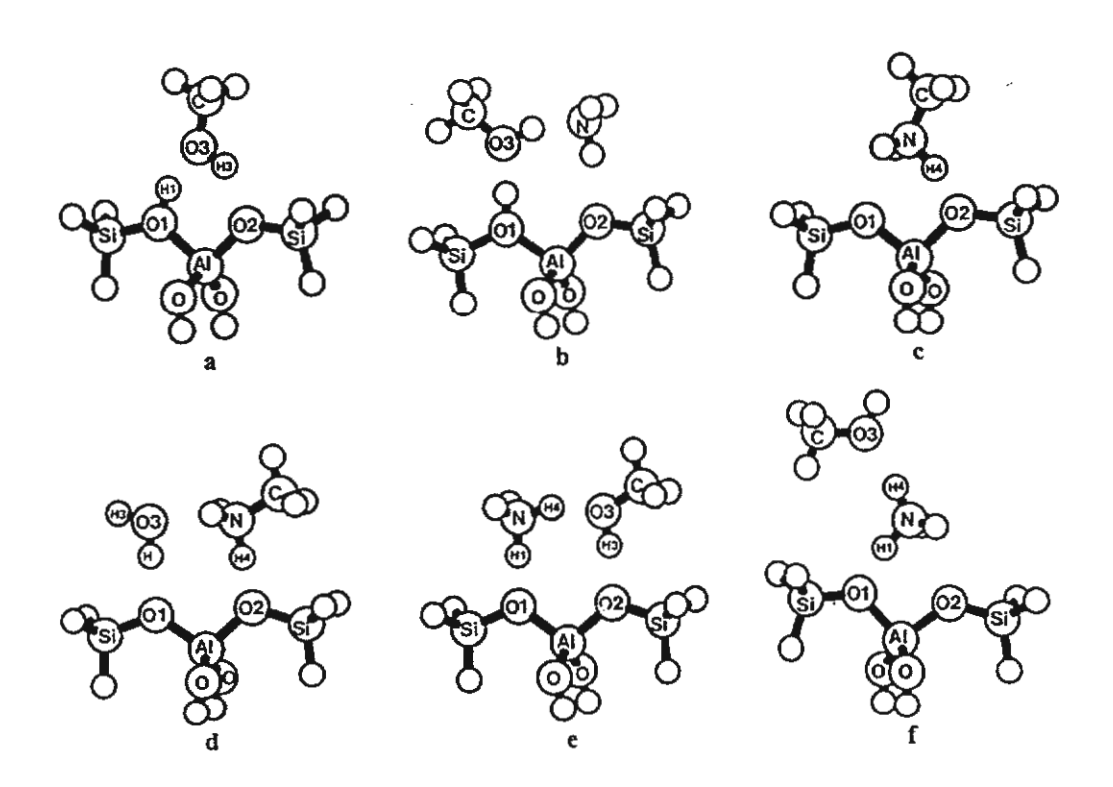


Figure 1. Optimized structures for different adsorption complexes (H₃SiOHAl(OH)₂OSiH₃ (3T), H₃SiOHAl(OH)₂OSiH₃/CH₃OH (1a), H₃SiOHAl(OH)₂OSiH₃/CH₃OH/NH₃ (1b), [H₃SiOAl(OH)₂OSiH₃]⁻/[CH₃NH₃]⁺/H₂O (1d), [H₃SiOAl(OH)₂OSiH₃]⁻/CH₃OH/[NH₄]⁺ (1e), [H₃SiOAl(OH)₂OSiH₃]⁻/[NH₄]⁺/CH₃OH/ (1f)) at B3LYP/6-31G(d) level of theory.

Full geometry optimization of the cluster models mentioned above was carried out with the DFT methods employing B3LYP density functional. This functional has been recently

demonstrated to yield accurate results about molecular structures, and vibrational frequencies for zeolites [10-11]. Transition state searches were performed using an eigenvalue-following algorithm [12]. On each optimized cluster, a vibrational analysis was made in order to obtain the normal modes. Final energies of some adsorption complexes were improved from point calculations at B3LYP/6-311+G(3df,2p) theoretical level. All density functional computations were performed using the program Gaussian-94 [13].

For the HF calculations, we employed the TURBOMOLE code [14] which is based on the direct SCF method. Geometry optimization was terminated when the gradient norm with respect to internal coordinates was less than 10^{-3} E_h/a₀. The energy change was then below 5×10^{-6} a.u.

The computations were carried out using DEC Alphastation 250 and HP 9000/700 workstations at the Laboratory for Computational and Applied Chemistry at Kasetsart University.

RESULTS AND DISCUSSION

Four different reaction pathways of methylamine synthesis have been investigated, as depicted in Figures 2-5.

The first reaction pathway for methylamine formation: One methanol molecule is adsorbed on the catalyst surface to yield ZOCH₃, followed by the interaction of ammonia to yield MeNH₂.

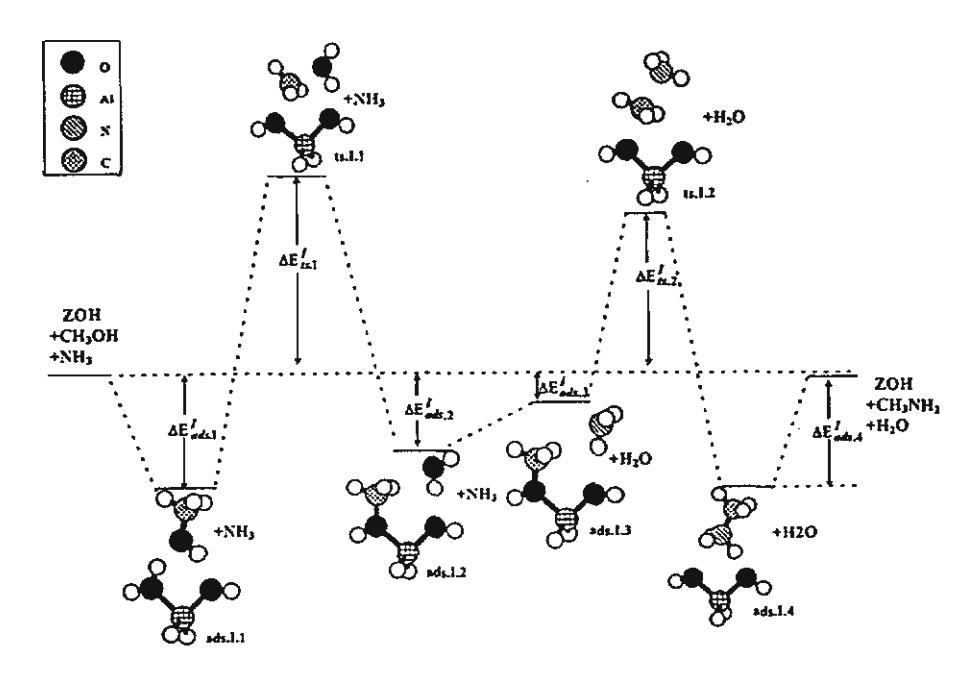


Figure 2. Path I: One CH₃OH is adsorbed on ZOH, ZOCH₃ generated, and the interaction of NH₃ with ZOCH₃ to yield methylamine.

The first reaction mechanism involves only one CH₃OH molecule adsorbed on the zeolitic acid site, ZOH/CH₃OH (see ads.I.1, Figure 2) which is then dehydrated and leaves a methyl group attached to the zeolite basic oxygen, ZOCH₃.

The adsorption energies of ZOH/CH₃OH were found to be -56.48 and -77.32 kJ/mol for 3T cluster models at HF and B3LYP levels of theory, respectively, which is in agreement with other theoretical values ranging from -56 to -89 kJ/mol [2,7,8] depending on the method and cluster size employed. Sauer's HF estimate of the adsorption energy of the large cluster (11T model fragment of faujasite) was -83.0 kJ/mol after correction for electron correlation, ZPE and BSSE. Experimental estimates of the heat of adsorption in acidic zeolites range from -63 [15] and -110 to -120 kJ/mol [referenced in ref. 2].

| Parameters | 3 <u>T</u> | la | lb | lc | ld | le | lf |
|--------------|------------|--------|--------|--------|--------|----------|--------|
| Al-01 | 194.67 | 190.80 | 189.45 | 179.55 | 180.01 | 182.70 | 182.71 |
| Ai-O2 | 173.89 | 177.18 | 176.69 | 183,14 | 182.78 | 180.57 | 179.35 |
| O1-H1 | 97.30 | 101.36 | 103.34 | - | 173.52 | 148.87 | 151.13 |
| 01-03 | - | 253.28 | 253.45 | - | 272.72 | 382.63 | 461.78 |
| O2-O3 | - | 267.96 | 372.47 | - | 398.68 | 267.46 | 553.16 |
| O3-H3 | - | 98.48 | 101.38 | - | 96.74 | 99.84 | 96.81 |
| 01-N | - | - | 406.18 | 263.98 | 361.00 | - 259.68 | 259.27 |
| O2-N | - | - | 299.77 | 256.69 | 260.72 | 379.21 | 268.22 |
| 03-N | - | - | 265.38 | - | 258.72 | 262.75 | 284.99 |
| O2-H3 | - | 181.22 | 340.31 | - | 487.34 | 168.09 | 620.88 |
| O2-H4 | - | - | 197.82 | 147.55 | 150.89 | 333.32 | 371.66 |
| N-HI | - | - | 331.31 | - | 274.99 | 110.81 | 109.61 |
| N-H4 | - | - | 102.81 | 110.77 | 109.87 | 106.16 | 103.57 |
| O1-A1-O2 | 89.66 | 97.84 | 102.83 | 97.88 | 103.20 | 104.86 | 98.23 |
| O1-H1-O3 | - | 157.51 | 177.90 | - | 175.70 | 116.14 | 139.10 |
| 01-H1-N | - | • | 130.57 | | 105.20 | 179.56 | 167.71 |
| O2-H3-N | - | - | 61.73 | - | 31.27 | 108.71 | - |
| O2-H4-N | - | - | 170.82 | 166.96 | 178.00 | 107.62 | - |
| O3-H4-N | - | ~ | 70.34 | - | 59.45 | 159.99 | 172.32 |
| Al-O1-HI | - | 113.35 | 122.80 | - | 131.69 | 125.00 | 105.94 |
| Al-O2-H4 | - | - | 131.03 | 105.78 | 120.04 | .96.47 | 99.44 |
| AI-O1-O3 | - | 98.22 | 124.04 | - | 130.12 | 81.58 | 134.47 |
| AI-02-N | - | - | 127.89 | 100.19 | 120.88 | 80.99 | 98.50 |
| -ΔE (kJ/mol) | | 77.31 | 132.40 | 101.61 | 151.27 | 148.04 | 132.80 |

Table 1: Optimized structure parameters (distances in pm and angles in deg.) and binding energies (kJ/mol) for different adsorption complexes (cf. Figure 1).

The activation energy, ΔE_{sct}^{I} , is quite high, +245.79 kJ/mol. However, this value compares well with the results of Sinclair and Catlow [5] 250 and 244 kJ/mol at the DFT/DZVP and DFT/DZVP levels of theory, respectively. The high value of ΔE_{sct}^{I} indicates that this catalytic route may therefore only play a minor role in methanol activation over acidic zeolites. A similar conclusion for DME formation from methanol has been noted by Catlow group [5].

The optimized geometrical parameters of zeolitic clusters with methylamine are reported for the first time and summarized in Table 1. The results for the surface complex cluster indicate that the adsorbed methylamine interacts strongly with the Brønsted acid sites of zeolite and form protonated methylamine cation, [CH₃NH₃]⁺, on the catalytic surface with the adsorption energy of -101.61 kJ/mol. The change in the structural parameters of zeolite upon complexation with methanol are impressive. The results are in line with Gutmann's rule [16], i.e. a lengthening of the bridging O-H bond, a shortening of Al-O adjacent to this bond, and a lengthening of Al-O (not adjacent to it).

The intermolecular O-H...N hydrogen bond in the ZOH/MMA complex, [H₃SiOAl(OH)₂OSiH₃][†], is evaluated to be 256.69 pm, less than that found in the neutral complexes. The contracted intermolecular distance of the complex reflects an increase of the binding energy (-101.61 versus -83.56 kJ/mol). The energy for conversion of [H₃SiOAl(OH)₂OSiH₃]/[CH₃NH₃][†] to [H₃SiOHAl(OH)₂OSiH₃]/[CH₃NH₂] is -18.05 kJ/mol. The result implies that the desorbed CH₃NH₂ is difficult to generate without the help of other adsorbates, e.g. NH₃ molecules in this study.

The second reaction pathway for methylamine formation: Simultaneous adsorption of CH₃OH and NH₃ on ZOH generating TS structure for methylamine formation.

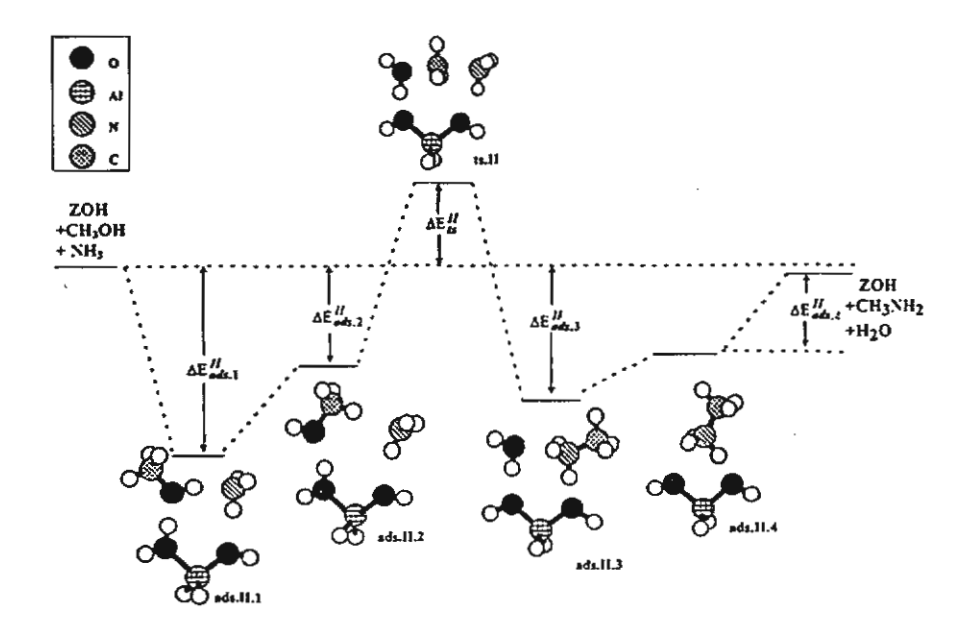


Figure 3. Path II: Simultaneous adsorption of CH₃OH and NH₃ on ZOH, generating a transition state structure for methylamine formation.

Structures of adsorption reactants, adsorption surface methoxy intermediates, and the adsorption products are shown in Figure 3. Selected optimized geometrical structures are tabulated in Table 1.

The starting adsorption reactants involve methanol and ammonia simultaneously adsorbed on ZOH (ads.II.1 in Figure 3). The adsorption energy ($\Delta E_{ads.II.1}^{II}$) for this adsorption complex is found to be -132.40 kJ/mol. Although no identical system has been published so far, our calculated adsorption energy, $\Delta E_{ads.II.1}^{II}$, of chemically different admolecules of methanol and ammonia should be compared also to the adsorption energy of chemically identical admolecules of two methanol molecules (-123.85 kJ/mol (B3LYP) for 3T/[CH₃OH]₂). These energy values can also be compared to the initial théoretical investigations of adsorption energy of two methanol molecules at the zeolitic surface [2,7-8]. Gale's DFT/BLYP estimated adsorption energy of the two methanols was -119.16 kJ/mol for 4Tcluster model [8]. Limtrakul [7] reported similar adsorption energies of -56.48 kJ/mol for the first and -35.52 kJ/mol for the second methanol from calculations at the HF theoretical level.

In order to search for the transition state complex of methylamine formation, the preferred configuration, (ads.II.2, Figure 3), has to be selected. This adsorption complex, ads.II.2, can be achieved by rotating the methanol molecule in such a way that the methyl group can be attached by the nucleophile, NH₃. The structure of transition state may be derived from the S_N2 reaction between the methoxonium cation and nucleophile NH₃. The activation energy barrier related to the adsorption complex, ads.II.2 is evaluated to be -126.09 kJ/mol, which is less stable than the ads.II.1 by 57.47 kJ/mol. The overall activation energy barrier related to the ads.II.1 for this reaction route becomes 183.56 kJ/mol. The activation energy at B3LYP/6-311G+(3df,2p)//B3LYP/6-31G(d) level of theory was 171.98 kJ/mol, which is about 12 kJ/mol lower than the fully optimized B3LYP/6-31G(d) structure.

The third reaction pathway for methylamine formation: Methanol and Ammonia are simultaneously adsorbed on ZOH generating ZOCH₃, which interacts with the ammonia promoter to yield methylamine.

The side-on MeOH/NH₃ adsorption, ads.III.2 (Figure 4) is supposed to be the precursor for the formation of surface methoxy intermediate, ads.III.4, which may further interact with ammonia to yield methylamine. However, the most stable adsorption reactants, ads.III.1, where ammonia is adsorbed on the zeolitic acid site, is about 40 kJ/mol more stable than the side-on MeOH/NH₃ adsorption (ads.III.2). The ΔE_{set}^{III} which is related to ads.III.1 is found to be 197.10 kJ/mol. This activation energy barrier is very much lower than ΔE_{set}^{I} obtained from the first type of reaction pathway. It is clearly due to the lesser strain in the transition-state structure, ts.III.1. The three-center angle of the transition-state structure is calculated to be ca. 170°, which is close to the optimum angle of 180° for an S_N2 mechanism. The result indicates that the influence of the adsorbed ammonia is to significantly decrease ΔE_{set}^{III} , which enhances the methylation reaction. Due to the lower activation energy, ΔE_{set}^{III} , as compared to ΔE_{set}^{II} of the first reaction route, this reaction route may play a significant role in methylamine synthesis.

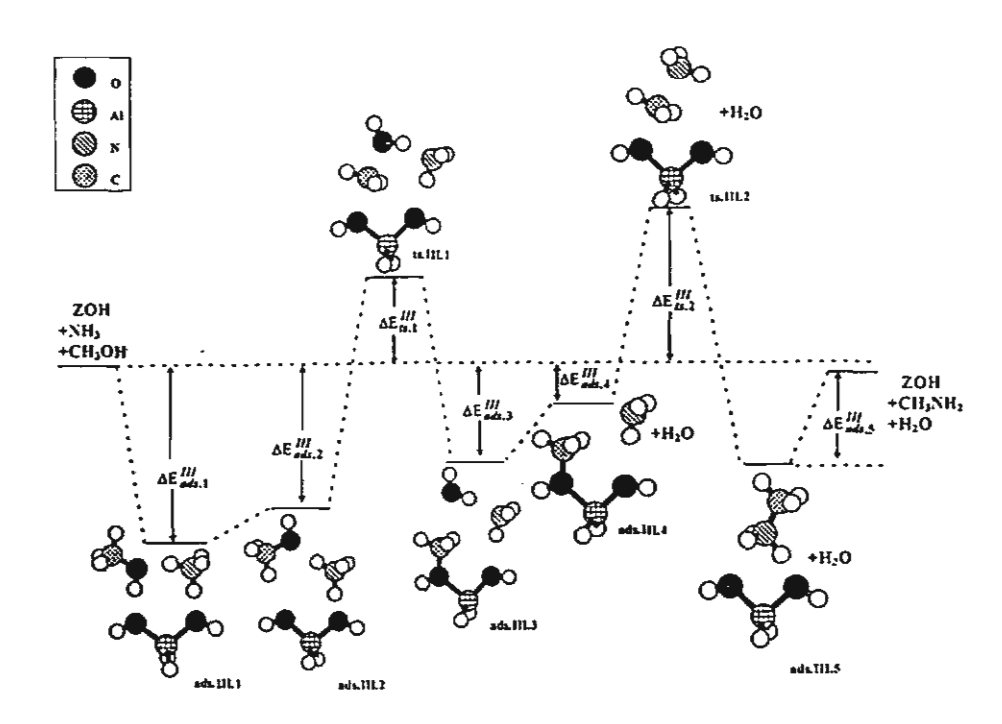


Figure 4. Path III: Both CH₃OH and NH₃ are adsorbed on ZOH, ZOCH₃ is generated via S_N2 with the help of the promoter NH₃, and the interaction of NH₃ with ZOCH₃ to yield methylamine formation.

The fourth reaction pathway for methylamine formation: Eley-Rideal mechanism where only NH₃ is adsorbed on the Brønsted acid site, followed by CH₃OH binding to the adsorbed NH₃, generating TS structure.

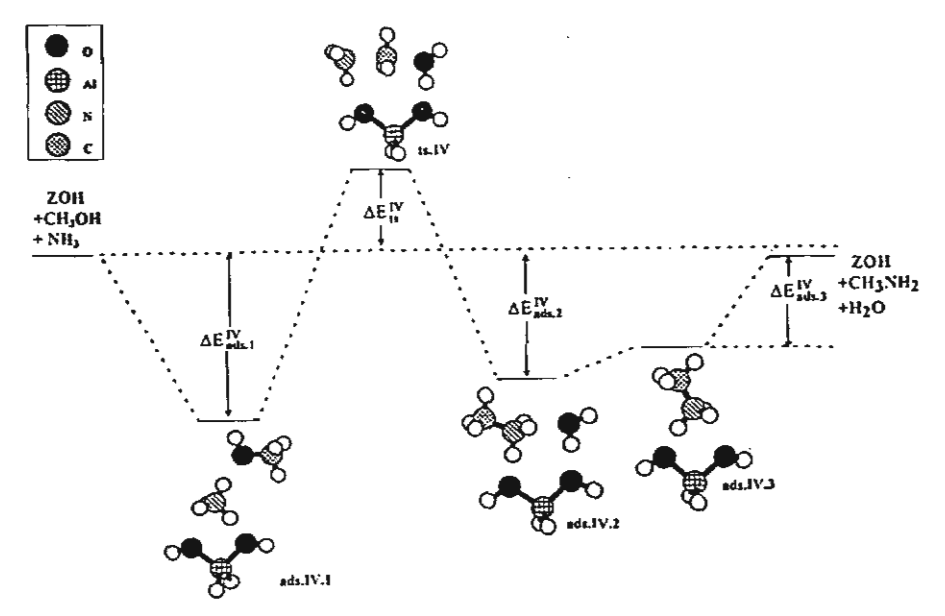


Figure 5. Path IV: Only NH₃ is adsorbed on the Brønsted acid site, CH₃OH is bound to the adsorbed NH₃, generating transition state structure which is converted to methylamine formation.

The aforementioned second and third reaction pathways, which involve the binding of both methanol and ammonia to Brønsted acid sites, follow a Langmuir-Hinshelwood mechanism.

In contrast, the last reaction pathway is dictated by the Eley-Rideal mechanism where only NH₃ is adsorbed on the Brønsted acid site, followed by CH₃OH binding to the adsorbed NH₃. To obtain the desired product, methoxonium cation is first generated via the Eley-Rideal precursor complex, which then reacts with ammonia, and loses water to yield a protonated methylamine. ΔE_{sc}^{tv} related to the Eley-Rideal configuration is found to be 183.85 kJ/mol.

CONCLUSIONS

We conclude that paths II, III, IV are the suggested reaction pathways, but paths (II and IV) involving the associative mechanism are the more preferred reaction routes due to a lower activation energy as compared to the path III. The results obtained in the present study are very useful from the experimental point of view, since the adsorption and coadsorption processes on the surface site are found to play a significant role in the catalytic process.

ACKNOWLEDGEMENTS

This research was supported by the Thailand Research Fund and KURDI.

REFERENCES

- 1. I.E. Maxwell, Cattech 1, 5 (1997).
- 2. F.Haase and J. Sauer, J. Am. Chem. Soc. 117, 3780.(1995).
- 3. R.A. van Santen and G.J. Kramer, Chem. Rev. 95, 637 (1995).
- 4. A. Kogelbaner and J.A. Lercher, J. Chem. Soc. Faraday Trans. 88, 2283 (1992).
- 5. P.E. Sinclair and C.R.A. Catlow, J. Chem. Soc., Faraday Trans. 93(2), 333 (1997).
- 6. S.R. Blaszkowski and R.A. van Santen, J. Phys. Chem. 101, 2292 (1997).
- 7. J. Limtrakul, Chem. Phys. 193, 79 (1995).
- 8. J.D. Gale, Topics in Catalysis 3, 169 (1996).
- 9. J. Limtrakul and U. Ongthong, J. Mol. Struct. 435, 181 (1997).
- 10. J. Limtrakul, P. Treesakol and M. Probst, Chem. Phys. 215, 77 (1977).
- 11. J. Limtrakul and D. Tantanak, Chem. Phys. 208, 331 (1996).
- 12. J. Baker, Comput. Chem. 7, 385 (1986); 8, 563 (1987).
- 13. M.J. Frisch, G.W. Trucks, H.B. Schlegel, P.M.W. Gill, B.G.Johnson, M.W. Wong, J.B. Foresman, M.A. Robb, M. Head-Gordon, E.S. Replogle, R. Gomperts, J.L. Andres, K. Raghavachari, I.S. Binkley, C. Gonzalez, R.L. Martin, D.J. Fox, D.J. DeFrees, J. Baker, J.J.P. Stewart and J.A. Pople, Gaussian 94 (Gaussian Inc., Pittsburgh, 1994).
- 14. R. Ahlrichs, M. Bär, M. Häser, H. Horn and C. Kömel, Chem. Phys. Lett. 162, 165 (1989).
- 15. U. Messow, K. Ouitzsch, and H. Herden, Zeolites 4, 255 (1984).
- V. Gutmann, The donor-acceptor approach to molecular interactions (Plenum Press, New York, 1978).

เคมีของซีโอไลต์

จำรัส ลิ้มตระกูล

ห้องปฏิบัติการวิจัยเคมีคอมพิวเตอร์ และเคมีประยุกต์ ภาควิชาเคมี คณะวิทยาศาสตร์ มหาวิทยาลัยเกษตรศาสตร์ กรุงเทพ 10900

E mail: jumras@chem.sci.ku.ac.th; Phone: 9428034-5

ซีโอไลต์คืออะไร? มีสมบัติ อย่างไร?

ชีโอไลต์เป็นสารประกอบอะลูมิในซิ ลิเกต (1) (crystalline aluminosilicates) มี โครงสร้างเป็นรูพรุนมีโพรงและช่องว่าง ขนาดตั้งแต่ 2-10 Å (ตารางที่ 1) ซึ่งเป็น ลักษณะพิเศษเฉพาะตัวที่เด่นชัด สมบัติของ ซีโอไลต์ที่นำเอาไปใช้ประโยชน์ เช่น การแลก เปลี่ยนไอออน (ion exchange) การดูดซับ (adsorption) การดูดขับแก๊ส สารอาหาร น้ำ ตลอดจนโมเลกุลอินทรีย์ และสมบัติที่สำคัญ มากอย่างหนึ่งคือเป็นตัวเร่งปฏิกิริยา

ตารางที่ 1 คุณลักษณะของชีโอไลต์ชนิดต่าง ๆ (2)

| สัญลักษณ์ | ชื่อ | ขนาดของโพรง (Å) | อัตราส่วน Si/Al |
|-----------|--------------|-----------------|------------------|
| FAU | Faujasite | 7.4 | 1.25 (Zeolite X) |
| | | | 2.80 (Zeolite Y) |
| LTL | Zeolite L | 7.1 | 3 |
| MOR | Modenite > | 6.5 × 7.0 | 5 |
| MFI | ZSM-5 | 5.3× 5.6 | 22 |
| | | 5.1 × 5.5 | |
| BEA | Zeolite Beta | 7.6 × 6.4 | 30 |
| | | 5.5 ×5.5 | |

เคมีของซีโอไลต์

จำรัส ลิ้มตระกูล

ห้องปฏิบัติการวิจัยเคมีคอมพิวเตอร์ และเคมีประยุกต์

ภาควิชาเคมี คณะวิทยาศาสตร์ มหาวิทยาลัยเกษตรศาสตร์ กรุงเทพ 10900

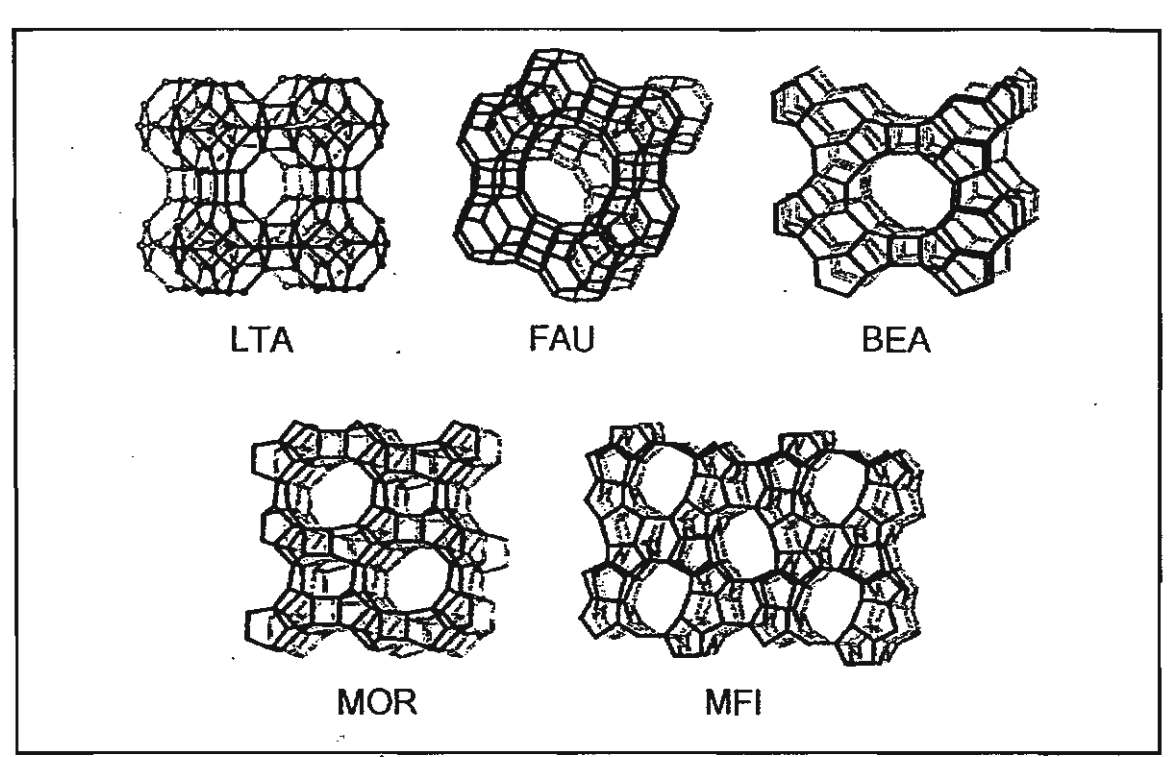
E mail: jumras@chem.sci.ku.ac.th; Phone: 9428034-5

ซีโอไลต์คืออะไร? มีสมบัติ อย่างไร?

ชีโอไลต์เป็นสารประกอบอะลูมิในชื ลิเกต (1) (crystalline aluminosilicates) มี โครงสร้างเป็นรูพรุนมีโพรงและช่องว่าง ขนาดตั้งแต่ 2-10 Å (ตารางที่ 1) ซึ่งเป็น ลักษณะพิเศษเฉพาะตัวที่เด่นชัด สมบัติของ ชีโอไลต์ที่นำเอาไปใช้ประโยชน์ เช่น การแลก เปลี่ยนไอออน (ion exchange) การดูดขับ (adsorption) การดูดขับแก๊ส สารอาหาร น้ำ ตลอดจนใมเลกุลอินทรีย์ และสมบัติที่สำคัญ มากอย่างหนึ่งคือเป็นตัวเร่งปฏิกิริยา

ตารางที่1 คุณลักษณะของซีโอไลต์ชนิดต่าง ๆ (2)

| สัญลักษณ์ | ชื่อ | ขนาดของโพรง (Å) | ขัตราส่วน Si/Al |
|-----------|--------------|-----------------|------------------|
| FAU | Faujasite | 7.4 | 1.25 (Zeolite X) |
| | | | 2.80 (Zeolite Y) |
| LTL | Zeolite L | 7.1 | 3 |
| MOR | Modenite : | 6.5 × 7.0 | 5 |
| MFI | ZSM-5 | 5.3× 5.6 | 22 |
| | | 5.1 × 5.5 | |
| BEA | Zeolite Beta | 7.6 × 6.4 | 30 |
| | | 5.5 ×5.5 | |



รูปที่ 1 แสดงโครงสร้างซีโอไลต์ชนิดต่างๆ

ซีโอไลต์ทำอะไรได้บ้าง?

1. การแลกเปลี่ยนไอออน (ion exchange)

ในปัจจุบันนิยมใช้ชีโอไลต์เป็นส่วน
ผสมในการทำสารชักล้าง โดยจะใช้ชีโอไลต์
แทนสารฟอสเฟต (phosphates) ซึ่งเป็นตัว
water softening agents ที่อันตรายต่อสิ่ง
แวดล้อม ซีโอไลต์ (zeolite A) มีโลหะ
โชเดี ยมซึ่งสามารถแลกเปลี่ ยนกับโลหะ
แคลเซียมและแมกนีเซียมได้เป็นอย่างดีและ
ไม่เป็นอันตรายต่อสิ่งแวดล้อม

การบำบัดนำ้เสีย ซีโจไลต์สามารถ ขจัด แอมโมเนียจากนำ้เสีย โดยการแลก เปลี่ยนแอมโมเนียมแคตใจจจนกับโลหะ โซเดียมที่อยู่ในโพรงซีโอไลต์ได้เป็นอย่างดี ดังนั้นซีโอไลต์ที่สังเคราะห์ขึ้นสามารถบำบัด นำ เสียได้ เป็นอย่างดี นอกจากนั้นยัง สามารถใช้ ขจัดไอโซโทปกัมมันตรังสี (cesium and strontium radioisotopes) จากกากนิวเคลียร์ (nuclear wastes)

2. การดูดซับ (adsorption)

มีการใช้ชีโอไลต์เป็นตัวดูดซับสาร ต่าง ๆ รวมทั้งการประยุกต์ใช้ในกระบวนการ ทำให้แห้ง (drying) กระบวนการทำให้ บริสุทธิ์ (purification) และ กระบวนการ แยกสาร (separation)

3. การเร่งปฏิกิริยา (catalysis)

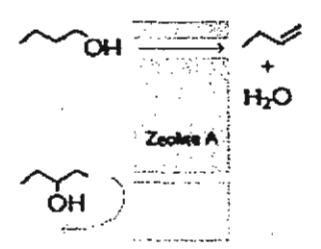
นักเคมีทำการสังเคราะห์สารที่มี
โครงสร้างคล้ายชีโอไลต์ และเรียกสารกลุ่มนี้
ว่า molecular sieves จากการสังเคราะห์
และออกแบบโครงสร้างจึงทำให้สารดังกล่าว
มีคุณค่าและ คุณประโยชน์ที่สำคัญใน
อุตสาหกรรมปิโตรเคมี เช่น ใช้เป็นตัวเร่ง
ปฏิกิริยาในกระบวนการเปลี่ยนแปลงเมธา
นอลเป็นไฮโดรคาร์บอน (methanol to
olefin) และ การแตกตัวด้วยตัวเร่งปฏิกิริยา
(catalytic cracking) เป็นต้น

ชีโอไลต์มีสมบัติเป็นกรด (Br nsted acid sites) และมีโครงสร้างเป็นภูพรุน และ เป็นโพรง ทำให้มีสมบัติโดดเด่น เช่น มี ความสามารถในการเลือกเกิดปฏิกิริยาตาม ภูปทรง (shape selectivity) ซึ่งอาจแบ่งได้ เป็น 3 แบบ ได้แก่ การเลือกเกิดปฏิกิริยาตามภูปทรงของสารตั้งต้น (reactant shape selectivity) การเลือกเกิดปฏิกิริยาตามภูปทรงของสารผลิตภัณฑ์ (product shape selectivity) และการเลือกเกิดปฏิกิริยาตาม ภูปทรงของสถานะแทรนซิชัน (transition state shape selectivity)

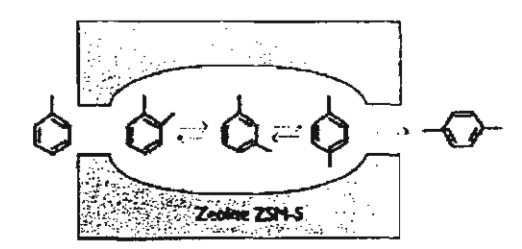
การเลือกเกิดปฏิกิริยาตามรูปทรง ของสารตั้งต้น (reactant shape selectivity) ชีโอไลต์เอสามารถเร่งปฏิกิริยาสูญเสียน้ำ (dehydration) ของ 1-butanol ได้อย่างดี แต่ ไม่ทำปฏิกิริยากับ 3-pentanol ซึ่งมีขนาด ใหญ่กว่า (ดูรูปที่ 2.1)

การเลือกเกิดปฏิกิริยาตามรูปทรง
ของสารผลิตภัณฑ์ (product shape
selectivity) ปฏิกิริยาเมธิลเลขัน
(methylation) ของโทลูอีนซึ่งเกิดขึ้นภายใน
โพรงของซีโอไลต์ ZSM5 จะเกิดขึ้นที่
ตำแหน่งพารา (para) เพื่อเกิดเป็นพาราไซลี
น (p-xylene) ซึ่งมีขนาดเล็กกว่าสาร
ผลิตภัณฑ์ชนิดอื่นๆ (คูรูปที่ 2.2)

การเลือกเกิดปฏิกิริยาตามรูปทรงของสถานะแทรนซิขัน (transition-state selectivity) ปฏิกิริยาการเกิดวงแหวน (cyclization) ของ 2,4-pentadiene สามารถเกิดขึ้นภายในโพรงของซีโอไลต์ mordenite แต่ไม่สามารถเกิดขึ้นภายในโพรงของซีโอ ไลต์ ZSM5 ซึ่งมีขนาดของโพรงเล็กกว่า สถานะแทรนซิขัน (คูรูปที่ 2.3)



2.1 การเลือกเกิดปฏิกิริยาตามรูปทรงของสารตั้งต้น (reactant shape selectivity)



2.2 การเลือกเกิดปฏิกิริยาตามรูปทรงของสารผลิตภัณฑ์ (product shape selectivity)



2.3 การเลือกเกิดปฏิกิริยาตามรูปทรงของสถานะแทรนซิขัน (transition-state selectivity) รูปที่ 2 แสดงลักษณะการเลือกเกิดปฏิกิริยาตามรูปทรงของสารตั้งต้น, สารผลิตภัณฑ์ และ สถานะแทรบซิชับ

งานวิจัยเกี่ยวกับซีโอไลต์

ชีโอไลต์มีมากกว่า 600 ชนิด (2538) แต่พอจะแบ่งกลุ่มตามชนิดของโครงสร้าง ได้ ประมาณ 40 ชนิด องค์ประกอบหลักที่ทำให้ ชีโอไลต์มีสมบัติแตกต่างกันคือ อัตราส่วน ของ ชิลิกอน และ อะลูมิเนียม การเปลี่ยน อัตราส่วนดังกล่าวมีผลก่อให้เกิดการเปลี่ยน แปลงกัมมันตภาพเชิงเร่งปฏิกิริยา (catalytic activity) และความเสถียรของ โครงสร้างชีโอ ไลต์

การแทนที่ธาตุ Si และ Al ด้วยธาตุ อื่น เช่น Ga, Ge, P, B และ Fe ในโครงสร้าง ชีโอไลต์ ทำให้ เกิด acidic bridging hydroxyl (≡AIOH-Ga≡, ≡Si-OH-Ga≡, ≡Si-OH-B≡) ซึ่งก่อให้เกิดการเปลี่ยนแปลง สภาพมีขั้ว (polarity) และความเป็นกรดของ ชีโอไลต์

การศึกษาและวิจัยถึงความสัมพันธ์
ของโครงสร้างและกับมันตภาพเชิงเร่ง
ปฏิกิริยาทำให้เราสามารถออกแบบและ
สังเคราะห์ซีโอไลต์ที่มีสมบัติใหม่ๆ เพื่อน้ำมา
ใช้ในปฏิกิริยาเคมีต่างๆ ได้ตามต้องการ และ
ขณะนี้ได้มีการศึกษาและวิจัยเกี่ยวกับซีโอ
ไลต์เมมเบรน (zeolite membrane) เพื่อใช้
ในการแยกสารประกอบไฮโดรคาร์บอน (3)
นอกจากนี้ได้มีการสังเคราะห์ transitionmetal oxide cluster ขึ้นภายในโพรงของซีโอ
ไลต์เพื่อนำมาใช้ในปฏิกิริยาออกซิเดชันของ
สารประกอบไฮโดรคาร์บอน (4)

กลุ่มเคมีชีโอไลต์และวิศวกรรมตัวเร่ง ของภาควิ ชาเคมี และวิ ศวกรรมเคมี มหาวิทยาลัยเกษตรศาสตร์ ได้ศึกษาและวิจัย ในหัวข้อต่อไปนี้ (5-14)

- Adsorption and coadsorption in zeolite
- Molecular aspects of heterogeneous catalysis
- Surface reaction dynamics in zeolitic catalysts
- Catalytic cracking (reaction & mechanism)
- Development of new and/or better catalytic reaction pathways via the explorative computational methods and the synthesis of new catalytic materials
- Other areas of developing use of zeolite like environmental chemistry

กิตติกรรมประกาศ

ขอขอบคุณสำนักงานกองทุนสนับ สนุนการวิจัยและสถาบันวิจัยและพัฒนา แห่งมหาวิทยาลัยเกษตรศาสตร์

เคกสารค้างคิง

- 1. Dyer, A. (1988). An introduction to zeolite molecular sieves. John Willey & Sons, New York.
- 2. Ono, Y. (1997). Solid acids and bases catalyze selective alkylations. Cattech.1, 31-38.
- 3. Gavalas, G.R., Yan, Y. and Davis, M.E. (1997). Preparation of selective zeolite ZSM-5 by a postsynthetic coking treatment, J. Membr. Sci.123, 95.
- 4. Pantu, P. (1997). Private communication.
- 5. Limtrakul, J. and Treesukol, P. (1997). Structures and potential energy hypersurface of faujasitic catalysts. Chem. Phys. 215, 77-87.
- 6. Limtrakul, J. and Tantanak, D. (1996). Cationic, structural, and compositional effects on the surface structure of zeolitic aluminosilicate catalysts. J.Chem.Phys. 208, 331-340.
- 7. Limtrakul, J. (1995). Adsorption of methanol in zeolite catalysts. Chem.Phys.193, 79-87.

- Limtrakul, J. and Tantanak, D. (1995).
 Structures, energetics and vibrational frequencies of zeolitic catalysts: a comparision between density functional and post-Hatree-Fock approaches. J. Mol. Struct. 358, 179-193.
- Limtrakul, J. and Yoinuan, J. (1994).
 Formation of ammonium cation at the Brønsted site in SAPO catalysts.
 Chem. Phys. 184, 51-57.
- 10.Limtrakul, J., Yoinuan, J. and Tantanak, D. (1994). Adsorption complexes of ammonia on germanium- and gallium-modified zeolites. J. Mol. Struct. 312, 183-194.
- 11.Limtrakul, J. (1993). Molecular modelling and catalytic properties of

- materials. *J. Mol. Struct.* 288, 105-110.
- 12.Limtrakul, J. and Hannongbua-Polman, S. (1993). Catalytic properties of a free hydroxyl on a silica, a zeolite, and modified zeolites: quantum-chemical model calculations. J. Mol. Struct. 280, 139-145.
- 13.Chareonpanich, M. et. al (1994).
 Selective production of BTX by hydrocracking of coal over zeolite catalyst. Energy Fuels 8, 1522.
- 14.Chareonpanich, M. et. al (1996).
 Hydrocraccking of aromatic hydrocarbon over USY- zeolite.
 Energy Fuels 10, 927.

ผลงาน

ผลงานที่ตีพิมพ์และกิจกรรมอื่น ๆ ที่เกี่ยวข้อง

- Limtrakul, J. and Tantanak D, J. Molecular Structure, 358 (1996) 179-193
 "Structures, energetics, vibrational frequies of zeolitic of zeolitic catalyst, a comparison with density functional and post Hartree-Fock",
- Limtrakul, J. and Tantanak, J. Chemical Physics, 208 (1996) 331-340.
 "Cationic, structure, and composition effects on the surface structure of zeolitic aluminosilicate catalysts".
- Limtrakul, J. and Treesukol P, J. Chemical Physics, 215 (1997) 77-87.
 "Structures and potential energy surface of faujasitic zeolite / water"
- Limtrakul J. and Onthong U. J Molecular Structure 435 (1998) 181-192.
 "Coadsorption of ammonia and methanol on H-zeolites and alkaline-exchanged zeolites
- Limtrakul J. "Structure and Reaction Pathways in Zeolitic Systems" in Zeolite Chemistry and Catalysis , M.M.J. Treacy, B. Marcus, J.B. Higgins and M. E. Bisher (Eds.) Materials Research Society, USA.

ผลงานอื่นๆ และรางวัลที่ได้รับ 2538-2541

- นักวิจัยที่มีผลงานดีเยี่ยมของเมธีวิจัย สกว. ประจำปี 2539
- นักวิจัยที่มีผลงานดีเยี่ยมของเมธีวิจัย สกว. ประจำปี 2540
- รางวัลผลงานวิจัยดีเด่นทางเคมีในรูปโปสเตอร์ในการประชุมวิทยาศาสตร์และเทคโนลียีแห่ง ประเทศไทย ครั้งที่ 22 ประจำปี 2539
- รางวัลผลงานวิจัยดีเด่นทางเคมีในการประชุมวิทยาศาสตร์และเทคโนลียีแห่งประเทศไทย ครั้งที่
 23 ประจำปี 2540
- รางวัลนักวิจัยดีเด่นแห่งชาติสาขาเคมี และเภสัช ประจำปี 2541 จากสภาวิจัยแห่งชาติ
- บุคลากรผู้มีผลงานดีเด่นทางวิชาการ มหาวิทยาลัยเกษตรศาสตร์ ประจำปีการศึกษา 2541
- ผลงานวิจัยดีเด่นสาขาวิทยาศาสตร์และเทคโนลียี "ครบรอบยีสิบงานวิจัย มก. สถาบันวิจัย มก.

จำนวนและรายละเอียดที่ได้รับเชิญเป็นวิทยากร

- Structure and reaction pathways in Zeolites, 12th International Zeolite Conference, 1998
 Baltimore, MD. USA.
- The role of molecular modelling in chemistry, สมาคมเคมี ห้องประชุมใหญ่ มหาวิทยาลัย เกษตรศาสตร์ กรุงเทพมหานคร
- ศักยภาพของนักวิทยาศาสตร์ไทย องค์ปาฐก "ปาฐกถาศาสตราจารย์ ดร.แถบ นีละนิธิ" 23 สิงหาคม 2541 ณ ห้องราชเทวี 2 โรงแรมเอเชีย กรุงเทพมหานคร
- Chemistry 1998 and Beyond การประชุมวิชาการวิทยาศาสตร์และเทคโนโลยีแห่งประเทศไทย ครั้งที่
 24 19-21 ตุลาคม 2541 ศูนย์ประชุมสิริกิติ์ กรุงเทพมหานคร
- Structure and Reactivity in Zeolites กรมวิทยาศาสตร์บริการ กระทรวงวิทยาศาสตร์เทคโนโลยีและ สิ่งแวดล้อม กรุงเทพมหานคร
- Catalyst Design 11 กันยายน 2541 คณะวิทยาศาสตร์ มหาวิทยาลัยเกษตรศาสตร์ กรุงเทพมหานคร
- หลักสูตร วท.บ.เคมี แนวใหม่ มหาวิทยาลัยทักษิณ สงขลา
- บรรณาธิการวารสาร KU Science Journal

การเชื่อมโยงทางวิชาการกับนักวิชาการอื่น ๆทั้งในและนอกประเทศ

- Chemical Engineering Department, Kasetsart University. In close collaboration with Chemical Engineering Department at Washington University, USA.
 Industrial applications of zeolite catalysis.
- Chemistry Department, University of Utah, Utah, USA.
 Development and Exploration of embedded Cluster Approach and Direct Dynamics for heterogeneous catalysis
- Laboratory for Molecular Spectroscopy, Bordeaux University, France.
 Surface Characterization of Advanced Materials
- Institutes of Inorganic and Theoretical Chemistry, University of Innsbruck and University of Vienna.
 - Computer Simulations of Surface Physical Chemistry and Drug Design.
- Molecular Simulations Inc., Sydney, Australia.
 Computer Aided Materials and Drug Design.
- Institute of Physical Chemistry & Electrochemistry, University of Karlsruhe, Germany.
 Development and Exploration of Computational chemistry codes.

Computer Simulations of Surface Physical Chemistry and Drug Design.

- Molecular Simulations Inc., Sydney, Australia.
 Computer Aided Materials and Drug Design.
- Institute of Physical Chemistry & Electrochemistry, University of Karlsruhe, Germany.

Development and Exploration of Computational chemistry codes.

ภาคผนวก

The Surface Structure and Catalytic Properties of Zeolite and Molecular Sieve Catalysts

Pl: Jumras Limtrakul

Chemistry Department, Faculty of Science, Kasetsart University

Executive Summary

Rational catalyst design, notably zeolites and molecular sieves, represents one of the most rewarding challenges in catalysis research. Zeolites possess three dimensional microporous crystalline solid. Their catalytically active acid-sites within the complex porous framework structure provide unique properties that make them very attractive industrial materials. They play a significant role in chemicals and fuels production worth over \$1000 billion per year. Zeolites and molecular sieves can be tailored or chosen to maximize the product of target molecules by employing state-of-the-art techniques. Our aim is to develop strategies for tailoring the structural and chemical properties of catalyst materials and to explore the potential of new catalytic materials.

 Structures, energetics and vibrational frequencies of zeolitic catalysts: a comparison between density functional and post-Hartree-Fock approaches Limtrakul, J. and Tantanak D, J. Molecular Structure, 358 (1996) 179-193.

We have carried out LSD and NLSD functional methods with 3-21G, 6-31G*, 6-311G* and DZVP basis sets to investigate the structures, energetics and vibrational frequencies for silanol, disiloxane, and different zeolite clusters. Some smaller models have also been calculated at the MP2 level. The individual geometrical parameters calculated at the BLYP and VWN levels with a modestly sized basis sets (6-311G*) generally yield good results compared to MP2 with much less computational effort. Comparing BLYP and VWN results with MP2, the former has a significant lengthening effect on the weaker A-O bond which does not occur with the latter. The Si-O(H)-Al and Si-O-H bond angles of zeolites are not appreciably affected by the inclusion of NLSD. However, the NLSD was found to be important for a better description of the floppy Si-O-

Si bond angle for disiloxane. The proton affinity of H3SiOHAlH3, a widely employed model of a Brønsted acid site in zeolites, is virtually identical to that of MP2/DZP and is also close to the result from G1 theory within the desired 10 kJ mol-1 accuracy. For this cluster model, the BLYP VOH value is calculated to within 130 cm-1 of the experimental value. We expect that the same accuracy from the BLYP/6-311G* procedure will be applied to larger zeolite clusters in the future.

Structures and potential energy surface of Faujasitic zeolite/water
 Limtrakul, J. and Treesukol, P., Chemical Physics, 215 (1997) 77-87.

We have presented a density functional study of faujasitic zeolites and their complexes with water using the B3LYP functionals and the basis sets 6-31G(d), 6-31G(d,p), 6-311G(d), 6-311G (d,p) and 6-311+G(d,p). The agreement between DFT/B3LYP-6-311+G(d,p) proton affinities and the corresponding CPF and G1 values are excellent. Comparing the older BLYP and VWN functionals, with the recently introduced B3LYP functionals, the latter yields superior accuracy. This artificial significant lengthening effect on the weaker Al-O bond in the BLYP and VWN calculations does not occur with B3LYP. The Si-O(H)-Al and Si-O-H bond angles of zeolites do not appreciably depend on the inclusion of non-local effects in the density functional. The 6-31G (d) basis set in DFT prediction of the faujasitic structure yields good results and is an economic choice for large systems. The predicted PA of the faujasitic catalyst is estimated to be 294±3 kcal/mol, which is in the range of experimentally determined value of 291-300 kcal/mol. The faujasite catalyst/water structure is stabilized at the bridging O-H group by two H-bonds with binding energy of -20.3 kcal/mol. Comparison with hydrogen halides and related complexes of water demonstrates that the faujasite is a strong acid. An analytical potential for the interaction to faujasitic zeolite with water was derived by fitting the ab initio interaction energies which we plan to employ in simulations studies of petrochemical catalyst/water systems.

Coadsorption of ammonia and methanol on H-zeolites and alkaline-exchanged zeolites
 Limtrakul J. and Onthong U. J. Molecular Structure 435 (1998) 181-192.

We have carried out HF and B3LYP methods with 6-31G* basis set to investigate the coadsorption of methanol and ammonia on H-zeolites (H-Z) and alkaline-exchanged zeolites (Na-Z). Comparing HF and B3LYP results with available experimental data, the B3LYP yields structural parameters which are in good agreement with experimental data. The Al...H distance of zeolite has been estimated experimentally as 238±4 pm, where as our B3LYP value is 239.7

pm. A comprehensive study of the coadsorption of absorbate molecules with the surface hydroxyl reveals several interesting points. Structure Na-Z/[CH3OH][NH3] is lower in energy than Na-Z/[NH3] [CH3OH], which suggests that the former is more favourable in the coadsorption process. The reaction mechanism of coadsorption of methanol and ammonia on H-Z is that the ammonia is found to stabilize to the BrØnsted acid site of H-Z, generating an ammonium cation, which acts as an active site for methanol.

 Cationic, structural, and compositional effects on the surface structure of zeolitic aluminosilicate catalysts

Limtrakul, J. and Tantanak, J. Chemical Physics, 208 (1996) 331-340.

The cationic, structural and compositional effects on the structure and bonding of different types of \equiv Si-OH-Al \equiv units in the secondary building unit of zeolite cluster models (OH)8HyAlxSi8-xO12)(x-y)- (x, y=0, 1, 2, 4) and the silica model (OH)8Si8O12 have been investigated with the DFT method. Full optimization of all mentioned structural isomer clusters have been carried out at VWN/6-31G* and BLYP/6-31G*. All isomers of the double four-membered ring aluminosilicate (D4R) demonstrate that Dempsey's rule may be violated in this type of zeolite. The well-known Loewenstein's \equiv Al-O-Al \equiv avoidance rule has been once again confirmed by us. The results of D4R with varying Si/Al ratio indicate that the higher the ratio, the lesser the proton is restricted which results in a higher acidic strength. The cations, H+ and Li+, are found to have a profound effect on the important structural parameters (Si-O, Al-O, O-H bonds and SiOHAl angle) of D4R. The marked difference between the cations is that the H+ is singly bonded while the Li+ is doubly bonded to the framework. This excellent results indicate that the catalytic activity of zeolites is also enhanced by the presence of cations, in addition to a compositional effect.